c1

A CONTRIBUTION TO THE STUDY OF LOCAL RIVER-BED SCOUR AROUND BRIDGE PIERS

by

CORNELIS ADRIANUS van der GUGTEN

B.A.Sc., University of British Columbia, 1967.

A THESIS SUBMITTED IN PARTIAL FULFILMENT OF
THE REQUIREMENTS FOR THE DEGREE OF

MASTER OF APPLIED SCIENCE

in the Department

of

CIVIL ENGINEERING

We accept this thesis as conforming to the
required standard

THE UNIVERSITY OF BRITISH COLUMBIA

September, 1972.

In presenting this thesis in partial fulfilment of the requirements for an advanced degree at the University of British Columbia, I agree that the Library shall make it freely available for reference and study. I further agree that permission for extensive copying of this thesis for scholarly purposes may be granted by the Head of my Department or by his representatives. It is understood that copying or publication of this thesis for financial gain shall not be allowed without my written permission.

C.A. van der Gugten

Department of Civil Engineering

The University of British Columbia
Vancouver 8, Canada

Date September 29, 1972.

ABSTRACT

This Thesis presents a review of the reported research on local sand-bed scour around bridge piers, describes the mechanics of local scour with particular reference to the horseshoe vortex, describes experiments on the effect of the vertical velocity distribution of the approach flow on local scour, and reports the results of these experiments.

The review of the previous research on local scour shows that the pier size is the most important parameter affecting the equilibrium depth of local scour, while the pier shape is of secondary importance. Two flow parameters are found to be important: the flow velocity and the flow depth, although their relative importance depends on the regime of the flow being considered.

The primary scouring agent is seen to be the horseshoe vortex system, which is a system of linked vortices that arises out of the vorticity always

present in shear flows, due to the interaction of the pier and the flow.

The experiments that were done consisted of observations and measurements of vertical velocity distributions, scour depths, and vortex patterns, for a circular cylinder in a laboratory flume. These experiments showed that the vertical velocity distribution of the boundary layer flow approaching the pier affects the structure of the horseshoe vortex system and the equilibrium depth of scour at the pier nose.

The Thesis concludes with a Summary and Conclusions, including recommendations for further research.

TABLE OF CONTENTS

Chapter		Page
	LIST OF TABLES	viii.
	LIST OF FIGURES	ix.
	LIST OF SYMBOLS	xiii.
	ACKNOWLEDGEMENTS	xx.
I	INTRODUCTION	1.
II	LITERATURE REVIEW	5.
	A. EARLY INVESTIGATORS	5.
	B. TISON AND ISHIHARA	6.
	1. Tison	6.
	2. Ishihara	7.
	C. INGLIS AND REGIME THEORY ADHERENTS	9.
	1. Inglis	9.
	2. Blench	9.
	3. Varzeliotis	10.
	D. LAURSEN	11.
	E. CHABERT AND ENGELDINGER	14.

Chapter		Page
II	F. BATA AND KNEZEVIC	16.
	1. Bata	16.
	2. Knezevic	16.
	G. TARAPORE	18.
	H. MOORE AND MASCH	20.
	I. BREUSERS: DELFT HYDRAULICS LABORATORY	22.
	1. Oosterschelde Bridge Model Studies	22.
	2. Scour Around Drilling Platforms	24.
	J. MAZA AND SANCHEZ	24.
	K. SHEN et al: COLORADO STATE UNIVERSITY	26.
	1. Introduction	26.
	2. Description of the Mechanics of Local Scour	26.
	3. Theoretical Analysis	28.
	4. Experimental Results	31.
	5. Reconciliation of Divergent Concepts	33.
	6. Methods of Reducing Scour	34.
	L. CARSTENS	35.
	M. TANAKA AND YANO, AND THOMAS	37.
	1. Tanaka and Yano	37.
	2. Thomas	38.
	N. SCHNEIDER	39.
	O. COLEMAN	43.
III.	THE MECHANICS OF LOCAL SCOUR	45.
	A. INTRODUCTION	45.
	B. THE BASIC VORTEX MECHANISM	46.
	C. ORIGIN OF THE HORSESHOE VORTEX	47.
	1. Vorticity	47.
	2. Vorticity in the Flow near a Cylinder	48.
	(a) The Approach Flow.	48.
	(b) Flow near the Cylinder.	49.

Chapter		Page
III.	D. CHARACTERISTICS OF THE HORSESHOE VORTEX	50.
	1. Structure	50.
	2. Formation	50.
	3. Strength	51.
	E. SUGGESTED RESEARCH	54.
IV.	EXPERIMENTAL WORK	55.
	A. PURPOSE AND SCOPE	55.
	B. EQUIPMENT AND EXPERIMENTAL ARRANGEMENT	56.
	1. General Arrangement	56.
	2. Sand Bed	57.
	3. Test Pier	57.
	4. Velocity-Distribution Control Gate	58.
	5. Current Flowmeter	58.
	6. Dye Injector	59.
	C. EXPERIMENTAL METHODS AND PROCEDURES	59.
	1. Starting-up	59.
	2. Generation of Vertical Velocity Profiles	60.
	3. Velocity Measurements	60.
	4. Flow Patterns	61.
	5. Scour Hole Development and Equilibrium Depth of Scour	62.
V.	EXPERIMENTAL RESULTS	63.
	A. GENERAL	63.
	B. APPROACH FLOW VELOCITY PROFILES	64.
	C. EQUILIBRIUM SCOUR DEPTH	65.
	1. Introduction	65.
	2. Results	66.
	3. Comparison with Results of Others	69.
	(a) Laursen	69.
	(b) Tarapore	70.
	(c) Breusers	70.
	(d) Maza and Sanchez	70.
	(e) Larras	71.
	(f) Shen *et al.*	71.
	(g) Coleman	71.

Chapter		Page
V.	D. VORTEX PATTERNS AND SCOUR HOLE DEVELOPMENT	72.
	1. The Horseshoe vortex System	72.
	2. Scour Hole Development: Beginning of Scour	73.
	3. Approach Flow Velocity Profile and Vortex Structure	75.
	4. Transport out of the Scour Hole	76.
VI.	SUMMARY AND CONCLUSIONS	78.
	A. PREVIOUS INVESTIGATIONS	78.
	B. MECHANISM OF LOCAL SCOUR	80.
	C. EXPERIMENTAL RESULTS	81.
	1. Introduction	81.
	2. Equilibrium Depth of Scour	81.
	3. Horseshoe Vortex Flow Patterns	82.
	D. RECOMMENDATIONS	83.
	1. Predicting Scour Depths	83.
	2. Further Research	84.
	BIBLIOGRAPHY	85.
	TABLES	98.
	FIGURES	101.

LIST OF TABLES

Table		Page
I	The variation of equilibrium scour depth with average velocity, for different pier diameters (circular pier) and different bed sediments, as reported by Breusers.	98
II	Values of the coefficient K_H used in the equation of Jaroslavtsiev.	99
III	Summary of Scour Experiments.	100

LIST OF FIGURES

Figure		Page
1.	Representation of curvature of the flow near an obstruction, as proposed by Tison.	101
2.	Laursen's non-dimensional plot of equilibrium scour depth (d_{se}) versus flow depth (H), for a rectangular pier of width b, at an angle of attack of 30^{o}.	102
3.	Schematic diagram showing variation of the equilibrium scour depth (d_{se}) with average flow velocity (u), as found by Chabert and Engeldinger (for any pier).	103
4.	Velocity diffusion into the scour hole, according to Tarapore.	104
5.	Schematic illustration of scour hole at equilibrium conditions, according to Tarapore.	105
6.	Approach flow velocity distribution and stagnation pressure on the plane of symmetry in front of a circular cylinder.	106
7.	Values of the coefficient K_{HU} to be used in the Maza and Sanchez version of Jaroslavtsiev's equation.	107

Figure		Page
8.	Idealized representation of the flow on the plane of symmetry in front of a circular cylinder; Shen et al.	108
9.	Control volume on the stagnation plane in front of a circular cylinder, Shen et al.	109
10.	Schematic representation of the velocity distribution and flow pattern in the scour hole on the plane of symmetry in front of a circular cylinder; Shen et al.	110
11.	Equilibrium scour depth versus pier Reynolds number (R_b) for circular cylindrical piers; Shen et al.	111
12.	Equilibrium scour depth versus pier Reynolds number (R_b), for circular cylindrical piers of different sizes; Shen et al.	112
13.	Equilibrium scour depth versus pier Reynolds number (R_b), for circular cylindrical piers and different grain sizes; Shen et al.	113
14.	Velocity distribution along the vertical, in the experiments of Tanaka and Yano.	114
15.	Types of circular cylindrical piers studied by Tanaka and Yano.	115
16.	Equilibrium depth of scour for different circular cylindrical pier types; Tanaka and Yano.	116
17.	Scour depth versus disc position, for a circular cylindrical pier; Thomas.	117
18.	The scour regions of Schneider (for any pier).	118
19.	Sketch of the vortex structure on the plane of symmetry in front of a circular cylinder in a laminar boundary layer, from a photograph of an experiment by Gregory and Walker, published in Thwaites[125].	119
20.	Sketch of laboratory flume cross-section showing general arrangement.	120

Figure		Page
21.	Flume sand grain-size distribution.	121
22.	View of velocity-control gate from a position downstream of the pier (gate is reflected in glass walls on either side).	122
23.	Velocity profiles, series 1.	123
24.	Velocity profiles, series 2-A.	124
25.	Velocity profiles, series 2.	125
26.	Velocity profiles, series 3 and 4.	126
27.	Velocity profile, series 5.	127
28.	Stability of velocity profile, series 1-A.	128
29.	Stability of velocity profile, series 2-A3.	129
30.	Scour hole development with time, series 1.	130
31.	Scour hole development with time, series 2-A.	131
32.	Scour hole development with time, series 2.	132
33.	Scour hole development with time, series 3.	133
34.	Scour hole development with time, series 4.	134
35.	Scour hole development with time, series 5.	135
36.	Vortex pattern, flat bed with low flow velocity.	136
37.	Vortex pattern, beginning of scour (cross-sectional view).	137
38.	Scour hole development with time, at $\theta = 30^{\circ}$ and $\theta = 0^{\circ}$, series 1-A.	138
39.	Vortex pattern, beginning of scour (plan view).	139
40.	Vortex patterns; partly developed scour hole; showing dependence of the individual vortices on the vertical velocity profile of the approach flow.	140

Figure		Page
41.	Vortex patterns; partly developed scour hole; showing effect of the vertical velocity profile of the approach flow.	141
42.	Scour hole development, showing motion of sand grains.	142
43.	Views of fully-developed scour hole: (a) looking downstream; (b) looking upstream.	143
44.	View of fully developed scour hole, looking diagonally upstream.	144

LIST OF SYMBOLS

Symbol	
A	A corner of the control volume ABCD (see Figure 9).
A_c	Area of the horseshoe vortex core.
A_o	Points on a vertical in the flow near the front of an obstruction (see Figure 1).
a	Cylinder radius
a_1	Parameter varying with type of flow: a_1 = 0.6 for main flow channel; a_1 = 1.0 for flood plain [1](Maza and Sanchez).
B	A corner of the control volume ABCD (see Figure 9).
B_d	Diameter of a circular disc fitted around a cylindrical pier (see Figure 15).
B_o	Points on a vertical in the flow in the region which remains unaffected by the pressure of an obstruction (see Figure 1).
b	Pier width or diameter.
b_1	Pier width projected onto a plane perpendicular to the approach flow direction.
C	A constant coefficient.

Symbol	
C	A corner of the control volume ABCD (see Figure 9).
C_1	Experimental constant (Ishihara).
C_2	A coefficient proportional to channel roughness and u'/H (Ishihara).
D	A corner of the control volume ABCD (see Figure 9).
D_c	Critical depth of flow = $(q^2/g)^{1/3}$
D_L	Lacey regime depth = $0.47\ (Q_m/f_L)^{1/3}$, in feet.
D_s	Total scoured depth, measured from the water surface, in feet.
dA	Element of surface area.
ds	Element of length.
d_{fo}	Blench's zero flood depth.
d_g	Characteristic grain size of bed sediment used by Carstens.
d_s	Depth of local scour below normal bed level.
d_{se}	Equilibrium or limiting value of d_s, for a given sediment, pier geometry, and flow conditions.
d_{sem}	Maximum possible value of d_{se}, for a given pier geometry.
d_{oo}	The grain size such that 00% of the material is finer, by weight.
e	The base of natural logarithms = 2.718.
F	The flow Froude number = $U/\sqrt{gH}$
F_b	Blench bed factor.
F_{bo}	Blench zero bed factor.
F_M	Total disturbing force on a bed sand-grain (Carstens).
F_R	Total retarding force on a bed sand-grain (Carstens).

Symbol

f	Function of .....
f_L	Lacey silt factor.
g	Acceleration of gravity.
H	Approach flow depth.
h	Height of pier modification above normal bed level (see Figure 15).
K	Pier shape coefficient (Larras).
K'	A constant coefficient in a uniform flow relation (Shen).
K_f	Pier shape coefficient (Jaroslavtsiev).
K_H	A coefficient which is a function of H/b_1 (see Table II).
K_{HU}	A coefficient which is a function of U^2/gb_1 and H/b_1 (see Figure 7).
K_s	Pier shape coefficient (Laursen).
K_U	A coefficient = $0.53\ (U^2/gb_1)^{-0.32}$ (Maza and Sanchez).
K_α	Coefficient for the angle of attack of the approach flow to the pier alignment (Laursen).
k	A coefficient representing the rate of velocity diffusion into the scour hole (Tarapore).
L	Characteristic length of flow obstruction.
ℓ	Distance along a flow streamline, starting at scour-hole edge.
m	A constant exponent in a uniform flow relation (Shen).
N_s	Carstens' sediment number = $u''/\sqrt{(s-1)gd_g}$.
N_{sc}	The critical value of N_s at which local scour is initiated.

Symbol

P	A point on the edge of the scour hole (see Figure 5).
p	Hydrostatic pressure.
$\overline{p}$	Stagnation pressure.
Q	Flow discharge.
Q_c	Critical value of Q at which local scour is initiated.
Q_m	Maximum flood discharge, in cubic feet per second.
$Q_{s\ in}$	Time rate of sediment transport into scour hole (volume).
$Q_{s\ out}$	Time rate of sediment transport out of scour hole (volume).
Q'_s	Time rate at which sediment is removed from the scour hole, in being deepened (weight).
Q'_{si}	Value of Q'_s at the beginning of the local scour process; ie. at $t = 0$.
$Q'_{s\ in}$	Time rate of sediment transport into scour hole (weight).
$Q'_{s\ in}$	$= q'_{s\ in}\ b$ (Schneider).
$Q'_{s\ out}$	Time rate of sediment transport out of scour hole (weight).
q	Flow discharge per unit width.
q_c	The value of q for the central approach flow just upstream of the pier, in cubic feet per second per foot.
q_s	Rate of bed-load sediment transport per unit width (Straub).
$q'_{s\ in}$	Time rate of sediment transport into the scour hole, per unit width (weight).
R_b	Pier Reynolds number $= Ub/\upsilon$.
r	Radius of curvature of flow streamlines.
S_F	Scour force at pier nose (Ishihara).

Symbol

s	Specific gravity of bed sediment.
t	Time, from the beginning of the local scour process.
t_c	Time constant (Schneider).
t_{se}	Time at which d_s reaches d_{se}.
U	Average velocity of approach flow.
U_c	The value of U at which local scour is initiated.
$U_{crit.}$	The value of U at which general bed-load transport is initiated.
u	The local velocity in the x-direction.
$u(\eta)$	Local velocity at the boundary (Tarapore).
$u(-\xi)$	Local potential velocity (Tarapore).
$\bar{V}$	Total velocity vector (Roper).
$\forall$	Volume of scour hole.
v	Local velocity in the y-direction.
v_x	Local velocity in the x-direction.
v_y	Local velocity in the y-direction.
v_z	Local velocity in the z-direction.
W	Stream or channel width.
W_s	Scour hole width.
w	Local velocity in the z - direction.
x,y,z	Axes of orthogonal co-ordinate system.
z	Elevation head.

Symbol

β	Included angle of pier nose.
Γ	Circulation $= \oint \overline{V} \cdot \overline{ds}$
γ	Specific weight of water.
δ	Boundary layer thickness.
ϵ	Constant exponent in a uniform flow equation (Shen).
λ	Void ratio of bed sediment.
ν	Kinematic viscosity of water.
ξ	Upward distance that the scour hole affects the main flow (Tarapore).
π	3.1416
ρ	Density of water.
ρ_s	Density of bed sediment.
σ	Standard deviation.
τ	Bed shear stress.
τ_c	Critical value of τ for the initiation of bed sediment transport.
ϕ	Angle of repose of the bed sediment.
χ	A parameter $= 3\, Q'_{si}\, t_c \tan^2\phi \,/\, \pi(1-\lambda)\rho_s\, gb^3$ (Schneider).
ψ	Sediment transport characteristic (Straub).
ψ_o	Flow streamline on the plane of symmetry of the approach flow (see Figure 5).
ψ_p	Flow streamline passing through point P on the edge of the scour hole (see Figure 5).
$\overline{\Omega}$	Total vorticity vector $= \overline{\nabla} \times \overline{V}$.
Ω_x	Vorticity with axis of rotation in the x-direction.
Ω_y	Vorticity with axis of rotation in the y-direction.

Symbol

Ω_z	Vorticity with axis of rotation in the z-direction.
ω	Angular velocity of the horseshoe vortex core.
$\overline{\nabla}$	Vector operator.
'	A superscript indicating that the parameter is to be evaluated at the surface of the flow.
"	A superscript indicating that the parameter is to be evaluated at the bed.

ACKNOWLEDGEMENTS

The author wishes to express his sincere thanks to his Supervisor, Professor E.S. Pretious, for his helpful advice, constant encouragement, and enduring patience throughout this study, especially during the last months, when he was already retired from the University.

Thanks are due to Professor H.W. Shen, of Colorado State University, for his suggestions and encouragement given to the author during a visit to the C.S.U. campus in the summer of 1968. Special thanks are due to Dr. Verne Schneider, then a post-graduate student at Colorado State, for his willingness to spend considerable time with the author in discussing and demonstrating various aspects of the local scour phenomenon during this visit.

The financial support of the National Research Council of Canada is gratefully acknowledged. The trip to Colorado was made possible through the N.R.C. operating grant to Professor Pretious.

CHAPTER I

INTRODUCTION

The successful foundation design of a structure founded in the sand-bed of a flowing stream, in order to safe-guard against excessive loss of bearing capacity, must include reasonably accurate methods for predicting the total amount of bed degradation at the foundations.

Degradation of the bed of a stream at a particular cross-section can occur due to changes in the general sediment-transport capacity of the flow at that section. For example, an increase in the velocity of the flow, due to increased discharge or reduced channel width, increases the capacity of the flow to carry sediment, and degradation results. Similarly, trapping or removing some of the sediment load of the flow (eg. by a dam) causes the stream to recover its full sediment load by scouring of the bed.

In addition to general degradation of the bed at a channel section, local bed-level changes can occur due to:

(1) meandering of the main flow channel (thalweg) between the banks of the stream,

(2) the downstream movement of bed dunes,

(3) local scour.

Local scour is the scour of the stream bed in the immediate vicinity of a structure (such as a groyne, training wall, wharf, bridge pier, or abutment) founded in that bed. It is primarily caused by the flow disturbance generated by such a structure.

It was the purpose of this thesis to investigate some of the aspects of the local scour phenomenon, with the aim of improving our understanding of the mechanics of the scour process and thus provide a sounder basis for predicting bed changes due to local scour.

The literature on local scour was reviewed fairly comprehensively, and is summarized in Chapter II. This review outlines the historical development of, and provides a basis for, the understanding of the local scour phenomenon. Although all of the references in the Bibliography were examined, only the more important and representative studies and findings are reported in the review.

Chapter III describes the mechanics of local scour of a sand-bed at a vertical cylinder, based on the findings summarized in Chapter II and on observations reported in the field of fluid dynamics. The origin and characteristics of the horseshoe vortex are discussed, particularly the various flow parameters that influence the strength of the horseshoe

vortex system.

After considering all of the available information on local scour developed in Chapters II and III, it was decided to investigate the influence of the approach flow velocity distribution. An outline of the experimental work done, and a description of the equipment and methods which were used, is given in Chapter IV. The experiments consisted of observations and measurements of velocity distributions, scour depths, and flow patterns in a laboratory flume.

Chapter V presents the results of the experimental work, and Chapter VI gives the summary and conclusions.

Symbols are defined where they first appear in the text, and also in the List of Symbols, p.xiii. Bibliographical references are indicated by raised, bracketed numerals. Footnotes are indicated by raised, unbracketed numerals, and are located at the end of each chapter.

The author was first encouraged to engage in studies in the field of local river-bed scour by his thesis supervisor, Professor E.S. Pretious, who had previously, in a consulting capacity, carried out private investigations of river-bed scour at bridge piers. These investigations were mainly concerned with finding the most adverse scour patterns that could occur at the piers of actual proposed or existing bridges in British Columbia. These included bridges over the Columbia River at Trail, the Columbia River at Kinnaird, the Kootenay River near Creston, the Fraser River at Agassiz, the Fraser River at Oak Street (Vancouver), and Morey Channel at Sea Island (Richmond).

The procedure used in these private investigations was to carry out a

hydraulic laboratory study using scale model piers and a moveable sand-bed, and to compare the results thus obtained with scour depths predicted by various formulas. It was found that often the predicted scour and the laboratory test results did not agree very well. It was this lack of a quick, rational, and safe method for predicting river-bed scour around flow obstructions, that motivated the present study.

CHAPTER II

LITERATURE REVIEW

A. EARLY INVESTIGATORS

The first reported[1] model studies involving bridge piers were carried out in Germany in the 1890's by H. Engels at the Technical University of Dresden[31]. These studies showed that the maximum scour of the bed occurs at the upstream end or nose of the pier. They also showed that riprap should be placed around the pier flush with the normal bed level, rather than on top of the bed. No other model studies were reported until the early 1920's, when T.H. Rehbock at the Technical University of Karlsruhe did some tests and found that the maximum depth of scour (which occurred at the pier nose) varied with flow velocity, bed materials, pier shape, and duration of flow, but the nature of these variations was not reported in detail[98]. The influence of the depth of

flow was apparently not investigated. The scour at the pier nose was attributed to cross-currents set up there.

B. TISON AND ISHIHARA

1. Tison

The first attempt at a theoretical approach to local scour was made by L.J. Tison in 1937[2]. His work has subsequently been republished in various places [128, 130, 131]. He considered the flow near the front of an obstruction in an open channel to be analogous to the flow of an irrotational vortex. On this basis he obtained an expression for a difference in piezometric head between the surface and the bottom of the flow close to the front of the obstruction:

$$\left(z'_{A_o} + \frac{p'_{A_o}}{\gamma}\right) - \left(z''_{A_o} + \frac{p''_{A_o}}{\gamma}\right) = \frac{1}{g}\left[\int_{A'_o}^{B'_o} \frac{u'^2}{r'}\,ds' - \int_{A''_o}^{B''_o} \frac{u''^2}{r''}\,ds''\right] \quad \ldots\ldots (1)$$

where z = the elevation head, p = the static pressure, γ = the specific weight of water, g = the acceleration of gravity, u = the local approach flow velocity, r = the radius of curvature of the flow streamlines, ds = an element of length taken along an orthogonal to the flow streamlines from A_o to B_o, A_o represents points on a vertical near the front of the obstruction, B_o represents points on a vertical in the flow which remains uninfluenced by the obstruction, single-primed symbols are for the flow at the surface, and double-primed symbols are for the flow at the bottom (see Figure 1).

For the case of an obstruction of uniform cross-section, r' = r" and ds' = ds". If, as commonly occurs in streams and laboratory flumes, the flow is not uniform, but a velocity gradient exists on the vertical plane, the surface velocity u' will be greater than the bottom velocity u", and the right-hand side of equation (1) will be positive. Thus there will be a pressure difference between surface and bottom, and as a result the flow will acquire a downward component in front of the pier and attack the bed, causing scour. Tison concluded that the greater the difference between u' and u", the greater would be the scour. In addition, smaller values of r' would also increase the scour. Tison verified each of these conclusions with laboratory tests. He used pier shapes ranging from square to lenticular, and obtained decreasing values of scour depth as the pier shape became more streamlined and permitted a more gentle curvature of the flow. By using a very coarse material for the upstream bed, he was able to change the velocity distribution so that u" became less and u' became greater, thus increasing the difference between u' and u", and obtained a greater scour hole depth. However, his results are only qualitative in nature and he did not present any specific relationship involving the depth of scour.

2. Ishihara

Shortly after Tison first published his work, Ishihara performed an extensive series of tests of scour at bridge piers [44]. It was found that the scour depth at the nose was mainly governed by the shape of the nose - a sharper nose producing less scour - and not at all by the shape of the pier tail or the length of the pier, for piers aligned with the

flow direction. The scour depth was found to increase with increased skewness of the piers; the more so for a sharper pier nose. The effect of constriction of the flow, expressed in terms of the ratio of stream width W to pier width b, was found to be small, for values of W/b from about 6 to 10, and nil for values of W/b greater than about 15. It was observed that scour decreased with decreasing flow depth, but that the rate of this decrease depended on the characteristics of the sand, the pier shape and the pier size.

In addition to his experimental work, Ishihara developed a theory for local scour at piers by assuming the flow near a pier to be similar to the flow in the bend of a river. He obtained an expression for the secondary downward flow component in a river bend by considering the main flow there to be analogous to the flow of an irrotational vortex, much after the manner of Tison (see above). By assuming that the "scour force" was proportional to the value of the downward flow component, and applying the results for the river bend directly to the case of flow around an obstruction, he obtained the expression:

$$S_F = C_1 C_2 \int_{B_o}^{A_o} \frac{U^2 H}{r} \, ds \qquad \ldots\ldots(2)$$

where S_F = the scour force at the pier nose, C_1 = an experimental constant, C_2 = a parameter which increases with increasing channel roughness and decreasing value of H/u', U = the average velocity of the approach flow, and H = the flow depth. This expression is substantially similar to that of Tison (equation (1)).

C. INGLIS AND REGIME THEORY ADHERENTS

1. Inglis

The first relationship explicitly involving the depth of scour at a bridge pier was formulated by Sir Claude Inglis (with A.R. Thomas and D.V. Joglekar) in 1939[3]. On the basis of model studies, using round-nosed piers of similar geometry but differing size, he obtained:

$$\frac{D_s}{b} = 1.70 \left[\frac{q_c^{2/3}}{b}\right] 0.78 \qquad .....(3)$$

where D_s = the total scoured depth measured from the water surface (in feet), b = the pier width (in feet), and q_c = the central approach-flow discharge per unit width (in square feet per second).

Inglis in 1949 presented a second relationship, this time on the basis of a considerable number of field data as well as the experimental data mentioned above. He obtained:

$$D_s = 2D_L \qquad .....(4)$$

where D_s is the total scoured depth as defined above, and D_L is the Lacey regime depth:

$$D_L = 0.47 \left[\frac{Q_m}{f_L}\right]^{1/3} \qquad .....(5)$$

where Q_m = the maximum flood discharge in cubic feet per second, and f_L = the Lacey silt factor.

2. Blench

Later, Blench[11], in 1957, reported the results of a plot, by Andru, using data of Inglis, Laursen, and others, of $D_s F_b^{1/3}$ vs. q,

without any attempt to differentiate between different types of obstructions. This data included scour at bridge piers, guide banks, spur noses, downstream of bridges, etc., and produced a "best fit" line of:

$$D_s F_b^{1/3} = 1.35\, q^{0.74} \qquad .....(6)$$

where D_s = the total scour depth below the water surface (in feet), F_b = the Blench bed-factor = U^2/H (U = average approach flow velocity in feet per second, H = approach flow depth in feet), and q = the approach flow discharge per unit width (in square feet per second).

In the same work, Blench proposes a relationship for maximum scour at bridge piers which is the same as equation (4) of Inglis, except that instead of the Lacey depth, D_L, Blench proposes a "zero flood depth," d_{fo}, which is supposed to represent the required regime depth of a canal having a bed factor corresponding to zero charge (ie. bed-load charge is zero: $F_b = F_{bo} = q^2/ d_{fo}^3$), with the discharge at the maximum, and using the reduced obstructed width[4].

3. Varzeliotis

In 1960, Varzeliotis did a laboratory study of local scour at bridge piers[134]. Using arguments based on regime theory to arrange his data, he obtained:

$$\frac{D_s}{D_c} = 1.7 \left[\frac{b\, g}{D_c F_{bo}}\right]^{\frac{1}{4}} \qquad .....(7)$$

where D_c = the critical depth of flow (= $[q^2/g]^{1/3}$). Although a better "fit" to the data is obtained using an index of 0.28, Varzeliotis used ¼ in the belief that natural laws usually follow simple indices.

D. LAURSEN

It was not until the early 1950's that experimental work directed towards the establishment of a design relation for local scour at bridge piers was started on a significant scale, by E.M. Laursen[59, 60, 61]. Laursen also formulated a number of concepts with respect to local scour which are useful in establishing a framework for the understanding of the local scour problem. These concepts can be enumerated as follows:

(a) The rate of scour equals the difference between the sediment transport rate into the scour hole and the sediment transport rate out of the scour hole. Symbolically:

$$\frac{dV}{dt} = Q_{s\ out} - Q_{s\ in} \qquad .....(8)$$

where $\frac{dV}{dt}$ = the time rate of change of volume of the scour hole, $Q_{s\ out}$ = the time rate at which sediment is carried out of the scour hole (in cubic feet per second), and $Q_{s\ in}$ = the time rate at which sediment is transported into the scour hole (in cubic feet per second)[5].

(b) The rate at which the volume of the scour hole increases will decrease as the hole gets bigger.

(c) There will be some limiting size of scour hole (for any given geometry and flow condition). When this occurs the scour depth is said to be at equilibrium, and $Q_{s\ out} = Q_{s\ in}$.

(d) This limiting size will be approached asymptotically.

On the basis of the first concept, Laursen distinguished between three different scour cases:

(a) No scour. This condition occurs when the velocity of the flow is too low to cause any local scour, and initial conditions are $Q_{s\ in} = Q_{s\ out} = 0$.

(b) "Clear-water" scour[6]. The flow disturbance due to the obstruction is strong enough to cause some scour, but sediment transport by the undisturbed approach flow does not occur. The initial conditions are:

$Q_{s\ in} = 0, Q_{s\ out} > 0$.

(c) Scour with general sediment motion. The initial conditions are $Q_{s\ out} > Q_{s\ in} > 0$.

All of Laursen's earlier work was done with flows which were capable of general sediment transport (case (c) above). He investigated the effects of bed sediment size, average velocity of the approach flow, and flow depth, on the equilibrium depth of scour at a pier. Although his data showed some scatter, he found no effect of bed sediment size or average flow velocity, and only the flow depth was found to have an effect on the equilibrium scour depth. He was able to present the influence of the flow depth in terms of a graph, using co-ordinates non-dimensionalized on the basis of the pier width (see Figure 2)[(61)].

Laursen (as had Posey[(93)] before him) observed that the basic scouring agent was a roller or vortex, with a horizontal axis, which formed in front of the pier nose. In order to explain the observed

effects of the average flow velocity, flow depth, and sediment size, Laursen reasoned along the following lines[59, 61].

At any given equilibrium scour condition in the general sediment transport region (case (c) above), the rate at which the roller moves sediment out of the hole is just balanced by the rate at which the approach flow moves sediment into the hole. If the average flow velocity is increased, the angular velocity of the roller could be expected to increase in a proportional way, and thus $Q_{s\ out}$ would increase. However, the velocity of the approach flow near the bed would also increase, and the net effect would be no change in the difference $Q_{s\ out} - Q_{s\ in}$. Similarly, if the sediment size would be increased, the transport rates into and out of the scour hole would decrease, but in the same proportion, so that there would be no change in the equilibrium scour depth.

When the flow depth is increased, however, the angular velocity of the roller is presumed to remain the same as long as the average flow velocity remains constant; thus $Q_{s\ out}$ does not increase. However, the velocity of the approach flow near the bed would be decreased somewhat, so that $Q_{s\ in}$ would decrease, and the net result would be an increase in the equilibrium scour depth.

Laursen concluded from his studies that the equilibrium depth of scour, for flows below the critical (Froude number < 1) and capable of general bed-load transport, depends only on the flow depth, pier size, pier shape, and the angle of attack of the approach flow. This dependence was presented in the form of design curves and tables[61]. These design

criteria can be reduced to the expression:

$$\frac{d_{se}}{b} = K_s K_\alpha \; 1.50 \; \left[\frac{H}{b}\right]^{0.3} \qquad .....(9)$$

where d_{se} = the equilibrium depth of scour below normal bed level, K_s is a factor for pier shape, and K_α is a factor for angle of attack. For a circular cylindrical pier, equation (9) reduces to:

$$\frac{d_{se}}{b} = 1.35 \; \left[\frac{H}{b}\right]^{0.3} \qquad .....(10)$$

Laursen later tried to incorporate local bed scour at bridge piers, for both the "clear-water" case and the case of general sediment transport, into a general theory of scour at bridge crossings[62, 63, 64, 65, 66, 67].

He did this by first developing an equation for the depth of scour in a long contraction, based on the Manning formula, his own sediment-concentration formula, and considerations of continuity of both the flow and the sediment discharges. Laursen then related the depth of local scour at a bridge pier to the general scour in a long contraction by introducing a special coefficient to account for the local non-uniformity of the flow in the former, and by assuming that the contracted width could be represented by 2.75 d_{se} and the uncontracted width by 2.75 d_{se} + 0.5b. Comparison of his theory to experimental data of Inglis and Chabert and Engeldinger (refs. 65 and 191, respectively, in Karaki and Haynie[51]), showed qualitative agreement only.

E. CHABERT AND ENGELDINGER

In 1956 Chabert and Engeldinger, in France, reported a large series of tests of local scour at bridge piers[7]. Their study involved scour in

both the region of "clear-water" scour and the region of general sediment transport. Their main contribution was that they found the equilibrium scour depth to increase roughly linearly with the bed shear stress throughout the region of "clear-water" scour, and that the maximum equilibrium depth of scour occurred in the transition region between "clear-water" scour and scour with general sediment transport - ie. when the average flow velocity is at about the critical for general bed-load transport (see Figure 3).

Chabert and Engeldinger also tested different sizes of bed material. They observed that the maximum equilibrium scour depth for a given pier increased with increasing sediment size, for median grain diameters[8] of 0.26 mm, 0.52 mm, and 1.50 mm. However, for a sand of median diameter = 3.00 mm, the maximum equilibrium scour depth was less than that for the 1.50 mm sand[9].

Later, Larras obtained a relation for local scour based on the data of Chabert and Engeldinger, as well as field data[10]:

$$d_{sem} = 1.42\ K\ b^{0.75} \qquad .....(11)$$

where d_{sem} is the maximum equilibrium depth of scour <u>below normal bed level</u>, in feet, and K is a factor to account for pier shape: K = 1.0 for circular piers, K = 1.4 for rectangular piers. The pier width b is measured in feet.

F. BATA AND KNEZEVIC

1. Bata

In 1960 Bata reported a study of the problem of local scour at bridge piers using field measurements, laboratory tests, and theoretical analysis[7]. He applied potential flow analysis to an assumed logarithmic velocity distribution of the flow approaching a circular pier. This analysis showed that vertically downward velocity components are present in front of the pier, and have a magnitude approximately one-half of the magnitude of the average approach flow velocity, for the region which extends upstream about three or four pier radii in front of the pier. These vertical velocity components were thought to be the main cause of local scour.

Bata plotted his laboratory and field data as d_{se}/H versus U^2/gH (the flow Froude number), and obtained a linear relationship. This was noted to be similar to the formula of Jaroslavcev (Jaroslavtsiev), which has $d_{se} \alpha U^2$ (this formula is discussed below in connection with the work of Maza and Sanchez).

2. Knezevic

Knezevic in 1960 also reported a study of the local scour problem[53]. The relevant aspects of his study involved attempts to determine the conditions required for the start of local scour, the equilibrium depth of scour, and the influence of several methods of reducing the maximum depth of scour.

The results of the investigation into the conditions required for local scour were presented in terms of the critical discharge Q_c just

large enough to start local scour. It appears that Q_c was determined by extrapolation, to $d_{se} = 0$, of plots of d_{se} versus discharge Q, for various water depths. Although the data are not sufficient to provide accurate values for Q_c, they do indicate that Q_c is slightly less for a pier with a square nose than for a pier with a round nose. The data also show a definite increase in Q_c with increasing sand-grain size, for the sands used (d_{90} = 0.285 mm., 2.4 mm., and 4.5 mm).

Knezevic arranged his data for equilibrium depth of scour to obtain a relation of the form:

$$d_{se} = C \frac{(Q-Q_c)^{3/2}}{H^{5/4} g^{3/4}} \qquad .....(12)$$

where C = a constant. The value of C is supposed to vary only with the pier shape, but actually there was scatter with respect to both sand-grain size and flow depth. Average values were, for the circular nose, C = 8.7; for the rectangular nose, C = 9.8.

Knezevic conceived the scour-causing vortex at the base of the pier to be due to the vertically downward velocity components in front of the pier, as suggested by Tison (see above). On this basis two methods of reducing scour occurred to him. One method consisted of aspirating the downward flow in front of the pier by means of a horizontal hole or slot cut through the pier in the direction of the main flow. A definite reduction in the equilibrium depth of scour was observed, ranging from about 27% to 76%, depending on the shape of the pier and the size of the bed sand-grains. The size, shape, and location of the slot were not given.

A second method consisted of placing a series of bands around the

pier at various levels, in order to deflect and retard the downward flow just in front of the pier. Using three bands of steel plate 15 mm. wide and 2 mm. thick, placed around a pier 10 cm. wide, reductions of the order of 30% to 40% in the equilibrium scour depth were obtained.

G. TARAPORE

Tarapore in 1962 completed a Doctoral Thesis in which he reported laboratory measurements and presented a theoretical method for determining the local scour at an obstruction[119, 120]. In his theoretical investigation he assumed that the initial flow pattern was given by potential flow theory. As the scour hole developed, it was assumed that the free stream diffused into the scour hole in a manner analogous to that of a mixing layer situation, and the velocity distribution was given by:

$$u(z) = u(-\xi)\, e^{-k(z+\xi)/l} \qquad .....(13)$$

where $u(z)$ = the local velocity at depth z, in the x-direction, $u(-\xi)$ = the potential velocity, ξ = the distance that the effects of the scour hole have penetrated into the main flow, l = distance along a streamline, starting at the scour hole edge, and k = a coefficient representing the rate of velocity diffusion into the scour hole (see Figure 4). The rate of bed load transport was assumed to follow Straub's expression (1935):

$$q_s \alpha \frac{\psi}{\gamma^2} \tau(\tau - \tau_c) \qquad .....(14)$$

which, for high rates of transport ($\tau >> \tau_c$), can be simplified to:

$$q_s \alpha \frac{\psi}{\gamma^2} \tau^2 \qquad .....(15)$$

where q_s = the rate of transport of bed load (in cubic feet per hour per foot width), ψ = Straub's transportation characteristic, γ = the specific weight of water, τ = the bed shear stress, τ_c = the critical bed shear stress. The assumption for the bed shear stress was:

$$\tau \alpha \rho [u(\eta)]^2 \qquad .....(16)$$

where $u(\eta)$ = the value of the (diffused) velocity at the boundary, and ρ = the density of water. When the scour hole is at the equilibrium condition, it was assumed that the rate of transport into the hole equaled the rate of transport out of the hole, thus the transport rate between the streamline on the plane of symmetry of the approach flow, ψ_o, and the streamline passing through the point P on the edge of the scour hole, ψ_P, was constant (see Figure 5). In terms of an equation:

$$\int_{\psi_o}^{\psi_P} q_s dy \quad (x=0) \quad = \quad \int_{\psi_o}^{\psi_P} q_s dy \quad (x=-\infty) \qquad .....(17)$$

where the x and y coordinates are as shown in Figure 5. Substitution of equations (15) and (16) yields:

$$\frac{\psi}{\gamma^2} \rho^2 \int_{\psi_o}^{\psi_P} [u(\eta)]^4 dy \quad (x=0) \quad = \quad \frac{\psi}{\gamma^2} \rho^2 \int_{\psi_o}^{\psi_P} U^4 dy \quad (x=-\infty) \qquad .....(18)$$

Further substitution of equation (13), with $u(\eta) = u(z)$, and additional assumptions and manipulation, yields an integral equation which can be solved by numerical methods to yield the position of the point P (see Figure 5). The depth of scour can then be determined, if the shape of the scour hole is known. In addition, the values of k and $\xi/1$ have to be

estimated in advance from experimental data. Since $\xi/1$ represents the rate at which the influence of the scour hole is propagated towards the surface of the flow, this term is determined by plotting the experimental data as d_{se}/b versus H/b, and noting where d_{se}/b is no longer affected by the depth of flow. The value of k is obtained by solving the equation for a know experimental result.

Tarapore's plots of d_{se}/b vs. H/b show considerable disagreement between his own data and that of others which he included in his plot, and his selection of $H/b = 1.15$, as the value above which flow depth no longer influences scour depth, seems arbitrary. Tarapore calculated the depth of scour at an elliptical cylinder, according to the method outlined above, and obtained results which were about 10% to 15% less than the experimental results. The difference is explained as due to improper estimation of the scour hole shape. In addition, Tarapore concluded that the maximum depth of scour (below normal bed level) at a circular cylinder, for large depths of flow, is equal to 1.35 b.

H. MOORE AND MASCH

In 1963 Moore and Masch published a paper in which they attempted to achieve an understanding of the secondary flow caused by the presence of a pier in an otherwise undisturbed flow[80]. Their analysis is largely based on the fact that a pressure gradient exists along the stagnation line formed by the intersection of the plane of symmetry of the approach flow and the pier surface, if the approach flow velocity is not uniform (see Figure 6). If the flow is two-dimensional, then the stagnation

pressure head, $\bar{p}/\gamma$, at any location on the stagnation line, is just equal to the velocity head of the approach at that level, $u^2/2g$. Thus, if $u = u(y)$, $\bar{p} = \bar{p}(y)$, where y is the vertical coordinate. Since the sum of static pressure head and elevation head remains a constant, a net pressure gradient exists along the stagnation line. This pressure gradient induces an acceleration of the nearby fluid from the point of maximum pressure towards the regions of lower pressure. If viscous effects are neglected and one considers a streamline running downward along the stagnation line, the conservation of energy principle yields, for the secondary vertical flow at any point, a velocity head $v^2/2g$, which is just equal to the difference between the pressure head at that point and the maximum pressure head. Thus:

$$\frac{v(y)^2}{2g} = \frac{\bar{p}\ \text{max.}}{\gamma} - \frac{\bar{p}(y)}{\gamma}$$

$$= \frac{u\ \text{max.}^2}{2g} - \frac{u(y)^2}{2g} \qquad \text{.....(19)}$$

or:

$$v(y)^2 = u\ \text{max.}^2 - u\ (y)^2 \qquad \text{.....(20)}$$

Moore and Masch contended that the above concept provides the basis for the mechanism producing a strong vertically downward flow just in front of the pier and thus accounts for the fact that the maximum depth of scour occurs at the nose of the pier rather than at the point of maximum breadth, as would be expected if only the two-dimensional potential flow pattern were considered. This downward flow was thought to significantly contribute to the formation and maintenance of the

spiral vortex in the scour hole.

On the basis of their understanding of the scour process, Moore and Masch briefly discussed four methods of reducing scour. One method consists of placing horizontal discs around the pier, below or above normal bed level, with possibly a vertical lip around the outside edge to deflect the secondary flows upward away from the bed[11]. Another previously proposed method consists of placing an auxiliary pier or pile upstream of the pier to be protected[12]. Masch and Moore thought that such a pile would "destroy" the velocity gradient of the approach flow. The reduction in scour depths achieved by sharpening the pier nose is explained in terms of the reduction in the size and strength of the downward flow component effected by such a nose. A final method suggested by Moore and Masch consists of a swept-back leading edge, possibly required only near the bed, in order for the deflected flow component which then develops to counteract the downward flow induced by the velocity gradient of the approach flow.

I. BREUSERS; DELFT HYDRAULICS LABORATORY

1. Oosterschelde Bridge Model Studies

In 1964, Delft Hydraulics Laboratory published a report of a model study of scour around the piers of the Oosterschelde Bridge, under the direction of H.N.C. Breusers[(16)]. Experiments were carried out using circular cylindrical piers in order to investigate the influence of the average approach flow velocity, flow depth, pier diameter, and bed material. It was observed that with a bed sand of d_{50} = 0.20 mm.

($U_{crit.}$ = 0.25 m./sec. = 0.81 ft./sec.), maximum scour occurred when $U/U_{crit.}$ reached a value of 1.4, and did not increase for greater velocities ($U_{crit.}$ is defined as the value of U at which general bed load transport is initiated). It was found that the ratio d_{sem}/b decreased somewhat with increasing pier diameter, having a value of 1.5 for b = 11 cm. and 1.6 for b = 5 cm. (see Table I). This result was obtained for a flow depth H, for the 5 cm. pier, of 0.25 m. and a flow depth for the 11 cm. pier of 0.50 m., in the understanding that similarity would be better approximated using similar values of H/b rather than just H alone. The flume width was 0.95 m.

The influence of the flow depth on the equilibrium depth of scour (below normal bed level) was tested using the 11 cm. pier and flow depths of 0.15 m., 0.25 m., and 0.50 m., at the condition $U/U_{crit.}$ = 1.4. There was no significant difference in the equilibrium scour depths for the two larger flow depths, while for the smallest flow depth, the equilibrium scour depth was somewhat less. It is interesting to note that at the initial stages of scour, at a time t = 15 min. from the start of scour, the smallest flow depth produced a larger scour depth than the two larger flow depths.

Tests were also run with a bed material of polystyrene spheres (density = 1050 kg/m^3) of diameter 1.5 mm. ($U_{crit.}$ = 0.09 m/sec.) in a flume 3.5 m. wide. For the 11 cm. pier, maximum scour depth corresponding to d_{sem}/b = 1.7 was reached, at $U/U_{crit.}$ = 1.2. The ratio d_{se}/b reached a steady value of 1.65 at $U/U_{crit.} \geq 1.4$ (see Table I).

2. Scour around Drilling Platforms

In 1965, Breusers reported the results of a private study of scour around drilling platforms[17]. He obtained:

$$d_{sem} = 1.4\ b \qquad .....(21)$$

J. MAZA AND SANCHEZ

Maza and Sanchez reported a study of local scour at bridge piers in 1964[79]. They reviewed the literature available to them and found that there were basically two different relations. The first of these was proposed by Laursen and is given above. Essentially it was $d_{se} = f(b,$ H/b, pier shape, angle of attack). The second relationship is due to Jaroslavtsiev, and can be formulated as $d_{se} = f(U^2, H/b_1, U^2/gb_1,$ pier shape, d_{50}, type of flow), where b_1 represents the width of the pier projected onto a plane perpendicular to the approach flow direction. The restriction on Laursen's relationship is that it is valid only for $U \geq U_{crit.}$, whereas Jaroslavtsiev's relationship is valid only for $H/b >$ 1.5, and in addition d_{50} is included only if it exceeds 5 mm. In terms of a design equation, Jaroslavtsiev's relation can be expressed as:

$$d_{se} = K_f K_U (a_1 + K_H) \frac{U^2}{g} - 3\ d_{50} \qquad .....(22)$$

Here K_H is a function of H/b_1 and decreases with increasing H/b_1 up to a value of $H/b_1 \simeq 5$ (see Table II). In the interval $1.5 \leq H/b_1 \leq 6$, the relation can be approximated by $K_H = (H/b_1)^{-7/4}$. The parameter a_1 varies from 0.6 for a pier in a main flow channel to 1.0 for a pier on a flood plain. The term K_U is a function of the pier Froude number U^2/gb_1,

and can be expressed as $K_U = 0.53(U^2/gb_1)^{-0.32}$. The pier shape coefficient varies from $K_f = 10$ for circular piers to $K_f = 12.4$ for rectangular piers. All units are in meters except for d_{50} which is in millimeters.

Maza and Sanchez carried out a number of experiments and compared their data to the two scour relations. They found that their data fitted the relation of Jaroslavtsiev quite well for values of $H/b > 1.5$. Ninety percent of their data fell below Laursen's relation, and none exceeded it. On the basis of their results, Maza and Sanchez proposed a modified version of Jaroslavtsiev's equation, in the form:

$$\frac{d_{se}}{b_1} = K_f K_{HU} \frac{U}{gb_1} - \frac{3\, d_{50}}{b_1} \qquad .....(23)$$

with d_{50} in millimeters and all other lengths in meters. The parameter K_{HU} is primarily a function of U^2/gb_1, and secondarily of H/b_1, but the latter has little influence except for values of $U^2/gb_1 < 0.10$ (see Figure 7). For purposes of design, Maza and Sanchez recommend that the smaller of the values given by equation (23) and Laursen's relation, equation (9), be used, with the restriction that equation (23) is valid only for $H/b_1 > 1.5$, and the term with d_{50} be included only if $d_{50} \geq 5$ mm.

K. SHEN et al.: COLORADO STATE UNIVERSITY

1. Introduction

Since 1962, workers at Colorado State University, largely under the direction of H.W. Shen and S.S. Karaki, under a contract with the United States Bureau of Public Roads, have investigated the problem of local bed scour at bridge piers[109,110,111,112,113]. Experimental work has involved the study of the variation of the depth of scour with time, the dependence of the equilibrium depth of scour on the hydraulic parameters, the velocity patterns of the flow in and around the pier and scour hole, and the effectiveness of various methods of reducing scour. Theoretical work was aimed mainly at trying to understand the mechanics of the local scour phenomenon, especially with respect to the vortex at the pier base, and thus provide a conceptual framework for functionally relating the equilibrium scour depth to the important hydraulic and other parameters of the problem.

2. Description of the Mechanics of Local Scour

Shen, et. al. gave a preliminary description of the local scour phenomenon, using a circular cylinder as a convenient example[110]. The cylinder, by the pressure field it induces, apprehends the vorticity normally present in the flow as it is swept towards the cylinder, and concentrates it near its leading surface. This process can also be described as vortex tubes collecting in front of the cylinder, and being bent and stretched around the cylinder. This process reaches a state of approximate equilibrium when the rate of dissipation of vorticity at the boundaries (the cylinder surface and neighbouring bed) equals the rate at

which vorticity enters the region.

The primary flow structure associated with this concentration of vorticity is the horseshoe vortex or horizontal roller which forms at the base of the pier, and it is the basic scouring agent. If the adverse pressure gradient induced by the pier is sufficiently strong, it causes separation of the three-dimensional boundary layer upstream of the pier. This separated boundary layer rolls up to form the horseshoe vortex system (see Figure 8). In addition, due to the mechanism described by Moore and Masch (see above), a downward flow exists near the cylinder leading surface.

The horseshoe vortex system is in general grossly unsteady, and can include a secondary vortex in addition to the primary vortex. It is the latter however which is mainly responsible for the scouring action. Scouring begins when the shear stresses at the periphery of the primary vortex reach the critical for sediment transport. Scouring is actually initiated somewhat downstream of the leading edge of the cylinder, in the region where the free stream velocity imposed on the vortex action is high.

Shen, et al. proposed a division of the local scour phenomenon into two basic cases: scour at blunt-nosed piers and scour at sharp-nosed piers. A blunt-nosed pier is defined as one which induces an adverse pressure gradient strong enough to cause the upstream boundary layer to separate and roll up to form the horseshoe vortex. A sharp-nosed pier is defined as one which lacks this property.

3. Theoretical Analysis

The theoretical treatment of the horseshoe vortex was done mainly by A.T. Roper, and is outlined below[110,113]. Consider a control volume (of small thickness) ABCD situated on the plane of symmetry (stagnation plane) in front of a circular cylinder in a uniform, steady flow in an open channel, as shown in Figure 9. The flow in this control volume is supposed to be two-dimensional.

The circulation, Γ, about the control volume ABCD is defined to be:

$$\Gamma = \oint \bar{V} \cdot \overline{ds} \qquad .....(24)$$

where $\bar{V}$ = the total velocity vector, and ds = an infinitesimal element of length along the boundary of ABCD. For the flow right at the solid boundaries AD and CD, the "no-slip" condition applies, ie. the flow velocity there is zero. Therefore the product $\bar{V} \cdot \overline{ds}$ along these boundaries is zero. Further, Roper specified that AB is far upstream of the pier in the region where the flow is not affected by the presence of the pier. Consequently, the vectors $\bar{V}$ and $\overline{ds}$ are at right angles to one another, and their dot product is zero. This leaves only one term remaining, and we get:

$$\Gamma = \int_B^C u\,dx \qquad .....(25)$$

This simplification is possible regardless of the shape of the bed, thus, expression (25) is valid even if a large scour hole is present. The right-hand-side of equation (25) can be evaluated if u is known along BC. The latter requirement can be satisfied if BC is specified to be

situated above the region where the velocity varies with depth (the shear layer), and also well below the free surface. The value of u along BC is given by potential flow theory for flow around a circular cylinder (with co-ordinates as shown in Figure 9) as:

$$u(x) = -u_o \left[1 - \frac{a^2}{(a+x)^2}\right] \qquad .....(26)$$

where $-u_o$ = the free stream velocity at point B, and a = the cylinder radius. Substituting this expression for u into the right-hand-side of equation (25), and evaluating the integral, we get:

$$\int_B^C udx = \int_{x=x_o}^{x=o} -u_o \left[1 - \frac{a^2}{(a+x)^2}\right] dx$$

$$= u_o x_o - u_o \left[a - \frac{a^2}{a+x_o}\right] \qquad .....(27)$$

Substituting this back into equation (25), and re-arranging:

$$\Gamma = u_o x_o - \frac{ax_o}{a+x_o} u_o \qquad .....(28)$$

If AB is specified to be far upstream of the pier, so that $x_o >> a$, then $(a + x_o) \simeq x_o$, and:

$$\frac{ax_o}{a+x_o} u_o \simeq au_o$$

so that equation (28) becomes;

$$\Gamma = u_o x_o - au_o \qquad .....(29)$$

For the undisturbed flow without a pier, the circulation $\Gamma = u_o x_o$.

Therefore, the net effect of the pier is to reduce the circulation by an amount:

$$\Delta \Gamma \text{ pier} = -au_o \qquad .....(30)$$

Roper assumed that the reduction in circulation due to the pier is proportional to the strength of the horseshoe vortex core. Roper further assumed that the horseshoe vortex core rotates as a rigid body, and that its strength can be represented by the term ωA_c where ω is the angular velocity, and A_c the area, of the vortex core. Expressing these assumptions in the form of an equation:

$$au_o \quad \alpha \quad (\omega A_c)_{core} \qquad .....(31)$$

Roper argued that since flow separation is a viscous effect, the kinematic viscosity of the fluid, ν, was an important variable. Incorporating this into equation (31), and replacing the pier radius, a, by the pier diameter, b, a non-dimensional relation is obtained:

$$\frac{\omega A_c}{\nu} = f\left[\frac{bu_o}{\nu}\right] \qquad .....(32)$$

The term on the right-hand-side of the equation is the Reynolds number based on the pier width, R_b, so that:

$$\frac{\omega A_c}{\nu} = f\,[R_b] \qquad .....(33)$$

Now, since the horseshoe vortex is supposed to be the primary agent causing scour, the depth of scour should be related to the strength of the vortex core. Thus:

$$d_{se} = f(R_b) \qquad .....(34)$$

where R_b = the pier Reynolds number, and d_{se} = the equilibrium depth of scour below normal bed level.

This analysis implies that the pier actually reduces the vorticity in the control volume. Further, the concentration of vorticity in the horseshoe vortex means that vorticity is reduced elsewhere. Such a reduction is in fact observed in the region between the separation line and the horseshoe vortex itself, where the flow is relatively quiescent.

4. Experimental Results

The experimental work carried out at Colorado State University confirmed the findings of previous studies in that the shape of the scour hole around a blunt-nosed pier approximates the frustum of an inverted cone, with its sides at about the angle of repose, and that the maximum depth occurs at the upstream edge of the pier. For sharp-nosed piers aligned with the flow direction, it was found that the maximum depth of scour occurred at the downstream end of the pier.

A qualitative representation of the flow patterns observed in the scour hole is shown in Figure 10[109,110]. The velocity profiles are proportional to the measured values. The dashed lines indicate the dominant flow features, which are in general not fixed but unsteady in nature.

Shen and his co-workers examined all the data available to them from the literature, but considered as useable only the data of Chabert and Engeldinger, besides their own, as all other data were either incomplete or were obtained from experimental arrangements and methods which differed in their significant details. These other data were however

used for purposes of comparison.

Shen plotted the useable data, for sands with $d_{50} \leq 0.52$ mm., in terms of the equilibrium scour depth (long-term average value), d_{se}, versus the pier Reynolds number, R_b, as shown in Figure 11[113]. This plot produced the relation:

$$d_{se} = 0.00073\ R_b^{0.619} \qquad .....(35)$$

which forms an approximate envelope for all the data. This relationship is supported by the other data mentioned above.

The scatter of the data arises not only from the differences between the various experimental arrangements and methods used, and inherent errors therin, but is due to the shortcomings of the analysis itself, as enumerated by Shen in the following points.

(a) For a given pier geometry and sand size, the curve of d_{se} versus R_b rises rapidly to some maximum, beyond which it falls off somewhat, as shown in Figure 12.

(b) The curve described in (a) differs for each pier, as shown in Figure 12.

(c) A different sand size also gives a different curve, even if the pier geometry is constant, as shown in Figure 13.

Shen et al. therefore recommended that equation (35) be used to estimate the equilibrium depth of scour for the "clear-water" scour case only. The result will be on the safe side. A caveat was added, however, in that the laboratory results haye to be extrapolated several orders of magnitude in order to apply to the much higher pier Reynolds numbers of prototype conditions. For the case of scour where there is general

bedload transport, Shen et al. recommended that either the relation proposed by Breusers:

$$d_{sem} = 1.4\ b \qquad .....(21)$$

or the one of Larras:

$$d_{sem} = 1.42\ K\ b^{0.75} \qquad .....(11)$$

be used to determine the maximum equilibrium depth of scour below normal bed level.

5. Reconciliation of Divergent Concepts.

The pier Reynolds number relation (equation 35) was further analyzed, and it was found that by assuming a uniform flow relation of the type:

$$U = K'H^{\epsilon} \qquad .....(36)$$

where K' and ϵ are constants, equation (35) could be transformed to an expression of a form similar to Laursen's equation (9), or an expression of the form:

$$\frac{d_{se}}{H} = C\ [F^2\ (\frac{b}{H})^3\ ]^m \qquad .....(37)$$

where C and m are constants, and F is the flow Froude number, $U/\sqrt{gh}$. Shen therefore concluded that arguments about whether the depth of flow or the average approach velocity of the flow is more important are of no great consequence, since the two parameters are related according to equation (36)[110].

6. Methods of Reducing Scour

Shen and his co-workers also carried out a number of experiments (apparently in the bed-load transport range only) to test various methods of reducing the depth of local scour around bridge piers, the results of which can be summarized as follows:

(a) Sharp-nosed piers were made by fastening noses, of included angle $\beta = 15^{\circ}$ and $\beta = 30^{\circ}$, onto a standard rectangular pier. The location, shape, and size of the scour hole were quite variable and no correlation with any of the usual parameters was evident, except that some of the variation seemed to be due to slight angles of attack effected by bed forms near the nose of the pier. For some runs, in which the upper regime plane-bed condition obtained, no scour at all occurred.

(b) Rectangular piers on a protruding, flat, pile-supported footing situated below normal bed level afforded reductions of between 0% and 55%, the higher values being achieved with higher velocities.

(c) An arrangement similar to (b) but with a vertical lip around the edge of the footing yielded reductions of the order of 40%-50%. When the footing and lip are situated low enough, the arrangement presumably traps the horseshoe vortex and prevents it from affecting the erodible bed.

(d) A rectangular pier with roughness elements attached to the front did not give any significant reductions in the scour depth; the vortex system seems to be merely displaced slightly upstream. The roughness elements may have been too close together to retard any downward flow in front of the pier.

(e) A cylinder of one-half the width of the rectangular pier was placed in front of the latter, and a maximum reduction of about 60% was achieved when the cylinder was placed a distance of about two cylinder diameters upstream of the rectangular pier.

(f) A cylinder split in the direction of flow (ie. half cylinders separated by a distance of from 1/3 to 2/3 the cylinder radius) gave reductions of the order of 25% to 40%. It was observed that the horse-shoe vortex, although still present, was weaker than for the solid cylinder.

L. CARSTENS

Carstens attacked the local scour problem by separating the fluid, sediment, and flow parameters from the geometric variables[20]. A theoretical analysis of the forces acting on a typical bed particle, assuming a negligibly thin boundary layer, yielded a ratio of disturbing force, F_M, to retarding force, F_R, of:

$$\frac{F_M}{F_R} = f\,(\text{sediment particle geometry})\, N_s^{\,2} \qquad .....(38)$$

where $N_s = \dfrac{U''}{\sqrt{(s-1)g\, d_g}}$, the "sediment number." In the later, s = the sediment specific gravity, and d_g = the characteristic sediment grain diameter. For the case of clear water scour ($Q_{s\ in} = 0$), the rate of sediment transport out of the scour area, $Q_{s\ out}$, was assumed to be a function of the force ratio and the geometry of the situation. Thus a non-dimensional sediment transport function was hypothesized:

$$\frac{Q_{s\ out}}{u\ W_s d_g} = f[(N_s^2 - N_{sc}^2), \frac{d_s}{L}, \text{obstruction geometry, sediment particle geometry}] \quad .....(39)$$

where W_s = the scour hole width, L = a characteristic length of the obstruction, N_{sc} = the critical sediment number at which local scour is initiated, u = a reference velocity, and d_s = the scour depth below normal bed level.

Approximating the scour hole shape at a circular cylinder of diameter b by the frustum of an inverted cone of base diameter b and side slope equal to the angle of repose, ϕ, Carstens rewrites equation (8) as:

$$Q_{s\ out} = \frac{dV}{dt} = \frac{\pi}{\tan\phi}\left(\frac{d_s}{\tan\phi} + b\right)d_s \frac{d}{dt}(d_s) \quad .....(40)$$

Selecting the data of run 204 from Chabert and Engeldinger, and defining u = U, the average approach flow velocity, L = b, the pier diameter, and $W_s = b + 2(d_s/\tan\phi)$, Carstens constructs a plot of:

$$\frac{Q_{s\ out}/U(b + \frac{2\ d_s}{\tan\phi})\ d_g}{(N_s^2 - N_{sc}^2)^{5/2}} \quad \text{vs.} \quad \frac{d_s}{b},$$

the index 5/2 of the term $(N_s^2 - N_{sc}^2)$ having been obtained from experiments of Le Feuvre, who studied sediment transport rates out of a rigid-boundary depression in a closed conduit. This plot gave:

$$\frac{Q_{s\ out}}{U(b + \frac{2\ d_s}{\tan\phi})d_g} = 1.3\ 10^{-5}\ (N_s^2 - N_{sc}^2)^{5/2} \left(\frac{d_s}{b}\right)^{-3} \quad .....(41)$$

Equation (41) can be substituted into (40), and the result integrated, to yield an expression for scour depth with time. This expression shows that the scour depth increases continually with time, and although the rate of increase decreases, an equilibrium scour depth is never attained.

M. TANAKA AND YANO, AND THOMAS

1. Tanaka and Yano

Tanaka and Yano report a laboratory study involving the effect, on local scour, of various devices and modifications in conjunction with a circular cylinder[118]. They considered that the horseshoe vortex is generated by a combination of main flow separation upstream of the cylinder and the secondary downward flow along the front of the cylinder, and that the magnitude of local scour depended on the strength and size of the vortex.

The experimental arrangement consisted of a 30 cm. wide flume, with a bed sand of d_{50} = 0.4 mm. and a flow depth of 10 cm. Flow conditions were arranged to just obtain slight ripples on the bed, and were the same for all tests. The velocity distribution was measured at the test location and is shown in Figure 14. The basic pier used was a circular cylinder of 3 cm. diameter. The different types tested are listed below and are also illustrated shcematically in Figure 15.

(a) Type I: a normal cylinder extending to above the water surface.

(b) Type II: a cylinder with a hole 1 cm. square or 2 cm. square cut in the direction of the main flow.

(c) Type III: a cylinder fitted with a circular disc of diameter B_d = 9 cm., 12 cm., or 18 cm.

(d) Type IV: a cylinder submerged below the water surface.

(e) Type V: a cylinder floating above the normal bed surface.

The positions of the modifications of the type II and type III piers, and the top of the type IV, and bottom of the type V piers, were varied. The experimental results are summarized in Figure 16.

Tanaka and Yano noted that the effect of the discs was pronounced only within the boundary layer (δ = 5 cm.), and that the size of the disc (when placed at bed level) required to completely eliminate scour was of the order of the boundary layer thickness. They therefore concluded that the size of the vortex is related to the boundary layer thickness, especially since the vortex is a boundary layer effect. Thus, they argued that the effect of the pier modifications can be validly represented in terms of an expression of the form:

$$\text{scour hole size} = f\left(\frac{h}{\delta}\right) \qquad .....(42)$$

where h = the height of the modification above normal bed level, and δ = the boundary layer thickness.

Tanaka and Yano considered the vertical downflow in front of the pier to have little effect on local scour, for their experimental conditions.

2. Thomas

Thomas reports a study of the effect of a disc fitted around a circular cylinder, similar to Tanaka and Yano's type III[124]. He used discs of 10 cm. and 15 cm. diameters around a 5 cm. diameter pier, placed

in a flume 35 cm. wide. His results, shown in Figure 17, are not strictly comparable because he used a scour depth equal to the arithmetical average of the scour at the cylinder quarter points: front, back, and two sides. Further, no information is given with respect to the flow conditions, and the scour depth for the normal cylinder is not stated.

N. SCHNEIDER

Schneider, one of Shen's co-workers at Colorado State University, recently completed a doctoral dissertation on the mechanics of local scour[106]. In it, he gives a description of the mechanics of local scour, based on the accumulated information of previous studies, as well as an outline of the more important concepts and relations proposed by previous investigators. His own theoretical work was mainly directed towards formulating a relation for local scour based on the sediment continuity equation (equation (8)), and his experimental work consisted largely of determining sediment transport rates out of the scour hole. Other considerations included the effect of constriction of the flow, unsteadiness of the horseshoe vortex, design criteria, and safety factors.

Making the same assumption as Carstens with respect to the scour hole shape (see above), but transforming the rate of change of scour hole volume to the rate at which solids are removed, an expression similar to equation (40) is obtained;

$$Q_s' = \frac{\pi(1-\lambda)\rho_s g}{\tan\phi}\left[\frac{d_s^2}{\tan\phi} + bd_s\right]\frac{d}{dt}(d_s) \qquad .....(43)$$

where Q_s' = the rate at which the scour hole is deepened, in terms of weight of solids removed per unit time, λ = the void ratio of the sediment in the scour hole, and ρ_s = the sediment density. Equation (8) can then be expressed as:

$$\frac{dV}{dt}(1-\lambda)\rho_s g = Q_s' = Q_s'_{out} - Q_s'_{in} \qquad .....(44)$$

where $Q_s'_{out}$ = the time rate of sediment transport out of the scour hole (by weight), and $Q_s'_{in}$ = the time rate of sediment transport into the scour hole (by weight).

Schneider assumed that the value of Q_s' could be sufficiently well described by an exponential decay function of the initial value, Q_{si}':

$$Q_s' = Q_{si}' \; e^{-t/tc} \qquad .....(45)$$

where t_c = a time constant. Schneider further thought that $Q_s'_{in}$, rather than have it vary with scour hole size, could best be represented by the constant value given by the rate of transport coming in across a width equal to the pier width, ie. $Q_s'_{in} = q_s'_{in}\, b$. Equation (45) is thus divided by the pier width and then substituted into equation (43), which, when integrated, yields:

$$(\frac{d_s}{b})^3 + \frac{3}{2}(\frac{d_s}{b})^2 \tan\phi = X\,[1-e^{-t/t_c}] \qquad .....(46)$$

where $X = \dfrac{3Q'_{si}\, t_c \tan^2\phi}{\pi(1-\lambda)\rho_s g\, b^3}$. As time becomes large (ie. $t >> t_c$) equation (46) becomes:

$$(\frac{d_{se}}{b})^3 + \frac{3}{2}(\frac{d_{se}}{b})^2 \tan\phi = X \qquad .....(47)$$

This equation implies that for a given pier size and given sediment characteristics, the equilibrium scour depth depends only on the time constant and the initial rate of removal of sediment from the scour hole. The time constant is determined by combining equations (47) and (46) for $t = t_c$, and was found to be the time required for the ratio d_s/d_{se} to reach a value from 0.796 to 0.858, depending on the relative importance of d_{se}/b and $\tan\phi$. The value of t_c can thus be estimated from d_s versus t curves. Schneider decided to determine Q_{si}' by measuring $Q_s'_{out}$ in the laboratory and relating the former to the latter by means of equations (44) and (45). Since these measurements were made for the initial flat-bed condition, the exponential time term reduces to unity, and the value of t_c is not required in order to obtain Q_{si}'. Values of $Q_s'_{in}$ were obtained from existing data for sediment transport in flumes.

Schneider's measurements of $Q_s'_{out}$ yielded a relation:

$$\frac{Q_s'_{out}}{b} = 0.0754(U-U_c)^3 \qquad .....(48)$$

where U_c = the average approach flow velocity at which local scour is just initiated. This velocity was estimated to be equal to about 0.4 ft./sec., based on Knezevic's data (see above). The data did not display any systematic scatter with respect to sediment size, pier width, or position of sediment feeding device. Values of $q'_{s\ in}$ were observed to be about one order of magnitude lower than values of $Q_s'_{out}/b$ (at the initial flat-bed condition), for most flow conditions tested (ie. low velocities).

The time constant t_c was determined from data of Chabert and Engeldinger, and Shen, et. al.,[113] and plotted as graphs of $1/t_c$ versus U. Significant correlation with pier diameter is also evident, although the influence of sediment size is not clear. A comparison of measured values of t_c with values calculated from the known data, using equations (48), (44), (45), and (47), shows fair agreement, although a definite scatter is evident for higher values of t_c, with the calculated values being mostly lower than the actual measured values. Predicted scour depths based on the calculated values would thus tend to be greater than those that would actually occur.

One of the more interesting results of Schneider's work involves the well-known observation that in the region of scour with general bed-load transport, the equilibrium scour depth is independent of the velocity U (see Figure 3). A constant scour depth implies a constant value of the product $(Q_{si}' \cdot t_c)$, by equation (46). However, it has been noted that at initial conditions, at least for velocities of about two feet per second or less, $Q_{si}' \simeq Q_s'_{out}$, since $Q_s'_{in} \leq 10\%$ of $Q_s'_{out}$. Thus changes in initial values of $Q_s'_{out}$ (due to changes in velocity) are almost completely balanced by changes in t_c, and the actual incoming sediment supply has only a small effect on the equilibrium scour depth. The development of general sediment transport is thus not the true basis for the flattening of the d_{se} versus U curve; rather, it seems to be based on the mechanics of the vortex itself.

Schneider therefore proposed a separation of the local scour phenomenon into two regions. The first region, where the equilibrium

scour depth increases with velocity, he called the "vortex-bed-interaction-limited depth of scour region", since the equilibrium scour depth is limited by the shear stress that the vortex can exert on the bed. The flat region of the curve he called the "vortex-mechanics-limited depth of scour region", since the equilibrium scour depth is limited by the inherent inability of the vortex to penetrate below a certain depth. The equilibrium scour depth in this latter region can be affected somewhat by the incoming sediment transport. The two scour regions are shown schematically in Figure 18. This finding modifies the result of Chabert and Engeldinger as given in Figure 3.

O. COLEMAN

Coleman reports the results of analyzing laboratory data of H.W. Shen and of himself[28]. He obtained several groups of variables by dimensional analysis, and then used the experimental data to obtain a relationship between them. He got an expression for equilibrium depth of scour as follows:

$$d_{se} = 1.49\ b^{9/10}\ \left(\frac{U^2}{2g}\right)^{1/10} \qquad \ldots\ldots(49)$$

NOTES TO CHAPTER II

1. Timonoff[126] refers to studies by Minard (1856) and Durand-Claye (1873), but cites no specific works for these.
2. Reported in Karaki and Haynie[51].
3. Reported in Karaki and Haynie[51]. Some presentation of this work by Inglis can be found (inter alia) in Arunachalam,[4] Chitale[23], Inglis[42], Joglekar[46], and Thomas[121].
4. This condition corresponds to the condition of "clear-water" scour, just below the threshold of general sediment transport, as outlined by Laursen.
5. Sediment transport rates are here defined in terms of volume, in order to make the equation dimensionally homogeneous. Void ratios would have to be allowed for.
6. The term "clear-water" does not imply that visibility is good, but indicates only that there is no transport of bed sediment.
7. Reported in Karaki and Haynie, ref. 191.
8. Median grain diameter = d_{50} = the grain size such that 50% of the material (by weight) is finer.
9. Reported by Shen, et al.[113].
10. Reported by Shen, et al.[113], and Neill[83].
11. This idea had already been tested by Schneible, as reported in Laursen and Toch[61].
12. Tison seems to have been the first to suggest and test this method. He understood the auxiliary pile to reduce the curvature of the flow and thus reduce scour.

CHAPTER III

THE MECHANICS OF LOCAL SCOUR

A. INTRODUCTION

The purpose of this chapter is to arrive at an understanding of the mechanics of local scour, based on observations and findings of previous investigations and experiments as summarized in Chapter II, and on the results of other studies, notably those in the field of fluid dynamics. Such an understanding should then provide some basis for assessing the validity of the various hypotheses and methods of analysis of the local scour phenomenon, and also suggest some guidelines for further study.

B. THE BASIC VORTEX MECHANISM

There can be little doubt that the basic mechanism of local scour is the horizontal roller or vortex, shaped like a horseshoe in plan, that forms on the bed directly in front of a pier. This vortex, due to the high velocity at which it rotates, exerts shear stresses on the bed that are greater than the critical shear stress for transport of the bed-sand. Consequently, bed sand is moved away from the pier, and a scour hole develops.

The horseshoe vortex has been observed and reported by many investigators, including Posey[93, 95], Laursen[59, 61], Moore and Masch [80], Maza and Sanchez[79], Shen *et al.*[109, 110, 113], Tanaka and Yano[118], and Schneider[106]. Shen, Schneider, and Tanaka and Yano in particular, have recognized the importance of the vortex, and in their analyses have considered the vortex mechanism.

Any attempt to understand or explain local scour without taking into account this basic vortex mechanism is doomed to fail from the very outset. Thus, an approach like that of Tarapore (see section II. G above), which is based on potential flow theory and a concept of the free stream flow diffusing into the scour hole, can never lead to a proper understanding of the local scour phenomenon (although his experimental results remain valid in themselves). Similarly, the theoretical analyses of Tison and Ishihara (section II. B) and Carstens (section II. L) are misleading.

C. ORIGIN OF THE HORSESHOE VORTEX

1. Vorticity

Basically, the horseshoe vortex originates out of the vorticity which is always present in shear flows, that is, flows in which a velocity gradient exists.

A shear flow may be visualized as consisting of thin layers of fluid, with each layer moving at a slightly different velocity than the adjacent layers. This differential movement results in the sliding or shearing of adjacent layers over each other, and in so doing causes a rotation of the fluid particles on the plane of sliding. Vorticity represents the rate of rotation or the angular velocity of these fluid particles.

A line drawn through the fluid so that it everywhere corresponds to the local axis of rotation of the fluid particles is called a vortex line. If adgacent vortex lines are joined together to form a surface, the result is a vortex tube. The fluid within this tube is called a vortex tube or filament, or simply a vortex.

Mathematically, vorticity is a vector, and is expressed as:

$$\bar{\Omega} = \bar{\nabla} \times \bar{v} \qquad \ldots.(50)$$

Expressed in terms of orthogonal components, this becomes:

$$\Omega_x = \frac{\partial v_z}{\partial y} - \frac{\partial v_y}{\partial z} \qquad \ldots.(51)$$

$$\Omega_y = \frac{\partial v_x}{\partial z} - \frac{\partial v_z}{\partial x} \qquad \ldots.(52)$$

$$\Omega_z = \frac{\partial v_y}{\partial x} - \frac{\partial v_x}{\partial y} \qquad \ldots.(53)$$

A theorem (due to Helmholtz and Kelvin) states that for any given vortex, the product of the vorticity and the cross-sectional area of the vortex must remain constant. An important consequence of this theorem is that vortex lines cannot begin or end anywhere within the fluid itself, but must either form closed loops or terminate at the flow boundaries. Another theorem states that vortex lines move with the fluid. An excellent description of the characteristics of vorticity has been presented by Lighthill[71].

2. Vorticity in the Flow near a Cylinder

Consider the case of a uniform steady flow in an open channel, past a vertical cylinder located in the middle of the channel, with the x-direction in the direction of flow, the y-direction across the direction of flow, and the z-direction along the vertical.

(a) The Approach Flow

Consider first the approach flow upstream of the cylinder in the central part of the channel, where neither the cylinder itself nor the side walls have any effect (ie. a two-dimensional flow). The velocity of this flow has an x-component only (v_x). Also, a velocity gradient exists only in the vertical or z-direction, due to the frictional drag of the bed of the channel. The total vorticity of the flow, as expressed by equations 51 to 53, is therefore reduced to a single term:

$$\Omega_y = \frac{\partial v_x}{\partial z} \qquad \ldots.(54)$$

The vorticity appears in the flow as vortex tubes or filaments, with axes of rotation aligned in the y-direction, all parallel to one another.

The vortex tubes are concentrated at the bottom of the flow, near the bed, in the region where the velocity gradient is high. Since the flow being considered is steady and uniform, the distribution of the vorticity within the flow (the vorticity field) does not change in the downstream direction, and the rate at which vorticity is being produced is just equalled by the rate at which it is being dissipated.

(b) Flow near the Cylinder

As the flow from upstream approaches the cylinder it divides to pass around it, and each vortex tube, being carried downstream by the flow, is stretched as the streamlines diverge. This stretching begins somewhat upstream of the nose of the cylinder due to the cylinder-induced pressure field (blunt-nosed cylinders inducing a stronger pressure field and thus affecting the flow farther upstream, than sharp-nosed ones). This stretching reduces the cross-section of each vortex tube so that the vorticity increases.

As the flow passes around the cylinder, the vortex tubes are also bent around the cylinder, and actually become trapped or caught in front of the cylinder, since vortex tubes cannot be cut even by a sharp front. Thus not only do the vortex tubes continue to stretch and increase in vorticity, but new ones are constantly being added from upstream. This process results in intense vorticity and vortex motion at the front and sides of the cylinder. However, the vorticity does not increase without limit, since viscous and turbulence effects cause the diffusion and convection of vorticity to take place[99,110].

The process of vorticity intensification by stretching and accumulation, together with viscous and turbulence effects, accounts for the origin

and formation of the horseshoe vortex system, and, as such, accounts qualitatively for all scour at cylinder noses, since no other mechanism exists for the transport of sediment in this region.

D. CHARACTERISTICS OF THE HORSESHOE VORTEX

1. Structure

The horseshoe vortex is not just a simple and solitary horizontal vortex that forms at the nose of a cylinder or pier in open-channel flow, but actually consists of a number of linked vortices that operate together to scour the bed around the pier.

Shen et al.[110] observed a secondary "counter" vortex as shown in Figures 8 and 10. Thwaites[125] presents a photograph of an experiment by Gregory and Walker, of a cylinder in a laminar boundary layer, which shows at least three vortices. This has been sketched in Figure 19. Rainbird et al. report the same structure as this, but with still another vortex upstream of the other three[96]. Roper[101] reports three vortices, as does Thwaites, above, although his proposed sequence of vortex formation and shedding is in error.

2. Formation

The actual formation of the horseshoe vortex system occurs as follows. The adverse pressure gradient generated by the cylinder causes the approach flow to slow down and, due to the velocity gradient in the vertical direction, to acquire a downward component in front of the cylinder. Qualitatively, this is the mechanism described by Bata (section II. F) and Moore and Masch (section II. H), although their

quantitative analyses, based on two-dimensional inviscid flow, are not valid.

This downward flow in turn induces a flow in the upstream direction along the bed in front of the pier nose, with subsequent flow separation upstream of the pier. A large horizontal vortex is thus induced, which, by viscous interaction with the boundaries and the approach flow, generates yet other vortices.

Another way of describing what happens is to say that the adverse pressure gradient induced by the pier causes the separation and rolling-up of the boundary layer in front of the pier to form the horseshoe vortex system. The horseshoe vortex system is thus also seen to be the area of concentration of the vorticity present in the boundary layer of the approach flow. This is supported by Thwaites[125] and Bolcs[14], who both state that the horseshoe vortex system is constantly being replenished by fluid from upstream.

3. Strength

The action of local scour at a bridge pier can be divided into two parts:

(a) the resistance of the channel bed to scour.

(b) the scouring strength or power of the vortex.

For non-cohesive material, the bed resistance depends only on the grain characteristics of the bed sediment, and thus constitutes a minor part of the analysis. The major part in understanding local scour has to do with discovering the factors that influence the vortex. Any procedure that attempts to relate flow parameters directly to scour depth, without

considering the intermediary role of the vortex, can at best give only a partial understanding of the scouring process, even though it may yield a relationship valid for the conditions for which it was derived. The works of Inglis, Blench, Varzeliotis, Knezevic, Breusers, and Coleman (see Chapter II) all fall into this category.

The strength of the horseshoe vortex system will be influenced by the parameters that govern the generation of vorticity in the approach flow, the concentration and distribution of vorticity around the pier, the dissipation of vorticity at the flow boundaries, and its convection downstream past the pier. These parameters, for the case of a single pier in a wide channel, can be listed as follows:

(a) The average velocity of the approach flow.

(b) The velocity gradient of the approach flow.

(c) The pier geometry (size and shape).

(d) The scour hole geometry.

(e) The kinematic viscosity of the fluid.

The influences of most of these parameters on the maximum depth of scour have been studied by previous investigators.

The influence of the approach flow velocity has been studied by various researchers, notably Laursen[60,61], and Chabert and Engeldinger (see section II. E above).

The influence of pier size has been studied by most researchers in the field. Again, Laursen is one of the chief contributors in this area, having also studied the effect of the shape of the pier. Hawthorne[39] has shown analytically that the shape of the pier is significant.

The scour hole geometry affects only the instantaneous vortex strength, and not the final maximum scour depth. As scour progresses, the scour hole becomes larger and deeper, and the horseshoe vortex system, expanding with the scour hole, becomes weaker. This process continues until the vortex strength falls to a level such that the rate of sediment transport out of the scour hole is just equal to the rate of sediment transport into the scour hole, and a limiting equilibrium depth of scour is reached.

The kinematic viscosity of the fluid is of importance in the generation and dissipation of vorticity and in determining the magnitude of shear stresses in the flow. It is governed by the temperature of the fluid. Shen et al. recorded the temperature in their test runs[111] and included viscosity as an implicit variable in their analysis[110].

With the exception of Tison (see following paragraph), the vertical velocity gradient of the approach flow has, to the author's knowledge never been explicitly studied in connection with local scour at bridge piers. It must, however, have some influence, because it is important in the generation of vorticity and the formation of the horseshoe vortex system. Vinjé has suggested[136] that the velocity distribution of the approach flow is important, as has Ahmad[2].

Tison did some experiments in which he varied the velocity distribution by changing the bed roughness (see section II. B above). However he did not recognize the horseshoe vortex mechanism, and his results have qualitative value only.

Depth of flow has not been listed explicitly as a parameter influencing the vortex strength, because this is included in the velocity

distribution of the flow. Various researchers have studied the influence of flow depth on the maximum depth of scour, Laursen again being foremost among them. The overall result of these investigations is that the depth of flow is not important except for small depths. This suggests that the flow depth is not important except when it affects the velocity profile in the boundary layer of the approach flow.

Shen et al. have attempted to derive an expression for the horseshoe vortex strength based on the concept of vorticity (see section II. K above). They postulated that two-dimensional flow analysis is valid for the flow in the plane of symmetry in front of the cylinder. However, this must be considered as questionable, since, as Johnson points out[50], this plane of symmetry is entirely immersed in a three-dimensional flow field.

E. SUGGESTED RESEARCH

From the foregoing discussion, it is evident that there has been little investigation of the influence of the vertical velocity distribution of the approach flow on the mechanics of local scour, although a definite connection can be shown to exist, from basic principles of fluid dynamics. It was therefore decided to investigate this connection, in a preliminary and qualitative way.

CHAPTER IV

EXPERIMENTAL WORK

A. PURPOSE AND SCOPE

The main purpose of the experimental work was to investigate, in a preliminary and qualitative way, the influence of the velocity distribution of the approach flow on the local scour around a cylinder, particularly the horseshoe vortex system and the equilibrium scour depth.

The experiments consisted of observations and measurements of flow velocities, scour depths, and flow patterns.

In these tests, the only parameters which were deliberately varied were the velocity profile of the approach flow and the average flow velocity. The other parameters, such as sand size, pier size, pier shape and so on, were held constant, except the flow depth, which varied

slightly with the average flow velocity, and the water temperature which varied from 56°F to 68°F.

B. EQUIPMENT AND EXPERIMENTAL ARRANGEMENT

1. General Arrangement

The experimental work was carried out in a forty-foot-long steel and glass flume in the Civil Engineering Hydraulics Laboratory at the University of British Columbia. The flume was three feet deep and two and one-half feet wide, and consisted of basically three sections: a fifteen-foot steel approach section, a fifteen-foot glass-walled test section, and a ten-foot steel end section (see Figure 20).

Inflows to the flume were provided by a recirculating system in which water from a sump was pumped up to a constant-head supply tank. Discharges from the tank were controlled by a valve in the flume inlet line, and were measured by a mercury manometer connected across an orifice plate located upstream of the valve. The discharge calibration curve for the orifice plate was obtained and checked using two large weighing tanks (20,000 lbs. each) in which the flume discharge, over a given time interval, could be collected and weighed.

The water depth in the flume was regulated by an adjustable vertical overflow gate at the downstream end of the flume.

In the approach section were placed two sets of double metal-grid screens and a set of vanes to straighten the flow, as well as a platform float to suppress wave action and surface disturbances.

2. Sand Bed

A sand bed twelve inches deep was placed over the entire fifteen-foot length of the glass-walled section of the flume. Bed transition sections were constructed out of plywood and sheet metal to provide smooth, gradual transitions between the flume bottom and the surface of the sand bed at each end (see figure 20). In this way the flow was guided parallel to the sand bed without unnecessary and undesirable turbulence.

The same sand was used for all the tests, and had a grain size distribution as shown in Figure 21. The median grain size was 0.215 mm. The standard deviation σ, defined by:

$$\sigma = \frac{1}{2}\left(\frac{d_{84}}{d_{50}} + \frac{d_{50}}{d_{16}}\right) \qquad \ldots.(55)$$

was equal to 1.33.

The sand was obtained from stockpiles of material dredged from the Fraser River, B.C. Occasional pebbles and fragments of wood had to be screened out before placement in the flume.

3. Test Pier

The pier used in the tests was a hollow circular cylinder of clear plexiglass, of four inches outside diameter, which extended from the bottom to the top of the flume. The pier was positioned in the center of the flume as shown in Figure 20, and midway between the two sides. Its bottom end was prevented from shifting by sliding it onto a circular disc fixed to the flume bottom. The top end fitted into a V-shaped notch in a board which

was secured across the top of the flume, preventing movement of the pier in the downstream direction. This arrangement also permitted rotation of the pier.

The scour depth below local bed level could be read at any time by a scale, graduated in hundredths of a foot, which was attached to the inside surface of the pier. A 150-watt floodlamp shining through the glass wall of the flume was used to illuminate the scour hole area, and facilitated reading of the scale.

4. Velocity-Distribution Control Gate

A velocity-distribution control gate was placed 2½ feet upstream of the nose of the pier. This gate consisted of spaced 3/8-inch-diameter aluminium rods extending horizontally across the flume, and secured at each end between two narrow aluminum bars, one of which had a rubber strip attached to its inside surface to prevent slippage. These bars could be either tightened, to clamp the rods in place, or loosened, to allow the spacing of the rods to be easily changed. Figure 22 shows a view of the control gate from a position downstream of the pier (the image of the gate is reflected by the glass walls of the flume).

5. Current Flowmeter

Velocity measurements were made with an Armstrong-Whitworth Miniature Current Flowmeter (Type 176/1). The measuring head, located at the end of an 18-inch probe, had a protective cage 1.5 cm. in diameter, and basically consisted of a five-bladed plastic rotor mounted on a hard stainless steel spindle. The spindle terminated in fine burnished conical pivots which ran in jewels mounted in an open steel frame. The pivots and

jewels were shrouded to reduce the possibility of fouling. The revolutions of the rotor were counted on three Dekatron counters over a period of 8.33 seconds. The count was displayed for 6.67 seconds, and 1.67 seconds were required after that for a new count to begin. The velocity was read from a calibration curve which related the count to the local flow velocity.

A traversing mechanism enabled the measuring head to be positioned anywhere in the flow.

Since the flowmeter required a conducting liquid in order to function properly, a small amount of sodium silicate solution was added to the laboratory water supply.

6. Dye Injector

A simple dye injector was made by bending the lower four inches of a section of thin glass tubing at right angles to the main stem to form a horizontal leg. This leg was then stretched at the tip, using a Buntzen burner, to form a fine nozzle. The nozzle could be positioned anywhere in the flow, and aligned in any direction, by a simple traversing mechanism built out of wood.

C. EXPERIMENTAL METHODS AND PROCEDURES

1. Starting-up

With the flume initially dry, the sand bed was carefully levelled. Then, with the desired depth set by the vertical overflow gate at the end of the flume, the flume was slowly filled from both ends so that the sand bed would not be disturbed. The flume inlet valve was

then opened rapidly to the desired discharge, and the stop-watch started. This procedure resulted in a rapid but smooth rise to the desired discharge, and did not produce any irregular disturbing waves.

2. Generation of Vertical Velocity Profiles

Different vertical velocity profiles were generated by the velocity-distribution control gate, by varying the number and spacing of the individual bars of the gate. The gate setting for each velocity profile used in the test runs was determined in preliminary tests by trial and error.

The velocity-distribution control gate was located 2½ feet upstream of the front face of the test pier. This distance was selected as a compromise between two conflicting considerations. On the one hand, the gate had to be placed far enough upstream so that the local disturbance in the flow, caused by the individual bars of the gate, would be dissipated, and, on the other hand, the gate had to be placed near enough so that the velocity profile created by the gate would not decay appreciably before it reached the pier.

The head drop across the gate was quite small, being of the order of a hundredth of a foot or less.

3. Velocity Measurements

Velocity measurements were made with the Armstrong-Whitworth Miniature Current Flowmeter. Its calibration was carefully checked with a miniature Ott propeller meter which had just been factory-calibrated. All velocity measurements were made on the centerline of the flume. In

general, measurements were made at 0.05-foot intervals vertically over the entire depth, except that the measurement nearest the bed was made 0.02 feet above the bed. Each measurement consisted of taking the average of five consecutive readings of the flowmeter, each reading itself being integrated over 8.33 seconds, with 8.33 seconds elapsing between each reading, as described in Section B.5 above.

A horizontal traverse across the flume two feet upstream of the pier was made to determine the horizontal velocity profile.

In general, for each test, the vertical velocity profile was measured in the first hour or so of the test run, at a distance of 1.5 feet upstream of the pier face. After all the test runs had been completed and the pier removed, the velocity profile for each test series was measured at the location of the pier centerline in order to check the stability of the profile.

4. Flow Patterns

Flow patterns in the scour hole and around the pier were studied with the aid of dye, which was introduced into the flow at the desired location with the dye injector. The discharge of the dye was controlled so that it did not disturb the flow.

The flow patterns so observed were recorded by making on-the-spot freehand sketches. Photographs of the flow patterns were not made, partly due to oversight on the part of the author in the early stages of the work, and partly due to technical difficulties which arose subsequently.

5. Scour Hole Development and Equilibrium Depth of Scour

The depth of scour below the bed level could be measured at any time by the graduated scale attached to the inside of the pier (which could be rotated in any direction). Scour depths were recorded for each test run, at regular intervals, so that the scour hole development with time, of different tests, could be compared.

Each reported test run was continued until there was no longer any increase of scour depth with time, and this final scour depth was taken to be the equilibrium scour depth for the conditions of that test run.

As the scour hole developed, it was observed that occasional coarser particles were left behind in the scour hole to produce an armouring effect. When this occurred, the flow was momentarily stopped and the offending particles carefully removed.

The visibility in the test arrangement permitted a completely unobstructed view of the scouring process. The motion of the individual sand grains out of the scour hole was especially noted, and sketches were made to record these observations.

CHAPTER V

EXPERIMENTAL RESULTS

A. GENERAL

The experimental results consist of the following data:

1. Observations of scour depth at periodic intervals during the development of the scour hole, and the final equilibrium scour depth, for each of various average velocities and vertical velocity distributions of the approach flow.
2. Observations of the development of the scour hole, the scouring process, and the motion of the individual sand grains in and out of the scour hole.
3. Observations of the vortex patterns in the scour hole for various stages of scour hole development.

These results are described and discussed below.

B. APPROACH FLOW VELOCITY PROFILES

Eight different vertical velocity profiles were tested: series 1, 2-A, 2-B, 2-C, 2-D, 3, 4, and 5. Series I was tested at three different average velocities; series 3 and 4 were each tested at two different average velocities. Series 2-A was tested three different times at the same average velocity. The velocity profiles for all the tests are shown in Figures 23 to 27, inclusive.

There was some unsteadiness inherent in the approach flow. Repeated velocity measurements with the Armstrong-Whitworth flow meter at any one spot in the flow usually gave velocity variations of two or three per cent, and sometimes as much as five per cent, especially near the bed.

The velocity profiles of series 1 were the ones which occurred naturally in the flume without the velocity-distribution control gate, while the profiles of the other seven test series were artificially generated by the gate. All of the profiles generated by the gate tended to decay into the natural profile of series 1. It was not possible to test very steep velocity gradients, as these were difficult to generate, and moreover they decayed too rapidly while approaching the pier.

Figure 28 shows the stability of the natural profile of series 1-A. The profile was measured at a location 1.5 feet upstream of the pier (with the pier in place), and then at the pier center-line (with the pier removed). The greatest difference between the two measurements is about five per cent, which is within the range of unsteadiness of the approach flow.

Figure 29 shows the extent of the decay of the profile of series 2-A3, from 1.5 feet upstream of the pier, to the location of the pier center-line. The shift towards the natural (series 1) velocity profile is quite evident, and is representative of the behaviour of the other velocity profiles tested. This instability prevented any quantitative analysis of the influence of the approach flow velocity gradient from being carried out.

The experiments were designed to run within the "clear-water" scour range - ie. scour with no sediment transport of the sand bed in general (see above, section II. D). This was done so that the development of the scour hole and the final equilibrium value of the scour depth would not be obscured by general sediment transport with ripples or dunes moving through the scour hole. It also simplified the experimental procedure. Therefore, the average velocities used for the various tests were all less than the critical velocity for general sediment transport of the sand bed ($U_{crit.}$).

The critical velocity for general sediment transport was determined to be about 0.90 ft/sec. At this velocity, small ripples started to form on the sand bed of the flume. The actual velocities used in the experiments varied from 0.65 ft./sec. to 0.89 ft./sec.

C. EQUILIBRIUM SCOUR DEPTH

1. Introduction

The equilibrium scour depth, d_{se}, is defined as the scour depth at which, for given conditions of pier and channel geometry and flow

conditions, the rate of sediment transport out of the scour hole equals the rate of sediment transport into the scour hole. In the case of "clear-water" scour, both of these transport terms equal zero for the equilibrium condition.

For each test run, the depth of scour was measured at regular intervals, starting from the beginning of each test at t = 0, until there was no longer any increase of scour depth with time. This final value was taken to be the equilibrium scour depth, d_{se}. The time at which this depth was first reached is called t_{se}. The scour depth measurements have been plotted in Figures 30 to 35, inclusive.

Occasionally, larger particles would become uncovered in the scour hole as it deepened. When this happened the flow was momentarily stopped and the larger particles were carefully removed to prevent armouring. These occasions show up as uneven segments in the plots of scour depth versus time.

A comprehensive summary of the test data is given in Table III.

2. Results

The accuracy of the results is indicated by the results for the three different runs of series 2-A (see Figures 24 and 31). Within the limits of accuracy of the measuring equipment used, the flow conditions for these runs were all the same. The resulting equilibrium scour depths, however, were measured to be 0.37, 0.36, and 0.38 feet, a variation of about 5 per cent. The inherent experimental error is therefore considered to be at least 5 per cent.

A comparison of the results for the various vertical velocity profiles and range of average flow velocities tested, leads to the following observations;

(a) For any given velocity profile, d_{se} increases with increasing average flow velocity. This is clearly demonstrated by the results for series 1, 3, and 4. In each of these series, a higher average flow velocity resulted in a larger equilibrium scour depth.

(b) The velocity of the lower part of the flow, near the bed, is more important, in determining d_{se}, then the velocity of the upper part of the flow. Series 3-B and 4-A both had an average flow velocity of 0.77 ft./sec., and series 3-A had an average flow velocity of 0.85 ft./sec., yet the equilibrium scour depth for series 4-A was greater than that for either series 3-A or 3-B. This is because the velocity of the lower part of the flow was greater in series 4-A than in either of series 3-A or 3-B, even though these last two had higher flow velocities in the upper part of the flow (Figure 26).

(c) For similar vertical velocity profiles, the equilibrium scour depth decreases with decreasing velocities in the lower part of the flow. This is evident from the results of series 2. There was a continuous reduction in d_{se} as the velocities in the lower parts of the flow decreased, from series 2-A to 2-D.

(d) The equilibrium scour depth tends to increase with an increase in the vertical velocity gradient. This is not a direct observation but is implied by the test results of series 5 and 1-C, and series 1-A and 2-A.

Series 5 and series 1-C had about the same value of d_{se} (within the limits of accuracy of the experiment). However, series 5 had a higher flow velocity near the bed, which, based on the previous observations, should have resulted in a larger value of d_{se}. The additional factor which needs to be considered is the velocity gradient (the rate of change of velocity with depth) of the approach flow, especially in the lower part of the flow. For series 5, this velocity gradient was practically zero except right at the bed, whereas in series 1-C, there was a definite velocity gradient up to 0.30 ft. above the bed. This lack of velocity gradient in the lower part of the flow in series 5 counter-acted the increase in velocity, resulting in no net change in the equilibrium scour depth.

A similar effect was observed with series 1-A and 2-A. Again, the equilibrium depth of scour was about the same for both series, even though in series 2-A the velocity of the lower part of the flow was lower. However, the effect of this lower velocity was counter-acted by the greater velocity gradient of series 2-A, resulting in the same equilibrium scour depth as for series 1-A.

(e) The flow above a height above the equal to one pier diameter (0.33 ft) has some influence on the equilibrium depth of scour. For series 3-A and 4-B, the flow velocities up to a height of approximately 0.33 ft. above the bed were about the same. Above this height, however, the flow velocity for series 3-A was greater, and the velocity gradient was greater. This was reflected in an equilibrium scour depth which was 0.05 ft. larger (0.21 ft.) than that of series 4-B (0.16 ft.).

3. Comparison with Results of Others

The flow conditions for series 1-A (undisturbed velocity profile, $U \simeq U_{crit.}$) were probably closer to the flow conditions of experiments done by previous investigators, than those for any of the other test series reported herein. The data for series 1-A are therefore used in the following selected equations as proposed by different researchers in the past. The equilibrium scour depth for series 1-A was 0.37 ft. below normal bed level.

The symbols used in the following equations are defined in Chapter II where they first appear and in the List of Symbols.

(a) Laursen (see section II. D)

Laursen proposed a design curve for conditions of general sediment transport, which for a circular pier is given by:

$$\frac{d_{se}}{b} = 1.35 \left(\frac{H}{b}\right)^{0.3}$$

For the conditions of series 1-A, this gives:

$$d_{se} = 2.01\ b$$
$$= 0.67 \text{ ft.}$$

This result is rather high. A check of Laursen's test data showed that he only used flow depths in the range 0.2 ft. to 0.9 ft., with flow velocities from 1.00 ft./sec. to 2.50 ft./sec.[61]. With these flow conditions, the velocity probably varied throughout the entire depth of flow (ie. boundary layer thickens ≃ depth of flow), and Laursen's results cannot be expected to hold for flow conditions where the flow depth is considerably larger than the boundary layer thickness.

(b) Tarapore (see section II. G)

Tarapore found that the flow depth had no appreciable influence on d_{se} beyond a value of H = 1.15 b. He proposed, for the case of a circular pier with a large flow depth, and conditions of general sediment transport:

$$d_{sem} = 1.35\ b$$

For the conditions of series 1-A, this gives:

$$d_{sem} = 0.45\ ft.$$

(c) Breusers (see section II. I)

Breusers reported the results of two studies:

(i) Model study of the piers of the bridge across the Oosterschelde: Table I shows, for $U \simeq U_{crit.} \simeq 0.81$ ft./sec.(b = 0.36 ft., H = 1.64 ft):

$$d_{se} = 1.25\ b$$

For the conditions of series 1-A, this gives:

$$d_{se} = 0.42\ ft.$$

(ii) Private study of scour around drilling platforms:

$$d_{sem} = 1.4\ b$$

For the conditions of series 1-A, this gives:

$$d_{sem} = 0.47\ ft.$$

(d) Maza and Sanchez (see section II. J)

Maza and Sanchez proposed a modified form of an equation by Jaroslavtsiev, for the region of "clear-water" scour, subject to the condition that $H \geq 1.5\ b$:

$$\frac{d_{se}}{b} = K_f K_{HU} \left(\frac{U^2}{gb}\right) - \frac{3\, d_{50}}{b}$$

For the conditions of series 1-A, this gives:

$$d_{se} = 0.85\ b$$
$$= 0.28\ ft.$$

(e) Larras (see section II. E)

Based on field data and the data of Chabert and Engeldinger, Larras suggested a design equation:

$$d_{sem} = 1.42\ b^{3/4}$$

For the conditions of series 1-A, this gives:

$$d_{sem} = 0.62\ ft.$$

This result is rather high. This is because Larras' equation is dimensionally non-homogeneous; for small pier diameters it will predict scour depths that are too large, and for large pier diameters, it will predict scour depths that are too small.

(f) Shen et al. (see section II. K)

Shen and his co-workers at Colorado State University obtained the relation:

$$d_{se} = .00073\ (R_b)^{0.619}$$

For the conditions of series 1-A, $R_b = 2.53 \times 10^4$, which gives:

$$d_{se} = 0.39\ ft.$$

(g) Coleman (see section II. O)

Coleman proposed the following relation for the equilibrium depth of scour:

$$d_{se} = 1.49\ b^{9/10}\ (U^2/2g)^{1/10}$$

For the conditions of series 1-A,

$(U^2/2g)^{1/10} = (0.0122)^{1/10} = 0.644$, which gives:

$$d_{se} = 0.35 \text{ ft.}$$

The equations ofInglis, Blench, and Varzeliotis were not used. These equations apply to natural channels flowing at regime depths, and thus could not be applied to the flume experiments reported here, in which flow depths were fixed arbitrarily.

D. VORTEX PATTERNS AND SCOUR HOLE DEVELOPMENT

1. The Horseshoe Vortex System

The structure of the horseshoe vortex system, which forms the basic mechanism of local scour around a cylinder, is shown in Figure 36. This pattern was observed for test series 2-C, before the start of scour, at an average approach-flow velocity of 0.30 ft./sec.

Vortex 1 is the main or primary vortex, and it does most of the work involved in the scouring process. It has been observed by investigators in the field of fluid dynamics as well as investigators who specifically studied the local scour phenomenon (see Chapters II and III).

Vortices 2(a) and 2(b) are secondary vortices which are much weaker than the primary vortex. They are derived mostly from the interaction of the primary vortex with the rest of the flow and the flow boundaries. These secondary vortices have been observed by Shen et al.[108] (see also Figures 8 and 10), and by various investigators in the field of fluid dynamics[94,99,123].

Vortex 3, has, to the author's knowledge, not been reported previously in the literature. It was observed by the author on different occasions for different test series, and for different stages of scour hole development. This vortex, although undoubtedly influenced by the primary vortex, nevertheless does not derive its energy from it, but is maintained by the incoming flow from a level just above that which feeds the primary vortex.

The whole vortex system is constantly being fed by the incoming flow from upstream. It is quite unstable, and the individual vortices are repeatedly swept away and being reformed. The turbulence generally present in the approach flow is probably the main factor in this.

2. Scour Hole Development: Beginning of Scour

The development of the scour hole with time is indicated by the plots of Figures 30 to 35. In these figures, the plotted scour depth is the depth (below normal bed level) of the deepest part of the scour hole at the time of measurement.

Scour of the bed around the pier was observed to begin at symmetrically-located points on both sides of the pier about 30° from the front center of the pier face. The shear stresses on the bed are apparently greatest at these spots, due to the superposition of the two-dimensional free-stream flow on the horseshoe vortex action. These two scour spots were observed to increase in size until they met at the front centre of the pier. This occurred within the first minute of the test for almost all the test series. However, the 30°- points still remained the points

of deepest scour for some time - until the scour hole had developed to such a size that the depth all around the front part of the pier, including the 30° - points, was the same.

A sketch of the vortex pattern and scour hole at the beginning of its development, for test series 1-A, is shown in Figure 37. The stage of scour shown is for time t = 12 minutes. The depth of scour at the front center of the pier at this stage was 0.12 ft. below bed level, as shown, whereas the maximum scour depth, at the 30° - points, was 0.15 ft.

The action of each vortex was observed to be quite distinct: vortex 1 scoured out the main part of the scour hole, while vortex 3 scoured the bed area right at the pier face.

The length of time required for the scour hole around the front of the pier to develop to a uniform depth must depend at least partly on the relative strengths of vortices 1 and 3, which in turn depend on the shape of the velocity profile of the flow approaching the pier (see Section 3 below). This is demonstrated by the test results for series 1 and 2 (the only series for which scour depths at both 0° and 30° were measured). The time required for the scour hole to develop to a uniform depth for the series 1 tests was about two hours, while the time required for this in the series 2 tests varied among the individual tests from 6 minutes to 30 minutes.

The development of scour at the 30° - points, and at the front center of the pier, is shown graphically for series 1-A, in Figure 38.

The plan-view vortex pattern is shown in Figure 39, for test series 2-C at time t = 20 minutes. The horseshoe vortices, which have horizontal axes, are swept around the cylinder by the main flow. The domain of the main vortex is between the two dashed lines on the figure, while the domain of vortex 3 is between the dashed line nearest the pier and the pier itself.

The two-dimensional vortices shed from the sides of the pier due to the action of the free stream flow around the pier, superimpose themselves on vortex 3, and cause strong bursts of turbulent eddying which carry sediment for a considerable distance downstream along the wake.

3. Approach Flow Velocity Profile and Vortex Structure

The connection between the approach flow vertical velocity profile and the structure of the horseshoe vortex system is illustrated in Figures 40 and 41. A scour hole was developed by a flow of U = 0.85 ft./sec., to a depth of d_s = 0.20 ft. The flow was then slowed to U = 0.45 ft./sec. to observe the vortex patterns. The approach flow velocity profile is plotted on the right hand side of the figure.

Dye was carefully injected into the flow just upstream of the scour hole at various levels above the bed, in the plane of symmetry of the experimental arrangement. It was observed that each individual vortex within the vortex system was maintained by or derived from a specific flow level within the boundary layer (ie. within the depth range in which the flow velocity varied).

The boundary layer thickness of the observed flow was about 0.30 ft., as shown in Figure 40. From the bed up to a height of about 0.04 ft., the flow was very slow and went mostly into a very weak, type 2(b) vortex. From 0.04 ft. to 0.15 ft., most of the flow went into the primary vortex, with occasional surges into type 2(a) and type 3 vortices. From 0.15 ft. to 0.22 ft., most of the flow went into vortex 3, with some going into vortex 2(a), and occasionally into the main vortex. From 0.22 ft. to 0.29 ft., the flow went into vortex 3. Above a level of 0.29 ft. no flow was observed moving down towards the vortex system. This level corresponds approximately with the level at which the velocity of the approach flow becomes constant. The above observations are combined in a sketch in Figure 41.

4. Transport out of the Scour Hole

The transport of sand out of the scour hole was observed for various test series. The sand travels in basically two steps. First, sand is moved along the slope of the scour hole to points A and B as shown in Figure 42. Points A and B mark the locations of two "lines" or "avenues" of sediment transport out of the hole and downstream, which lie approximately at right angles to the slope.

Three vortices are active in moving the sand towards points A and B. Vortex 1 moves sand up the slope of the scour hole to point A. Vortex 2(a) moves sand down the slope, also to point A. Vortex 3 moves sand right into the pier face to point B. Vortex 2(b) is too weak to have any effect, and the sand in this area simply slides down towards point A by the action of gravity.

Transport line A is located along the outside edge of vortex 1 (see Figure 39), and line B is located right along the surface of the pier. These lines are quite narrow at the front of the scour hole, but widen towards the rear.

The average slope of the scour hole was measured several times (see for example Figure 41) and was found to be 30°. However, as can be seen from the figures, the slope of the scour hole is not constant. The steepest part of the slope is right under the main vortex, and is partially maintained by the shear stresses exerted by the vortex. When the flow is stopped, this part of the slope slumps down.

Several photos of the fully-developed scour hole are shown in Figures 43 and 44.

CHAPTER VI

SUMMARY AND CONCLUSIONS

A. PREVIOUS INVESTIGATIONS

The reported study of local bed scour at bridge piers goes back over the last eighty years or so. During this time, different investigators tried to understand how scour of an erodible bed at a bridge pier or other flow obstruction occurred, and, on the basis of their various ideas and concepts, tried to establish relationships between the depth of local scour and the other parameters of the problem, usually by conducting experiments on scale models in a hydraulic laboratory.

The parameters that were shown by these experiments to be most important, can be divided into two groups - the parameters describing the

pier geometry, and the parameters describing the flow conditions.

The pier geometry is adequately described by two parameters. The most important one is the pier size, expressed as the pier width, or diameter, b. The second parameter is the pier shape, and is usually expressed as a constant coefficient and applied as a direct factor in scour equations.

There are two main flow parameters which the various investigators have found to be important. These are the flow velocity and the flow depth. However, there is not universal agreement as to their relative importance. Some investigators, especially Laursen, stressed the importance of the flow depth, while discounting the flow velocity. Others, such as Shen et al., stressed the flow velocity as being more important.

The relative importance of these two flow parameters depends on the regime of flow which is being considered. For a flow regime in which there is no general transport of bed sediment, the flow velocity has a definite effect on the equilibrium depth of scour, d_{se}. However, this effect decreases rapidly once conditions of general sediment transport are established (see Figures 3 and 18). If the flow regime is such that the flow depth is small, and the velocity profile of the boundary layer is affected by changes in flow depth, then the equilibrium depth of scour will be affected also. However, if the depth of flow is large, and the boundary layer velocity profile is fully deveploped, then variations in flow depth will not affect the equilibrium depth of scour. This conclusion is implied by the findings of Tarapore (p.20, above), Breusers (p. 23,

above), and Maza and Sanchez (p. 25, above).

For any given pier in an erodible bed, the equilibrium depth of scour (d_{se}) increases with flow depth and flow velocity, only up to a certain limiting value. Increasing the flow depths and velocities beyond this point will no longer affect the depth of scour. This limiting value is known as the maximum equilibrium depth of scour (d_{sem}), and is governed only by the pier size and shape. This has been implicitly recognized by a number of investigators who have proposed relationships for maximum equilibrium scour depth (d_{sem}) based only on pier size and shape (eg. Tarapore, Breusers).

B. MECHANISM OF LOCAL SCOUR

The basic mechanism of local scour is the horseshoe vortex. The horseshoe vortex is formed by the action of the pier in apprehending the vorticity normally present in the flow, and concentrating it near the bed at the pier nose. The pier induces an adverse pressure gradient in the flow, which causes it to acquire a downward component in front of the pier. This in turn causes separation of the boundary layer in front of the pier, which then rolls up to form a large vortex with a horizontal axis and shaped like a horseshoe in plan. Interaction of this vortex with the boundaries and the approach flow generates yet other vortices, so that a system of linked vortices develops. This is called the horseshoe vortex system.

Any attempt to understand or explain local scour without considering the basic vortex mechanism cannot succeed. Thus, the analyses of Tison, Ishihara, Tarapore, and Carstens, do more to confuse the situation than they do to explain it, although their experimental results are valid in themselves.

C. EXPERIMENTAL RESULTS

1. Introduction

A consideration of the factors that influence the strength of the horseshoe vortex led to the decision to investigate the effect of the vertical velocity distribution of the approach flow on the equilibrium depth of scour, and on the horseshoe vortex flow patterns. Experiments were therefore carried out to do this. A flow regime with a large depth of flow, and flow velocities below the critical for the beginning of general sediment transport, were used.

2. Equilibrium Depth of Scour

The main results of the experiments on the equilibrium depth of scour can be summarized as follows.

(a) The equilibrium depth of scour increases with increasing average approach flow velocity, for the range of flow velocities used.

(b) The equilibrium depth of scour depends more on the velocity of the lower part of the flow than on the velocity of the upper part of the flow.

(c) The equilibrium depth of scour increases with an increase in the gradient of the vertical velocity profile of the approach flow.

The equilibrium depth of scour obtained for an undisturbed velocity profile at an average velocity slightly less than the critical velocity required for the beginning of general sediment transport (series 1-A), was

equal to 0.37 ft. (1.12 b). This value was compared to scour depths calculated from various equations proposed by previous investigators.

The equations of Laursen (equation 10) and Larras (equation 11) gave very high values for the equilibrium scour depth, and were considered to be inapplicable, for the reasons stated in Chapter V. Equations of Tarapore and Breusers, for the maximum equilibrium depth of scour, d_{sem}, are also inapplicable, since these were derived for the most severe flow conditions possible, with a state of general sediment transport, and would include the effect of such factors as dune troughs passing through the scour hole.

The remaining equations, of Breusers, Maza and Sanchez, Shen et al., and Coleman, gave values for d_{se} of 0.42 ft., 0.28 ft., 0.39 ft., and 0.35 ft., respectively. These four equations give an average of 0.36 ft., which compares well with the 0.37 ft. actually obtained.

3. Horseshoe Vortex Flow Patterns

The main results of the observations of flow patterns in the horseshoe vortex system are as follows.

a) The horseshoe vortex system is a system of linked vortices, and is made up of a primary vortex (vortex 1), several secondary vortices (vortices 2(a) and 2(b)), and a tertiary vortex (vortex 3). This tertiary vortex has not been reported before.

b) The work of moving the sand grains out of the scour hole is done mainly by the primary vortex; the secondary vortices do very

little work. Vortex 3 scours the region of the bed right next to the pier face.

c) The whole vortex system is continually being fed by the incoming flow from upstream. Approach flow turbulence is therefore reflected in the alternate collapse and reformation of the individual vortices.

d) Each individual vortex within the horseshoe vortex system is derived from and maintained by a specific flow level within the boundary layer, and the flow over the entire thickness of the boundary layer is used to supply the horseshoe vortex system.

D. RECOMMENDATIONS

1. Predicting Scour Depths

The present state of knowledge and understanding of local scour at bridge piers is such that, in general, the scour depth for a given pier geometry and flow regime cannot be predicted with confidence.

More experimental work has been done with circular cylindrical piers than with any other type. However, even for these, the only relationship that has been established with any confidence is the relationship for the maximum depth of scour, d_{sem}. This seems to be adequately defined by Breusers' equation, $d_{sem} = 1.4\ b$ (equation 21).

For particular flow conditions, pier geometries, and bed sediment characteristics be safely predicted only on the basis of hydraulic laboratory

studies in which actual prototype conditions are accurately reproduced on a small scale. Further, models of several different scales should be tested to check for scale effects. The experimental work reported here indicates that the vertical velocity distribution should also be considered as one of the flow characteristics that need to be properly scaled.

2. Further Research

The following areas are suggested as particularly in need of further research and investigation.

(a) Experimental data covering a broad range of vertical velocity distributions needs to be obtained, so that the influence of this flow parameter can be quantitatively determined.

(b) The effect of the depth of flow on the vertical velocity gradient, and thus on the equilibrium scour depth, should be investigated further.

(c) Previous experimental data should be reviewed in the light of the observed effects of the vertical velocity gradient of the approach flow.

BIBLIOGRAPHY

BIBLIOGRAPHY

1. Ahmad, M. "Experiments on Design and Behaviour of Spur Dykes," Proceedings, Minnesota International Hydraulics Convention, Minneapolis, Minnesota, August, 1953, pp. 145-159.

2. Ahmad, M. [Discussion of E.M. Laursen's "Scour at Bridge Crossings"], Journal of the Hydraulics Division, Am.Soc. of Civil Engrs., Vol. 86, No. HY9 (November 1960), pp. 144-151.

3. Allen, J. "The Effect of Engineering Structures on the Regime of Waterways, with Special Reference to Bridge Piers, Sluice-Dams, and Spillways," Scale Models in Hydraulic Engineering, Chapter III. London; Longmans, Green and Co., 1947.

4. Arunachalam, K. "Scour Around Bridge Piers," Journal of Indian Roads Congress, Vol. 29, No. 2 (August 1965), pp. 189-210.

5. Arunachalam, K. [Discussion of C.R. Neill's "Measurements of Bridge Scour and Bed Changes in a Flooding Sand-Bed River"], Proceedings, Institution of Civil Engineers, Vol. 36, Feb., 1967, pp. 402-404.

6. Baines, W.D. [Discussion of F.D. Masch and W.L. Moore "Drag Forces in Velocity Gradient Flow"], Journal of the Hydraulics Division, Am. Soc. of Civil Engrs., Vol. 87, No. HY1 (January 1961), pp. 271-273.

7. Bata, G. Scour Around Bridge Piers. Unpublished translation, Colorado State University, Fort Collins, Colorado. Translated from the Serbian by Markovic. Original entitled Erozija oko Novosadskog Mostovskog Stuba, published by Institut za vodoprivredu, Jaroslav Cerai Beograd, Yugoslavia, 1960.

8. Barr, D.I.H. [Discussion of C.R. Neill's "Measurements of Bridge Scour and Bed Changes in a Flooding Sand-Bed River"], Proceedings, Institution of Civil Engineers, Vol. 36, Feb., 1967, pp. 404-406.

9. Barr, D.I.H., and Herbertson, J.G. [Discussion of S. Komura's "Equilibrium Depth of Scour in Long Contractions"], Journal of the Hydraulics Division, Am.Soc. of Civil Engrs., Vol. 93, No. HY3, (May 1967), pp. 220-221.

10. Bauer, W.J. [Discussion of E.M. Laursen's "Scour at Bridge Crossings"], Journal of the Hydraulics Division, Am. Soc. of Civil Engrs., Vol. 86, No. HY9 (November 1960), pp. 132-133.

11. Blench, T. "Problems Related to Breadth, Depth, and Slope," Regime Behaviour of Canals and Rivers, Chapter 7. London: Butterworths, 1957.

12. Blench, T. [Discussion of E.M. Laursen's "Scour at Bridge Crossings"], Journal of the Hydraulics Division, Am. Soc. of Civil Engrs., Vol. 86, No. HY5 (May 1960), pp. 193-194.

13. Blench, T. [Discussion of C.R. Neill's "Measurements of Bridge Scour and Bed Changes in a Flooding Sand-Bed River"], Proceedings, Institution of Civil Engineers, Vol. 36, Feb., 1967, pp. 407-408.

14. Bolcs, A. "Flow Investigations in a Water Flow Channel at Subsonic and Supersonic Velocities", Escher Wyss News, Zurich, Vol. 42, (1969), No. 1, pp. 18-29.

15. Bradley, J.N. [Discussion of E.M. Laursen's "Scour at Bridge Crossings"], Journal of the Hydraulics Division, Am. Soc. of Civil Engrs., Vol. 86, No. HY8 (August 1960), pp. 69-70.

16. Breusers, H.N.C. Ontgronding Pijlers Oosterscheldebrug. Delft Hydraulics Laboratory, Report R262, Delft, January, 1964.

17. Breusers, H.N.C. "Scour Around Drilling Platforms," Bulletin Hydraulic Research, International Assoc. for Hydraulic Research, Vol. 19, 1964 and 1965, p. 276.

18. Breusers, H.N.C. "Time Scale of Two-Dimensional Local Scour," Proceedings, Twelfth Congress of the International Assoc. for Hydraulic Research, Fort Collings, Colorado, September, 1967, Vol. 3, pp. 275-282.

19. Breusers, H.N.C. [Discussion of H.W. Shen et al. "Local Scour Around Bridge Piers"], Journal of the Hydraulics Division, Am.Soc. of Civil Engrs., Vol. 96, No. HY7 (July, 1970), pp. 1638-1639.

20. Carstens, M.R. "Similarity Laws for Localized Scour," Journal of the Hydraulics Division, Am. Soc. of Civil Engrs., Vol. 92, No. HY3 (May 1966), pp. 13-36.

21. Carstens, M.R. [Closure to Discussion of M.R. Carstens' "Similarity Laws for Localized Scour"], Journal of the Hydraulics Division, Am. Soc. of Civil Engrs., Vol. 94, No. HY1 (January 1968), pp. 303-306.

22. Chaplin, T.K. [Discussion of R.J. Garde et al. "Study of Scour Around Spur-Dikes"], Journal of the Hydraulics Division, Am. Soc. of Civil Engrs., Vol. 88, No. HY2 (March 1962), p. 192.

23. Chitale, S.V. [Discussion of E.M. Laursen's "Scour at Bridge Crossings"], Transactions, Am. Soc. of Civil Engrs., Vol. 127, Part I (1962), pp. 191-196.

24. Chitale, S.V. [Discussion of E.M. Laursen's "An Analysis of Relief Bridge Scour"], Journal of the Hydraulics Division, Am. Soc. of Civil Engrs., Vol. 90, No. HY1 (January 1964), p. 287.

25. Chitale, S.V. [Discussion of C.R. Neill's "Measurements of Bridge Scour and Bed Changes in a Flooding Sand-Bed River"], Proceedings, Institution of Civil Engrs., Vol. 36, Feb., 1967, pp. 410-411.

26. Chow, V.T. Open Channel Hydrualics, Toronto, McGraw-Hill, 1959, p. 25.

27. Clutter, D.W., and Smith, A.M.O. "Flow Visualization by Electrolysis of Water," Aerospace Engineering, Vol. 20, No. 1 (January 1961), pp. 24-27.

28. Coleman, N.L. "Analyzing Laboratory Measurements of Scour at Cylindrical Piers in Sand Beds," Proceedings, Fourteenth Congress of the International Assoc. for Hydraulic Research, Paris, September, 1971, Vol. 3, pp. 307-313.

29. Corbett, D.M., et al. Stream-Gaging Procedures, U.S.G.S. Water-Supply Paper 888, Washington, 1943, p. 36.

30. Edgecombe, A.R.B. [Discussion of C.R. Neill's "Measurements of Bridge Scour and Bed Changes in a Flooding Sand-Bed River"], Proceedings, Institution of Civil Engineers, Vol. 36, Feb., 1967, p. 397.

31. Engels, H. "Experiments Pertaining to the Protection of Bridge Piers against Undermining," Hydraulic Laboratory Practice. J.R. Freeman, ed., New York: Am.Soc. of Mech. Engrs., 1929, p.92.

32. Garde, R.J., Subramanya, K., and Nambudripad, K.D. "Study of Scour Around Spur-Dikes," Journal of the Hydraulics Division, Am. Soc. of Civil Engrs., Vol. 87, No. HY6 (November 1961), pp. 23-37.

33. Goldstein, S., ed. "Cylinders of finite span. The effect of aspect ratio on drag," Modern Developments in Fluid Dynamics, Vol. II, New York: Dover, 1965, p. 439.

34. Gole, C.V., and Chitale, S.V. "River Bed Scour at Bridge Constrictions," Proceedings, Twelfth Congress of the International Assoc. for Hydraulic Research, Fort Collins, Colorado, September, 1967, Vol. 3, pp. 330-337.

35. Gourlay, R. [Discussion of C.R. Neill's "Measurements of Bridge Scour and Bed Changes in a Flooding Sand-Bed River"], Proceedings, Institution of Civil Engineers, Vol. 36, Feb., 1967, pp. 398-400.

36. Gradowczyk, M.H., Maggiolo, O.J., and Folguera, H.C. "Localized Scour in Erodible-Bed Channels," Journal of Hydraulic Research, International Assoc. for Hydraulic Research, Vol. 6, No. 4 (1968), pp. 289-326.

37. Hallmark, D.E., and Smith, G.L. "Stability of Channels by Armorplating," Journal of the Waterways and Harbours Division, Am.Soc. of Civil Engrs., Vol. 91, No. WW3 (August 1965), pp. 117-135.

38. Hallmark, D.E., and Smith, G.L. [Closure to Discussion of D.E. Hallmark and G.L. Smith "Stability of Channels by Armorplating"], Journal of the Water-Ways and Harbours Division, Am. Soc. of Civil Engrs., Vol. 92, No. WW3 (August 1966), pp. 91-92.

39. Hawthorne, W.R. "The Secondary Flow About Struts and Airfoils," Journal of the Aeronautical Sciences, Vol. 21 (1954), pp. 588-608.

40. Herbich, H.P., and Brennan, L.M. Prediction of Scour at Bridges, Ontario Dept. of Highways Report RR115, April 1967.

41. Herbich, J.B. "Prevention of Scour at Bridge Abutments," Proceedings, Twelfth Congress of the International Assoc. for Hydraulic Research, Fort Collins, Colorado, September, 1967, Vol. 2, pp. 74-87.

42. Inglis, Sir Claude C. "Maximum depth of scour at heads of guide banks and groynes, pier noses, and downstream of bridges," The Behaviour and Control of Rivers and Canals, Part II, Chapter 8. Poona: Government of India, Central Waterpower Irrigation and Navigation Research Station, 1949.

43. Inglis, Sir Claude C. [Discussion of C.R. Neill's "Measurements of Bridge Scour and Bed Changes in a Flooding Sand-Bed River"], Proceedings, Institution of Civil Engineers, Vol. 36, Feb., 1967, pp. 406-407.

44. Ishihara, T. An Experimental Study of Scour Around Bridge Piers. Unpublished translation, Colorado State University; Fort Collins, Colorado. Translated from Journal of the Japan Society of Civil Engineers, Vol. 24, No. 1 (1938), pp. 28-55, Vol. 28, No. 9 (1942), pp. 787-821, and Vol. 28, No. 11 (1942), pp. 974-1005.

45. Jarocki, W. "Effect of Piers on Water Streams and Bed Form," Ninth Convention, International Assoc. for Hydraulic Research, Dubrovnik, 1961, pp. 1147-1149.

46. Joglekar, D.V. "Role of Models in River Training Works," Symposium on Role of Models in the Evolution of Hydraulic Structures and Movement of Sediment. Central Board of Irrigation and Power (India), Publication No. 53, 1952, pp. 115-129.

47. Joglekar, D.V. [Discussion of E.M. Laursen's "Scour at Bridge Crossings"], Journal of the Hydraulics Division, Am. Soc. of Civil Engrs., Vol. 86, No. HY9 (November 1960), pp. 129-132.

48. Johnston, J.P. "On the Three-Dimensional Turbulent Boundary Layer Generated by Secondary Flow," Transactions, Am. Soc. of Mech. Engrs., Vol. 82, Series D (Journal of Basic Engineering, March, 1960), pp. 233-246.

49. Johnston, J.P. [Closure to Discussion of J.P. Johnston's "On the Three-Dimensional Turbulent Boundary Layer Generated by Secondary Flow"], Transactions, Am. Soc. of Mech. Engrs., Vol. 82, Series D (Journal of Basic Engineering, March 1960), p. 248.

50. Johnston, J.P. "The Turbulent Boundary Layer at a Plane of Symmetry in a Three-Dimensional Flow," Transactions, Am. Soc. of Mech. Engrs., Vol. 82, Series D (Journal of Basic Engineering, September, 1960), pp. 622-628.

51. Karaki, S.S., and Haynie, R.M. Mechanics of Local Scour, Part II, Bibliography. Report No. CER 63SSK46, Civil Engineering Section, Colorado State University, Fort Collins, Colorado, November, 1963.

52. Kemp. P.H., and Grass, A.J. "The Measurement of Turbulent Velocity Fluctuations Close to a Boundary in Open Channel Flow," Proceedings, Twelfth Congress of the International Assoc. for Hydraulic Research, Fort Collins, Colorado, September, 1967, Vol. 2, pp. 201-209.

53. Knezevic, B. Contributions to Research Work of Erosion around Bridge Piers. Unpublished translation, Colorado State University, Fort Collins, Colorado, Translated from the Serbian by Markovic. Original entitled Prilog Proucavanju Erozye oko Mostovskih Stubova, published by Institut za vodo privredu, Jaroslav Cerai Beograd, Yugoslavia, 1960.

54. Komura, S. "Equilibrium Depth of Scour in Long Contractions," Journal of the Hydraulics Division, Am. Soc. of Civil Engrs., Vol. 92, No. HY5 (September 1966), pp. 17-37.

55. Komura, S. [Closure to Discussion of S. Komura's "Equilibrium Depth of Scour in Long Contractions"], Journal of the Hydraulics Division, Am. Soc. of Civil Engrs., Vol. 93, No. HY6 (November 1967), pp. 427-429.

56. Krishnamurthy, M. [Discussion of H.W. Shen et al. "Local Scour Around Bridge Piers"], Journal of the Hydraulics Division, Am. Soc. of Civil Engrs., Vol. 96, No. HY7 (July 1970), pp. 1637-1638.

57. Lacey, G. [Discussion of C.R. Neill's "Measurements of Bridge Scour and Bed Changes in a Flooding Sand-Bed River"], Proceedings, Institution of Civil Engineers, Vol. 36, Feb., 1967, pp. 411-414.

58. Larras, J.A. [Discussion of H.W. Shen et al. "Local Scour Around Bridge Piers"], Journal of the Hydraulics Division, Am. Soc. of Civil Engrs., Vol. 96, No. HY6 (June 1970), p. 1368.

59. Laursen, E.M. "Observations on the Nature of Scour," Proceedings, Fifth Hydraulics Conference, State University of Iowa, Studies in Engineering, Bulletin 34, 1952, pp. 179-197.

60. Laursen, E.M., and Toch, A. "A Generalized Model Study of Scour Around Bridge Piers and Abutments," Proceedings, Minnesota International Hydraulics Convention, Minneapolis, Minnesota, August, 1953, pp. 123-131.

61. Laursen, E.M., and Toch, A. Scour Around Bridge Piers and Abutments. Iowa Highway Research Board, Bulletin No. 4, May, 1956.

62. Laursen, E.M. Scour at Bridge Crossings. Iowa Highway Research Board, Bulletin No. 8, August, 1958.

63. Laursen, E.M. "Scour at Bridge Crossings," Journal of the Hydraulics Division, Am. Soc. of Civil Engrs., Vol. 86, No. HY2 (February 1960), pp. 39-54.

64. Laursen, E.M. [Closure to Discussion of E.M. Laursen's "Scour at Bridge Crossings"], Transactions, Am. Soc. of Civil Engrs., Vol. 127, Part I (1962), pp. 207-209.

65. Laursen, E.M. "An Analysis of Relief Bridge Scour," Journal of the Hydraulics Division, Am. Soc. of Civil Engrs., Vol. 89, No. HY3 (May 1963), pp. 93-118.

66. Laursen, E.M. [Closure to Discussion of E.M. Laursen's "An Analysis of Relief Bridge Scour"], Journal of the Hydraulics Division, Am. Soc. of Civil Engrs., Vol. 90, No. HY4 (July 1964), p. 231.

67. Laursen, E.M. "Some Aspects of the Problem of Scour at Bridge Crossings," Proceedings of the Federal Inter-Agency Sedimentation Conference. Miscellaneous Publication No. 970, Agricultural Research Service, U.S. Dept. of Agriculture, 1963, pp. 304-309.

68. Laursen, E.M. [Discussion of H.W. Shen et al. "Local Scour Around Bridge Piers"], Journal of the Hydraulics Division, Am. Soc. of Civil Engrs., Vol. 96, No. HY9 (September 1970), pp. 1896-1899.

69. Leliavsky, S. An Introduction to Fluvial Hydraulics. London: Constable, 1955.

70. Levi, E., and Luna, H. "Dispositifs pour Reduire L'Affouillement au Pied des Piles de Ponts," Ninth Convention, International Assoc. for Hydraulic Research, Dubrovnik, 1961, pp. 1061-1069.

71. Lighthill, M.J. "Introduction: Boundary Layer Theory," Laminar Boundary Layers, ed. L. Rosenhead, Clarendon Press, Oxford, 1963, pp. 46-109.

72. Liu, H.K., Chang, F.M., and Skinner, M.M. Effect of Bridge Constriction on Scour and Backwater. Report No. CER60 HKL22, Civil Engineering Section, Colorado State University, Fort Collins, Colorado, February, 1961.

73. McDowell, D.M. [Discussion of C.R. Neill's "Measurements of Bridge Scour and Bed Changes in a Flooding Sand-Bed River"], Proceedings, Institution of Civil Engineers, Vol. 36, Feb., 1967, pp. 401-402.

74. Maddock, T., jr. [Discussion of M.R. Carstens' "Similarity Laws for Localized Scour"], Journal of the Hydraulics Division, Am. Soc. of Civil Engrs., Vol. 92, No. HY6 (November 1966), pp. 271-273.

75. Masch, F.D., jr. The Effect of a Velocity Gradient on the Drag Coefficient for Circular Cylinders. M.S. Thesis, University of Texas, August, 1957.

76. Masch, F.D., jr., and Moore, W.L. "Draf Forces in Velocity Gradient Flow," Journal of the Hydraulics Division, Am. Soc. of Civil Engrs., Vol. 86, No. HY7 (July 1960), pp. 1-11.

77. Masch, F.D., jr, and Moore, W.L. [Closure to Discussion of F.D. Masch, jr. and W.L. Moore "Drag Forces in Velocity Gradient Flow"], Journal of the Hydraulics Division, Am. Soc. of Civil Engrs., Vol. 88, No. HY4 (July 1962), pp. 229-230.

78. Mavis, F.T. [Discussion of M.R. Carstens' "Similarity Laws for Localized Scour"], Journal of the Hydraulics Division, Am. Soc. of Civil Engrs., Vol. 92, No. HY6 (November 1966), pp. 273-278.

79. Maza Alvarez, J.A., and Sanchez Bribiesca, J.L. Contribution to the Study of the Local Scour at Bridge Piers. Unpublished English abstract, Colorado State University, Fort Collins, Colorado. Original entitled Contribucion al Estudio de la Socavacion Local en Pilas de Puenta, published by Universidad Nacional Autonoma De Mexico, Facultad de Ingenieria, Publicacion Num. 84, 1964.

80. Moore, W.L., and Masch, F.D. "Influence of Secondary Flow on Local Scour at Obstructions in a Channel," Proceedings of the Federal Inter-Agency Sedimentation Conference. Miscellaneous Publication No. 970, Agricultural Research Service, U.S. Dept. of Agriculture, 1963, pp. 314-320.

81. Neill, C.R. [Discussion of R.J. Garde et al. "Study of Scour Around Spur-Dikes"], Journal of the Hydraulics Division, Am. Soc. of Civil Engrs., Vol. 88, No. HY2 (March 1962), pp. 191-192.

82. Neill, C.R. "Alluvial Processes and River Channel Regime," Transactions, Engineering Institute of Canada, Vol. 7, No. A-3, July, 1964.

83. Neill, C.R. River Bed Scour. Canadian Good Roads Association, Technical Publication No. 23, Ottawa, December, 1964.

84. Neill, C.R. "Measurements of Bridge Scour and Bed Changes in a Flooding Sand-Bed River," Proceedings, Institution of Civil Engineers, Vol. 30, February 1965 (paper no. 6775), pp. 415-436.

85. Neill, C.R. [Closure to Discussion of C.R. Neill's "Measurements of Bridge Scour and Bed Changes in a Flooding Sand-Bed River"], Proceedings, Institution of Civil Engineers, Vol. 36, February, 1967, pp. 414-421.

86. Neill, C.R. "Mean Velocity Criterion for Scour of Coarse Uniform Bed-Material," Proceedings, Twelfth Congress of the International Assoc. for Hydraulic Research, Fort Collins, Colorado, September, 1967, Vol. 3, pp. 46-54.

87. Neill, C.R. "Note on Initial Movement of Coarse Uniform Bed-Material," Journal of Hydraulic Research, International Assoc. for Hydraulic Research, Vol. 6, No. 2 (1968), pp. 173-176.

88. Neill, C.R. [Discussion of H.W. Shen et al. "Local Scour Around Bridge Piers"], Journal of the Hydraulics Division, Am. Soc. of Civil Engrs., Vol. 96, No. HY5 (May, 1970), pp. 1224-1227.

89. Nimmo, W.H.R. [Discussion of C.R. Neill's "Measurements of Bridge Scour and Bed Changes in a Flooding Sand-Bed River"], Proceedings, Institution of Civil Engineers, Vol. 36, February, 1967, pp. 408-410.

90. Peake, D.J., and Galway, R.D. "The Three-Dimensional Separation of a Plane Incompressible Laminar Boundary Layer Produced by a Circular Cylinder Mounted Normal to a Flat Plate," Recent Developments in Boundary Layer Research. AGARDograph 97, Part 2, AGARD, NATO, Paris, May, 1965, pp. 1049-1080.

91. Pierce, F.J. "The Turbulent Flow at the Plane of Symmetry of a Collateral Three-Dimensional Boundary Layer," Transactions, Am. Soc. of Mech. Engrs., Vol. 86, Series D (Journal of Basic Engineering, June 1964), pp. 227-233.

92. Plate, E.J., and Goodwin, C.R. "The Influence of Wind on Open Channel Flow," Coastal Engineering Specialty Conference. Santa Barbara: Am. Soc. of Civil Engrs., October, 1965, pp. 391-423.

93. Posey, C.J. "Why Bridges Fail in Floods," Civil Engineering (New York), Vol. 19, February, 1949, p. 42 and 90.

94. Posey, C.J. "Some Basic Requirements for Protection Against Erosion," Proceedings, Minnesota International Hydraulics Convention, Minneapolis, Minnesota, August 1953, pp. 85-88.

95. Posey, C.J. "Scour at Bridge Piers: 2. Protection of Threatened Piers," Civil Engineering (New York), Vol. 33, No. 5 (May 1963), pp. 48-49.

96. Rainbird, W.J., et al. "Some Examples of Separation in Three-Dimensional Flows," Canadian Aeronautics and Space Journal, Vol. 12, 1966, pp. 409-423.

97. Rajaratnam, N. [Discussion of Z. Thomas' "An Interesting Hydraulic Effect Occurring at Local Scour"], Proceedings, Twelfth Congress of the International Assoc. for Hydraulic Research, Fort Collins, Colorado, September 1967, Vol. 5, p. 449.

98. Rehbock, T. "The River-Hydraulic Laboratory of the Technical University of Karlsruhe," Hydraulic Laboratory Practice. J.R. Freeman, ed., New York: Am. Soc. of Mech. Engrs., 1929, pp. 135, 137, 161, 201.

99. Richardson, P.D. "The Generation of Scour Marks Near Obstacles," Journal of Sedimentary Petrology, Vol. 38, No. 4, December, 1968, pp. 965-970.

100. Romita, P.L. [Discussion of E.M. Laursen's "Scour at Bridge Crossings"], Journal of the Hydraulics Division, Am. Soc. of Civil Engrs., Vol. 86, No. HY9 (November 1960), pp. 151-152.

101. Roper, A.T. A Cylinder in a Turbulent Shear Layer. Ph.D. Disseration, Colorado State University, Fort Collins, Colorado, August, 1967.

102. Roper, A.T. [Discussion of H.W. Shen et al. "Local Scour Around Bridge Piers"], Journal of the Hydraulics Division, Am. Soc. of Civil Engrs., Vol. 96, No. HY7 (July 1970), pp. 1636-1637.

103. Roper, A.T., Schneider, V.R., and Shen, H.W. "Analytical Approach to Local Scour," Proceedings, Twelfth Congress of the International Assoc. for Hydraulics Research, Fort Collins, Colorado, September, 1967, Vol. 3, pp. 151-161.

104. Sanden, E.J. Scour at Bridge Piers and Erosion of River Banks. Department of Highways, Alberta. Presented at Thirteenth Annual Conference of the Western Assoc. of Canadian Highway Officials, October 3, 1960.

105. Sarma, K.V.N. [Discussion of M.R. Carstens' "Similarity Laws for Localized Scour"], Journal of the Hydraulics Division, Am. Soc. of Civil Engrs., Vol. 93, No. HY2 (March 1967), pp. 67-71.

106. Schneider, V.R. Mechanics of Local Scour. Ph.D. Dissertation, Colorado State University, Fort Collins, Colorado, December, 1968.

107. Schraub, F.A., et al. "Use of Hydrogen Bubbles for Quantitative Determination of Time-Dependent Velocity Fields in Low Speed Water Flows," Transactions, Am. Soc. of Mech. Engrs., Vol. 87, Series D (Journal of Basic Engineering, June, 1965), pp. 429-444.

108. Shankarachar, D., and Chandrasekhara, T.R. [Discussion of H.W. Shen et al. "Local Scour Around Bridge Piers"], Journal of the Hydraulics Division, Am. Soc. of Civil Engrs., Vol. 96, No. HY8, (August 1970), p. 1747.

109. Shen, H.W., Ogawa, Y., and Karaki, S.S. "Time Variation of Bed Deformation near Bridge Piers," International Association for Hydraulic Research, Eleventh Congress, Leningrad, 1965, Volume III, paper no. 3.14.

110. Shen, H.W., Schneider, V.R., and Karaki, S. Mechanics of Local Scour. Report No. CER66HWS22, Civil Engineering Department, Engineering Research Center, Colorado State University, Fort Collins, Colorado, June, 1966.

111. Shen, H.W., Schneider, V.R., and Karaki, S. Mechanics of Local Scour, Data Supplement. Report No. CER66-67 HWS27, Civil Engineering Department, Engineering Research Center, Colorado State University, Fort Collins, Colorado, June, 1966.

112. Shen, H.W., Schneider, V.R., and Karaki, S. Mechanics of Local Scour, Supplement, Methods of Reducing Scour. Report No. CER66HWS36, Civil Engineering Department, Engineering Research Center, Colorado State University, Fort Collins, Colorado, June, 1966.

113. Shen, H.W., Schneider, V.R., and Karaki, S. "Local Scour Around Bridge Piers," Journal of the Hydraulics Division, Am. Soc. of Civil Engrs., Vol. 95, No. HY6 (November 1969), pp. 1919-1940.

114. Shen, H.W., Schneider, V.R., and Karaki, S. [Closure to Discussion of H.W. Shen et al. "Local Scour Around Bridge Piers"], Journal of the Hydraulics Division, Am. Soc. of Civil Engrs., Vol. 97, No. HY9 (September 1971), pp. 1513-1517.

115. Skogerboe, J.V. [Discussion of D.E. Hallmark and G.L. Smith "Stability of Channels by Armorplating"], Journal of the Waterways and Harbours Division, Am.Soc. of Civil Engrs., Vol. 92, No. WW1 (February 1966), pp. 143-145.

116. Stabilini, L. "Scour at Bridge Piers: 1. Cause and Effect," Civil Engineering (New York), Vol. 33, No. 5 (May 1963), pp. 46-47.

117. Steinheuer, J. "Three Dimensional Boundary Layers on Rotating Bodies and in Corners," Recent Developments in Boundary Layer Research. AGARDograph 97, Part 2, AGARD, NATO, Paris, May, 1965, pp. 577-611.

118. Tanaka, S., and Yano, M. "Local Scour Around a Circular Cylinder," Proceedings, Twelfth Congress of the International Assoc. for Hydraulic Research, Fort Collins, Colorado, September, 1967, Vol. 3, pp. 193-201.

119. Tarapore, Z.S. A Theoretical and Experimental Determination of the Erosion Pattern Caused by Obstructions in an Alluvial Channel with Particular Reference to Vertical Circular Cylindrical Piers. Ph.D. Thesis, University of Minnesota, February, 1962.

120. Tarapore, Z.S. "Determination of the Depth of Scour Around an Obstruction in an Alluvial Channel," Proceedings, Twelfth Congress of the International Assoc. for Hydraulic Research, Fort Collins, Colorado, September, 1967, Vol. 3, pp. 17-25.

121. Thomas, A.R. [Discussion of E.M. Laursen's "Scour at Bridge Crossings"], Journal of the Hydraulics Division, Am. Soc. of Civil Engrs., Vol. 86, No. HY9 (November 1960), pp. 142-143.

122. Thomas, A.R. [Discussion of C.R. Neill's "Measurements of Bridge Scour and Bed Changes in a Flooding Sand-Bed River"], Proceedings, Institution of Civil Engineers, Vol. 36, Feburary, 1967, p. 407.

123. Thomas, A.R. [Discussion of H.W. Shen et al. "Local Scour Around Bridge Piers"], Journal of the Hydraulics Division, Am. Soc. of Civil Engrs., Vol. 96, No. HY9 (September 1970), pp. 1894-1896.

124. Thomas, Z. "An Interesting Hydraulic Effect Occuring at Local Scour," Proceedings, Twelfth Congress of the International Assoc. for Hydraulic Research, Fort Collins, Colorado, September, 1967, Vol. 3, pp. 125-134.

125. Thwaites, B. Incompressible Aerodynamics. Oxford: Clarendon Press, 1960.

126. Timonoff, V.E. "Experiments on the spacing of bridge piers....," Hydraulic Laboratory Practice. J.R. Freeman, ed., New York: Am. Soc. of Mech. Engrs., 1929, p. 359.

127. Tison, G., jr. [Discussion of R.J. Garde, et al. "Study of Scour Around Spur-Dikes"], Journal of the Hydraulics Division, Am. Soc. of Civil Engrs., Vol. 88, No. HY4 (July 1962), pp. 301-306.

128. Tison, L.J. "L'erosion et le Transport des Materiaux Solides Dans les Cours d'Eau," Reports and Papers for the Postponed Meeting, International Assoc. for Hydraulic Structures Research, Liege, 1939, pp. 71-90.

129. Tison, L.J. "Studies of the Critical Tractive Force of Entrainment of Bed Materials," Proceedings, Minnesota International Hydraulics Convention, Minneapolis, Minnesota, August, 1953, pp. 21-35.

130. Tison, L.J. [Discussion of E.M. Laursen's "Scour at Bridge Crossings"], Journal of the Hydraulics Division, Am. Soc. of Civil Engrs., Vol. 86, No. HY9 (November 1960), pp. 134-137.

131. Tison, L.J. "Local Scour in Rivers," Journal of Geophysical Research, Vol. 66, No. 12 (December 1961), pp. 4227-4232.

132. Toomre, A. "The Viscous Secondary Flow Ahead of an Infinite Cylinder in a Uniform Parallel Shear Flow," Journal of Fluid Mechanics, Vol. 7, No. 1 (1960), pp. 145-155.

133. Van Beesten, C. [Discussion of C.R. Neill's "Measurements of Bridge Scour and Bed Changes in a Flooding Sand-Bed River"], Proceedings, Institution of Civil Engineers, Vol. 36, February, 1967, pp. 400-401.

134. Varzeliotis, A.N. Model Studies of Scour Around Bridge Piers and Stone Aprons. M.Sc. Thesis, University of Alberta, Edmonton, Alberta, September, 1960.

135. Veiga da Cunha, L. [Discussion of H.W. Shen et al. "Local Scour Around Bridge Piers"], Journal of the Hydraulics Division, Am. Soc. of Civil Engrs., Vol. 96, No. HY8 (August 1970), pp. 1742-1747.

136. Vinje, J.J. "On the Flow Characteristics of Vortices in Three-Dimensional Local Scour," Proceedings, Twelfth Congress of the International Assoc. for Hydraulic Research, Fort Collins, Colorado, September 1967, Vol. 3, pp. 207-217.

TABLES

TABLE I

THE VARIATION OF EQUILIBRIUM SCOUR DEPTH WITH AVERAGE VELOCITY, FOR DIFFERENT PIER DIAMETERS (CIRCULAR PIER) AND DIFFERENT BED SEDIMENTS, AS REPORTED BY BREUSERS

Pier Diameter b (cm.)	Flow Depth H (cm.)	Bed Sediment		Critical Velocity for Sediment transport $U_{crit.}$ (cm/sec.)	Velocity Ratio $\frac{U}{U_{crit.}}$	Scour Depth Ratio $\frac{d_{se}}{b}$	Max. Scour Depth Ratio $\frac{d_{sem}}{b}$
		Type	d_{50} (mm.)				
11	50	sand	0.2	25	0.8 1.0 1.2 1.4 1.6	1.1 1.25 1.4 1.5 1.5	1.5
5	25	sand	0.2	25	0.8 1.0 1.2 1.4 1.6	1.3 1.4 1.5 1.6 1.6	1.6
11	50	poly-styrene	1.5	9	1.0 1.2 1.4 1.6	1.5 1.7 1.65 1.65	1.7
21	50	poly-styrene	1.5	9	1.0	1.5	

TABLE II

VALUES OF THE COEFFICIENT K_H USED IN THE EQUATION OF JAROSLAVTSIEV

Flow Depth Ratio	H/b_1	.6	1.0	1.5	2.0	2.5	3.0	3.5	4.0	5.0	6.0	8.0
Coefficient	K_H	.92	.67	.46	.31	.22	.15	.10	.08	.05	.05	.05

TABLE III

SUMMARY OF SCOUR EXPERIMENTS

Test Pier: circular cylinder, dia. b = 0.33 ft. Bed Sand: d_{50} = 0.215 mm., $U_{crit.}$ = 0.90 ft./sec.

Test Series	Average Velocity U ft./sec.	Equilibrium Scour Depth d_{se} ft.	Time to reach d_{se} t_{se} min.	Depth of flow H ft.	$\frac{H}{b}$	$\frac{d_{se}}{b}$	$\frac{U}{U_{crit.}}$	Water Temp. °F.
1-A	0.89	0.37	720	1.26	3.8	1.12	0.99	63
1-B	0.85	0.33	690	1.24	3.7	1.00	0.95	58
1-C	0.77	0.31	1260	1.20	3.6	0.94	0.86	63
2-A1	0.85	0.37	1170	1.24	3.7	1.12	0.95	68
2-A2	0.85	0.36	1440	1.24	3.7	1.09	0.95	62
2-A3	0.85	0.38	1470	1.24	3.7	1.15	0.95	61
2-B	0.85	0.35	1320	1.24	3.7	1.06	0.95	65
2-C	0.85	0.31	1200	1.24	3.7	0.94	0.95	63
2-D	0.85	0.28	960	1.24	3.7	0.85	0.95	60
3-A	0.85	0.21	240	1.24	3.7	0.64	0.95	56
3-B	0.77	0.18	300	1.20	3.6	0.55	0.86	58
4-A	0.77	0.30	810	1.20	3.6	0.91	0.86	61
4-B	0.65	0.16	180	1.12	3.4	0.48	0.72	62
5	0.79	0.30	720	1.20	3.6	0.91	0.88	62

FIGURES

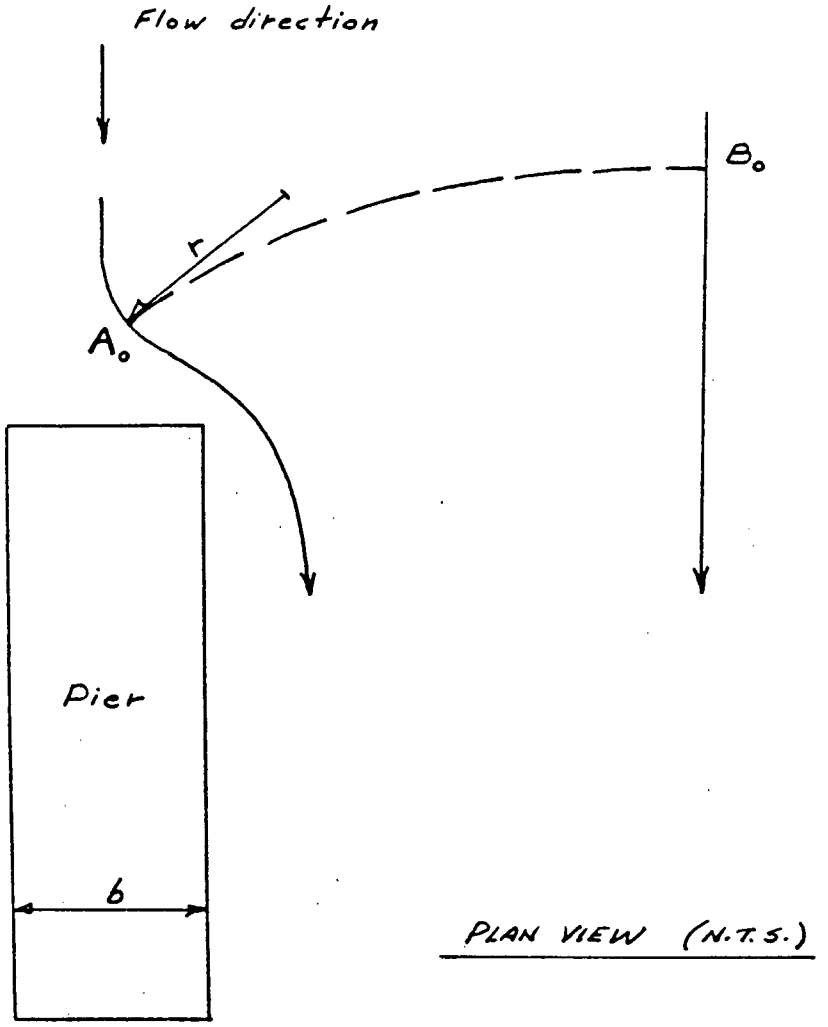

Figure 1. Representation of curvature of the flow near an obstruction, as proposed by Tison.

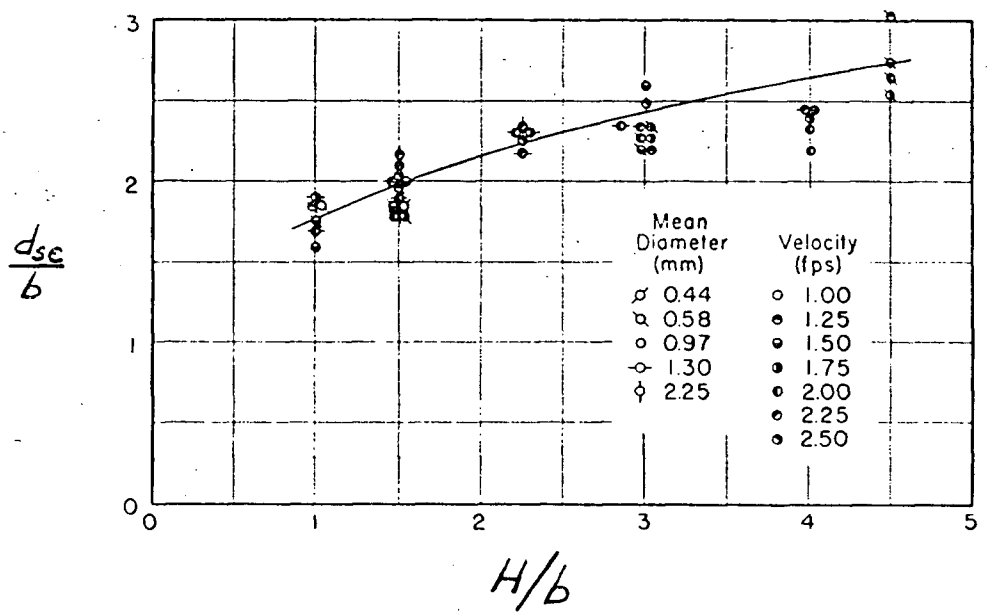

Figure 2. Laursen's non-dimensional plot of equilibrium scour depth (d_{se}) versus flow depth (H), for a rectangular pier of width b, at an angle of attack of 30^{o}.

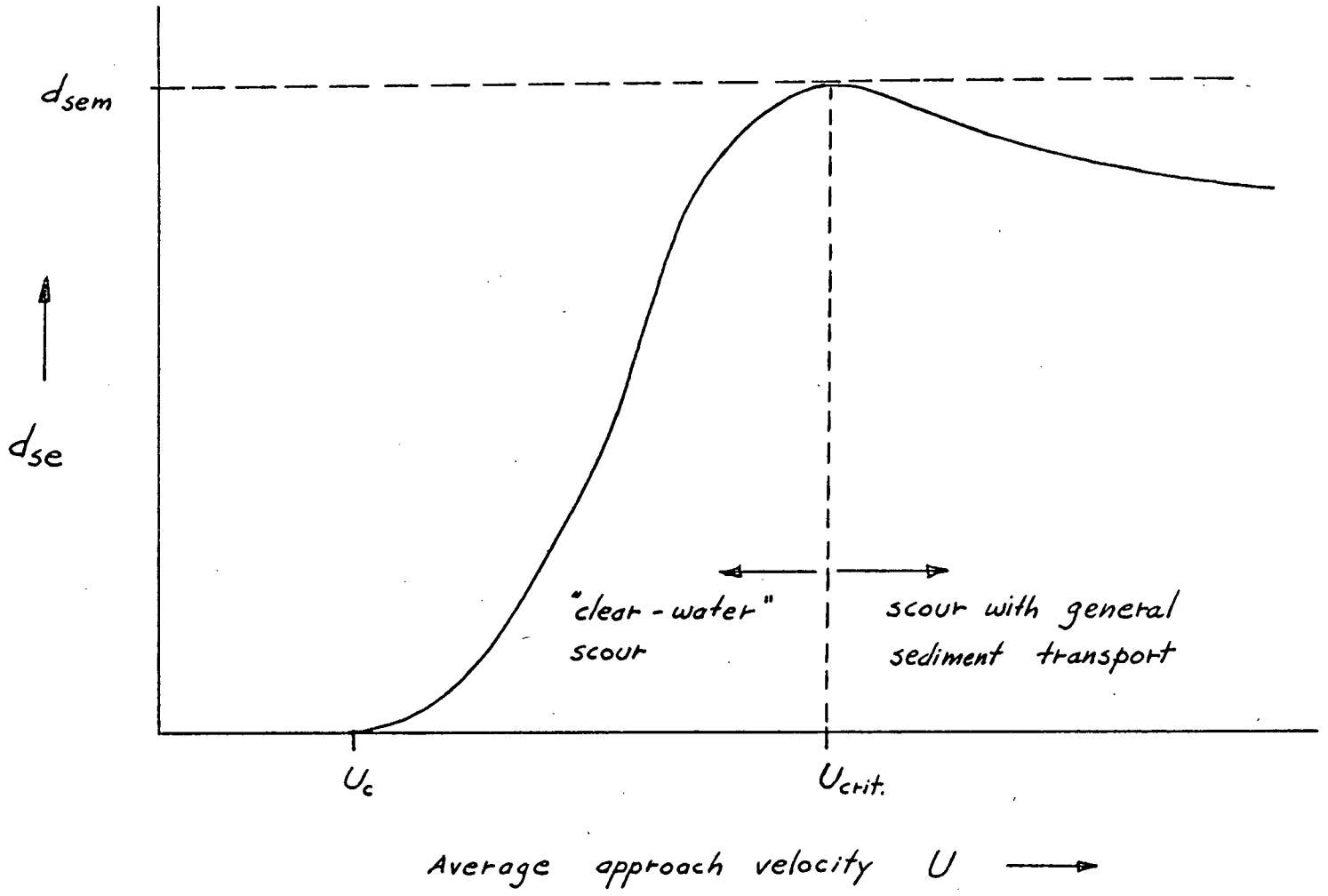

Figure 3. Schematic diagram showing variation of the equilibrium scour depth (d_{se}) with average flow velocity (U), as found by Chabert and Engeldinger (for any pier).

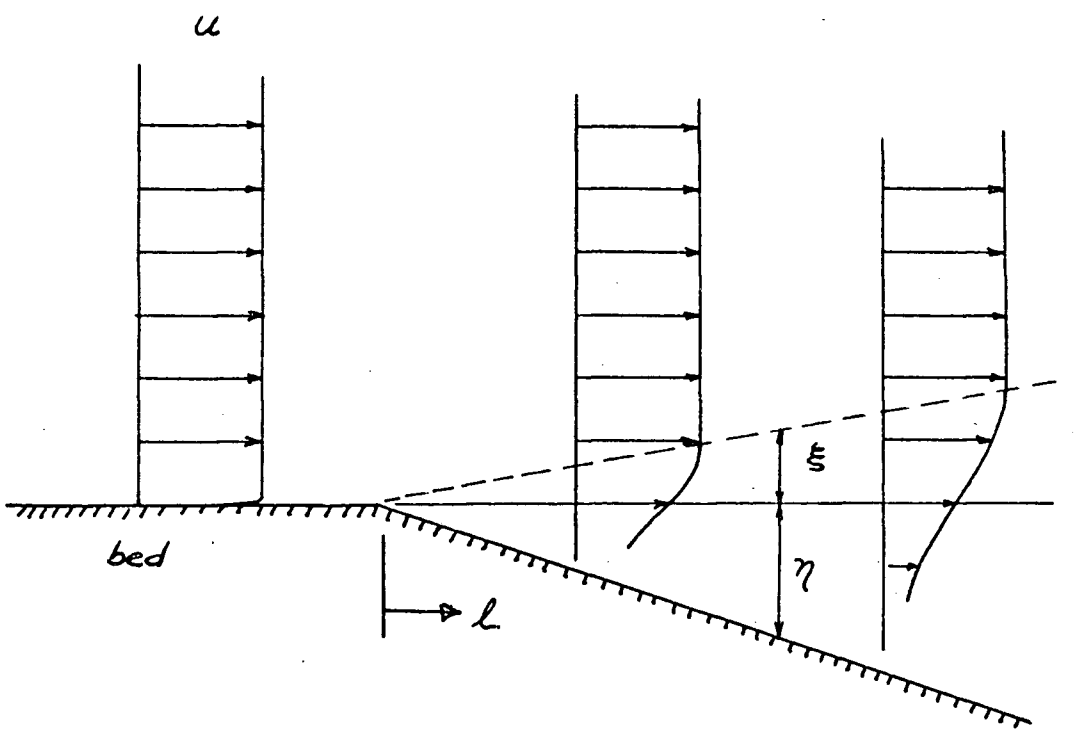

Figure 4. Velocity diffusion into the scour hole, according to Tarapore.

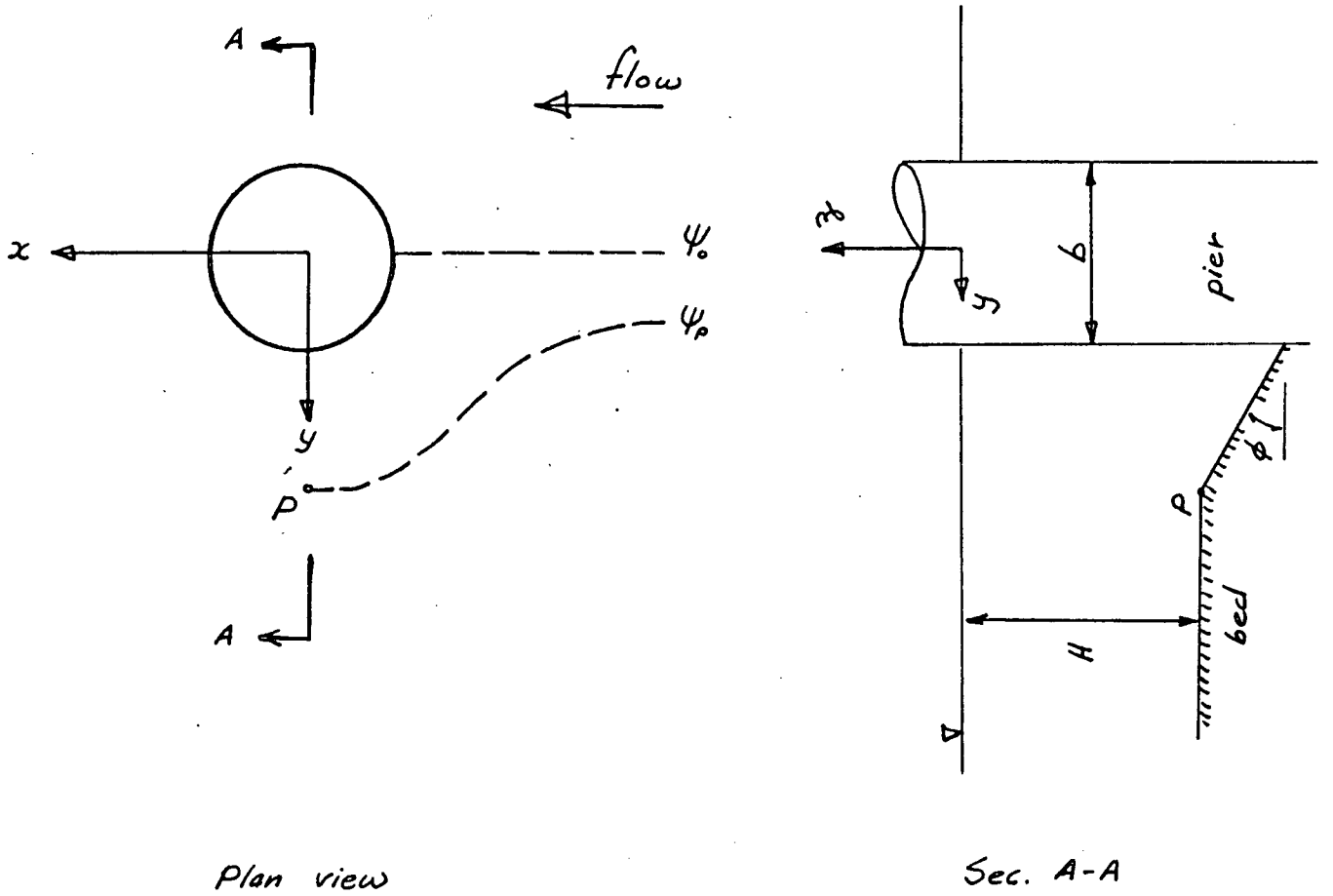

Figure 5. Schematic illustration of scour hole at equilibrium conditions, according to Tarapore.

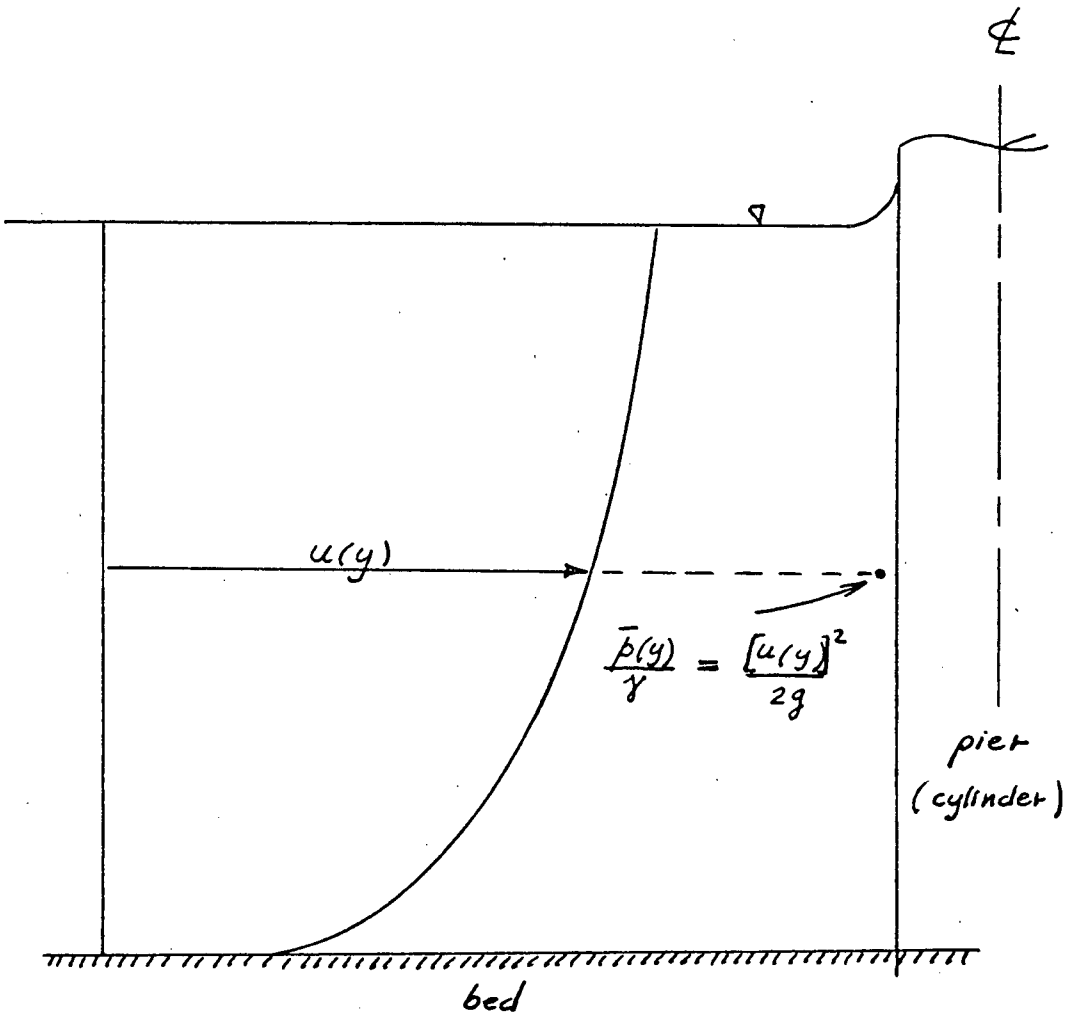

Figure 6. Approach flow velocity distribution and stagnation pressure on the plane of symmetry in front of a circular cylinder.

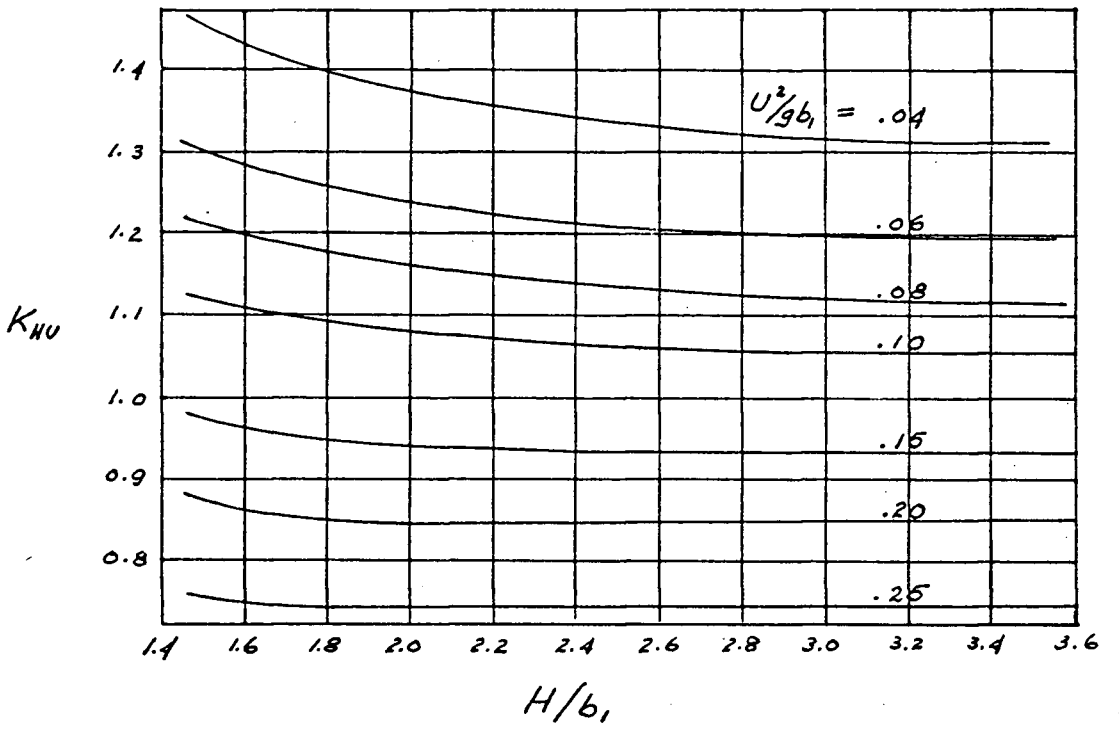

Figure 7. Values of the coefficient K_{HU} to be used in the Maza and Sanchez version of Jaroslavtsiev's equation.

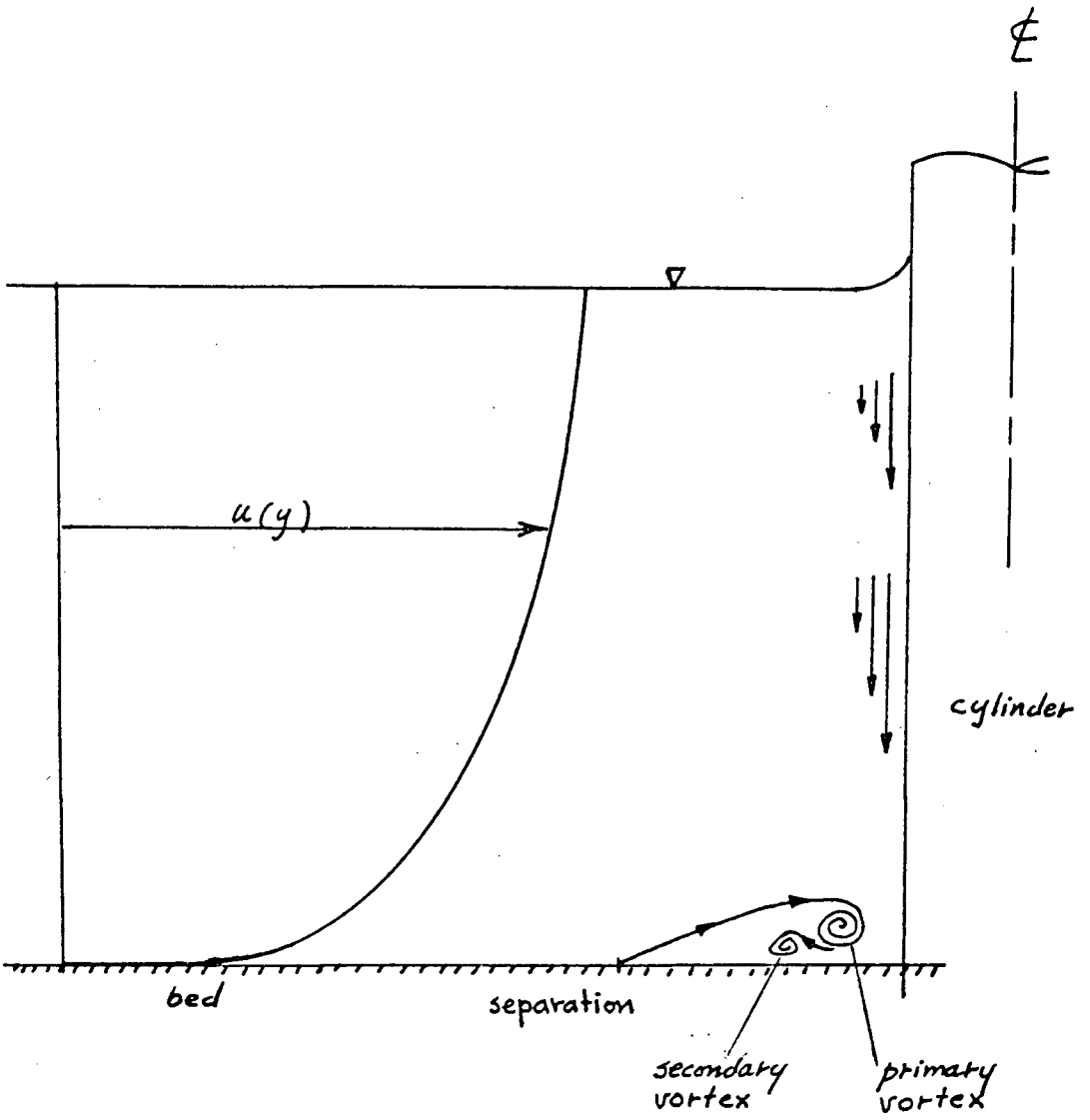

Figure 8. Idealized representation of the flow on the plane of symmetry in front of a circular cylinder; Shen et al.

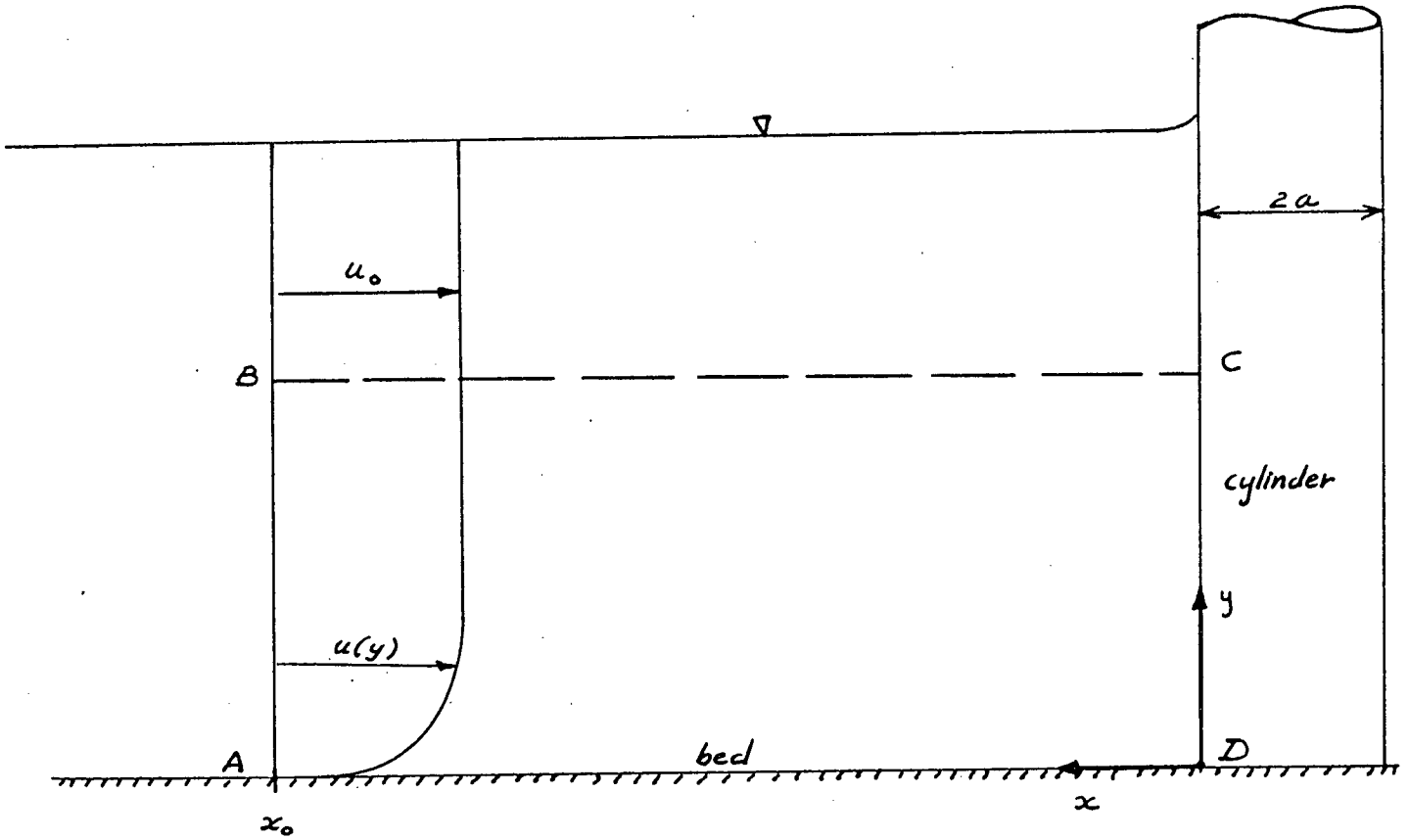

Figure 9. Control volume on the stagnation plane in front of a circular cylinder; Shen et al.

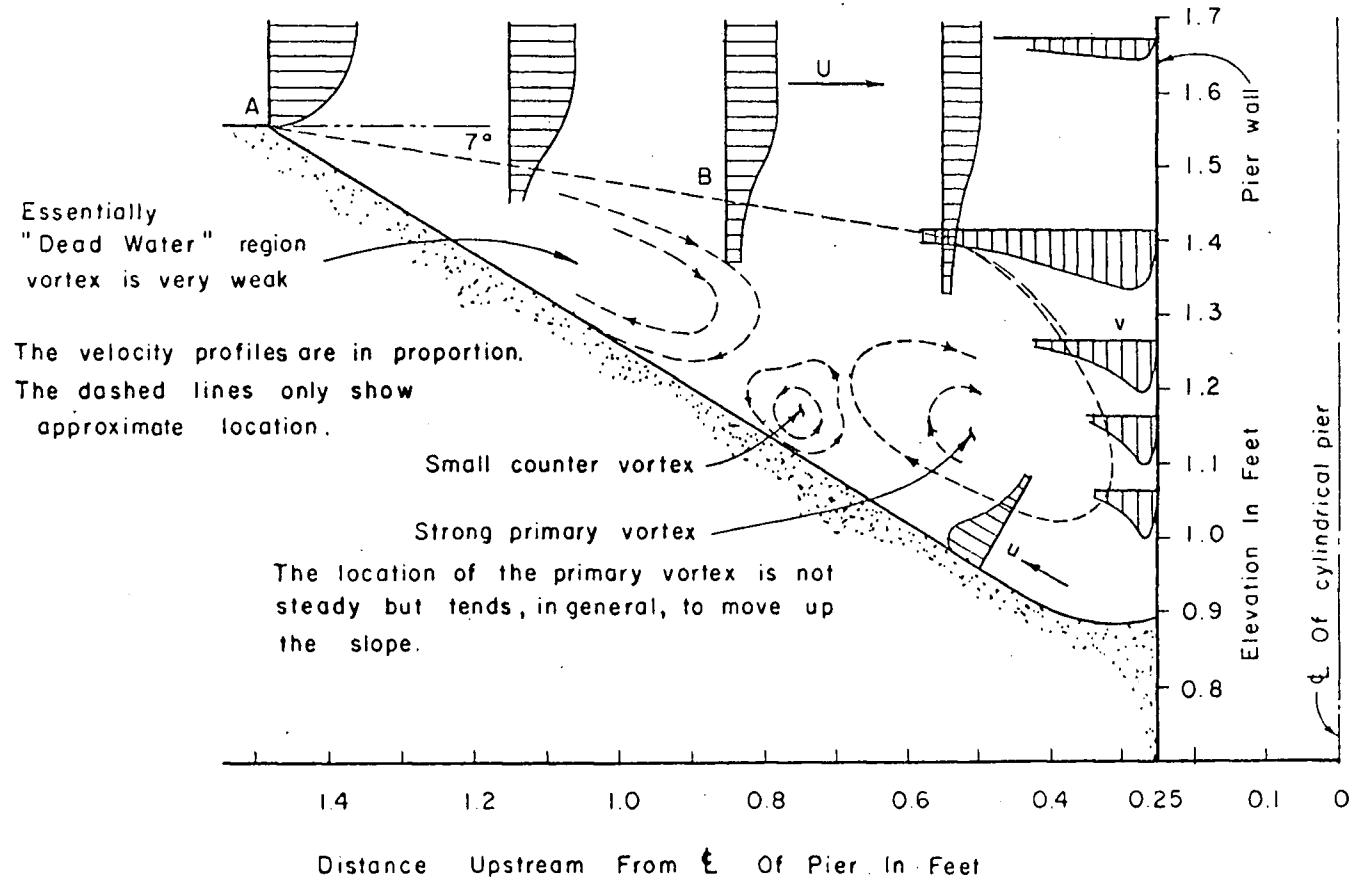

Figure 10. Schematic representation of the velocity distribution and flow pattern in the scour hole on the plane of symmetry in front of a circular cylinder; Shen et al.

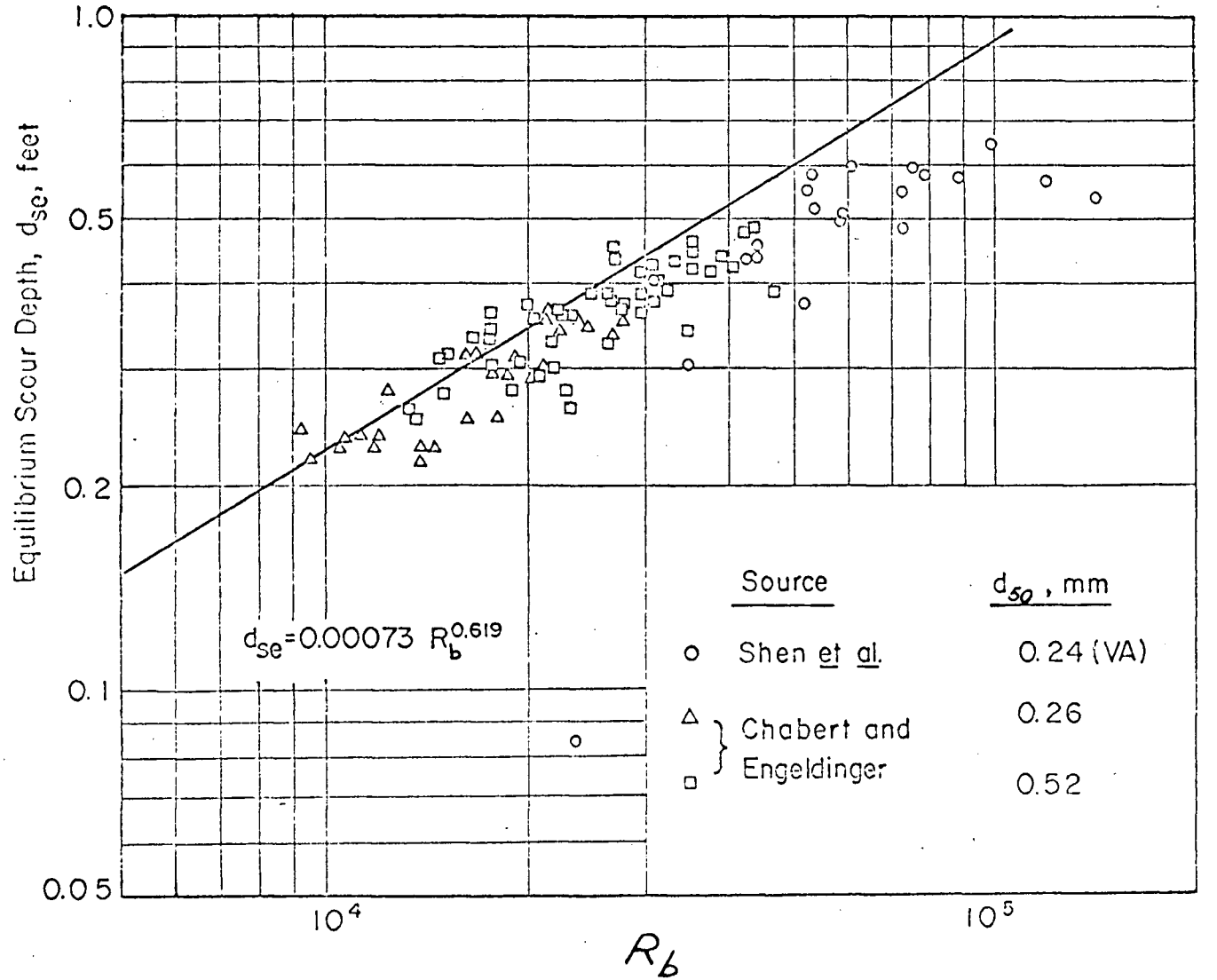

Figure 11. Equilibrium scour depth versus pier Reynolds number (R_b) for circular cylindrical piers; Shen et al.

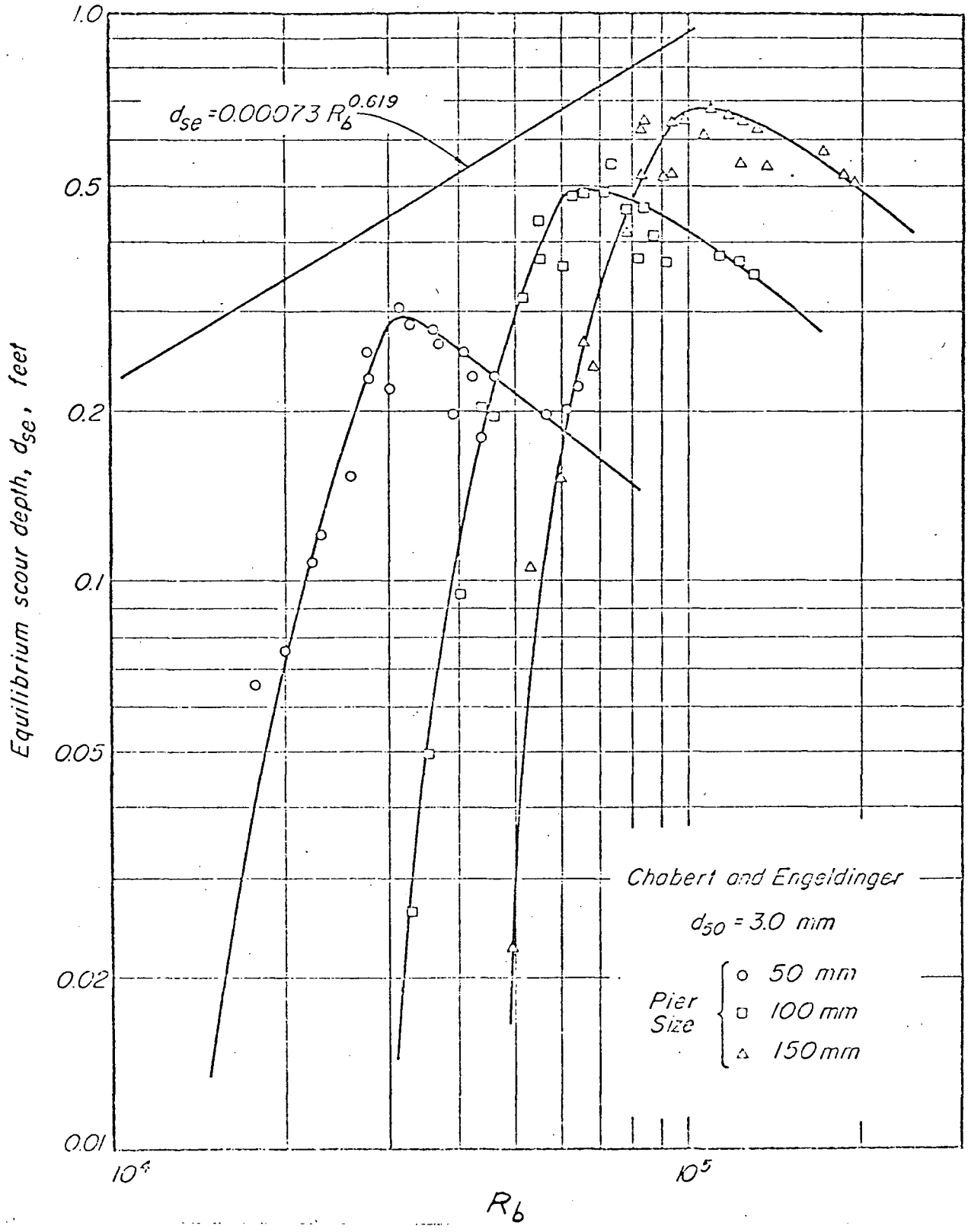

Figure 12. Equilibrium scour depth versus pier Reynolds number (R_b) for circular cylindrical piers of different sizes; Shen et al.

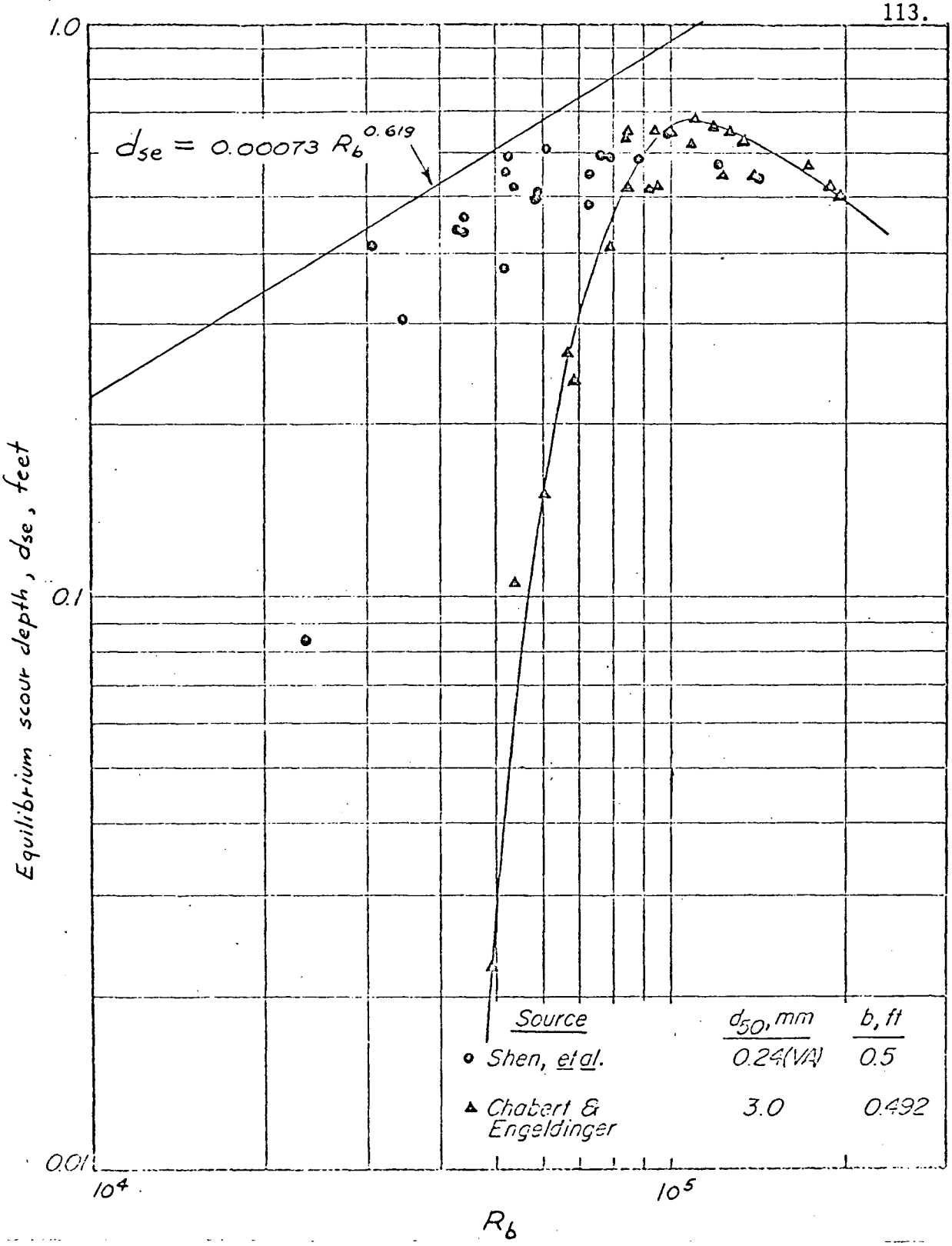

Figure 13. Equilibrium scour depth versus pier Reynolds number (R_b), for circular cylindrical piers and different grain sizes; Shen et al.

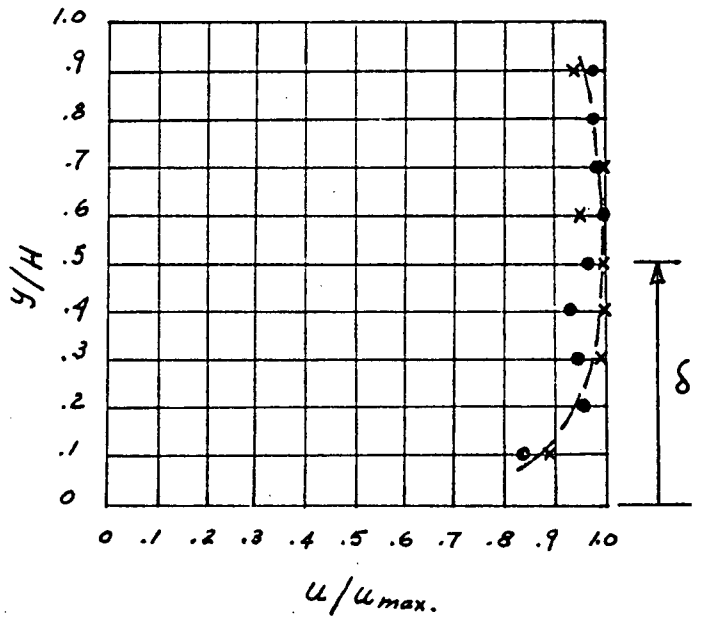

H = 10 cm. • run 1

u_{max} = 27.7 cm./sec. × run 2

Figure 14. Velocity distribution along the vertical, in the experiments of Tanaka and Yano.

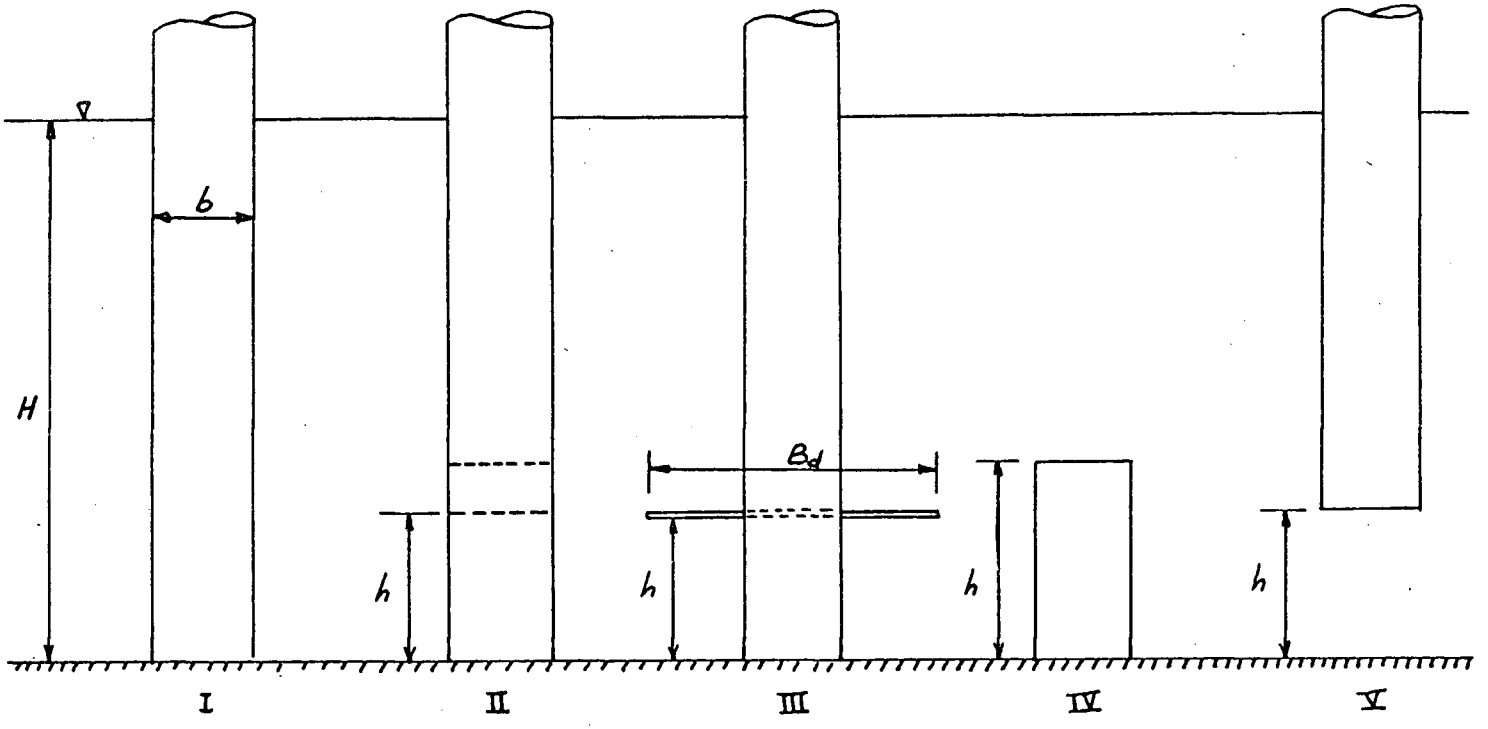

Figure 15. Types of circular cylindrical piers studied by Tanaka and Yano.

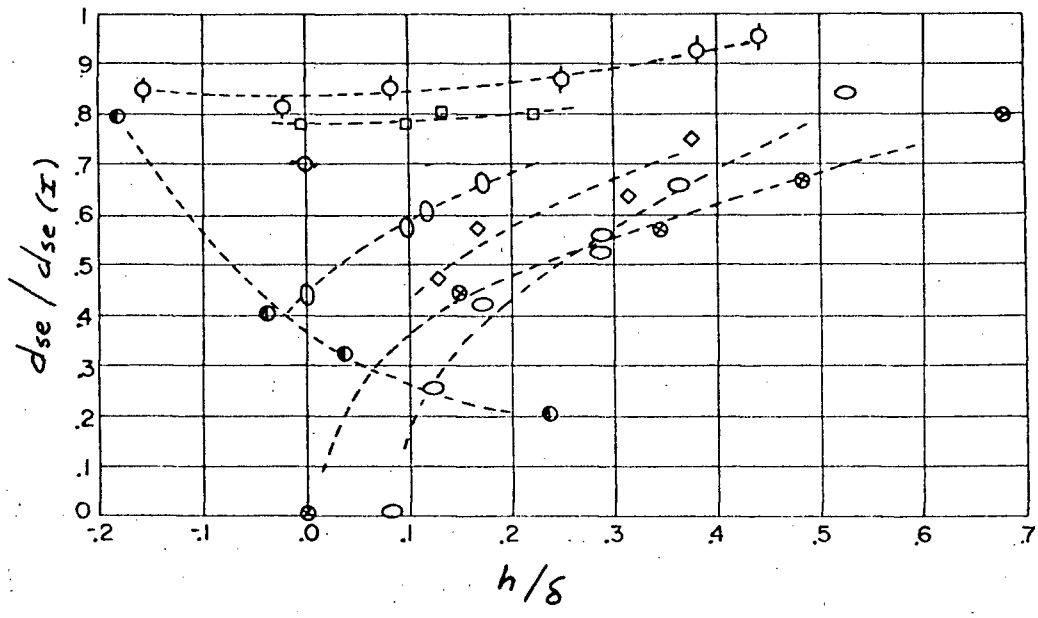

$d_{se(I)}$ = 5 cm. b = 3 cm. δ = 5 cm.

- II, 1 cm. sq. hole
- II, 2 cm. sq. hole
- III, B_d/b = 3
- III, B_d/b = 4
- III, B_d/b = 5
- III, B_d/b = 6
- IV
- V

Figure 16. Equilibrium depth of scour for different circular cylindrical pier types; Tanaka and Yano.

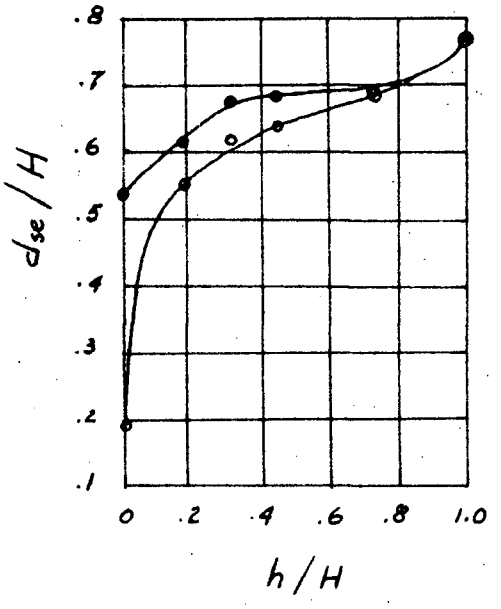

Figure 17. Scour depth versus disc position, for a circular cylindrical pier; Thomas.

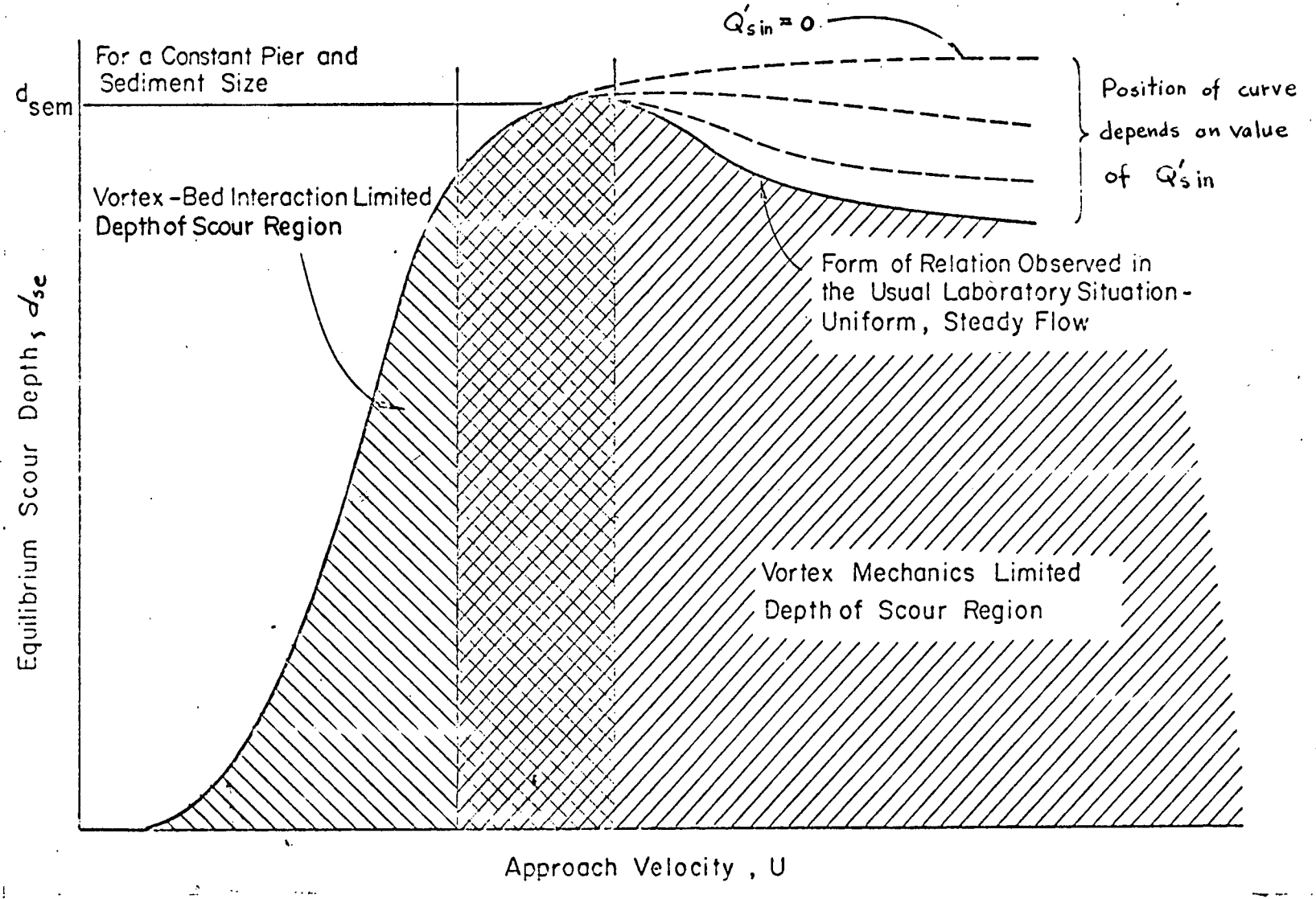

Figure 18. The scour regions of Schneider (for any pier).

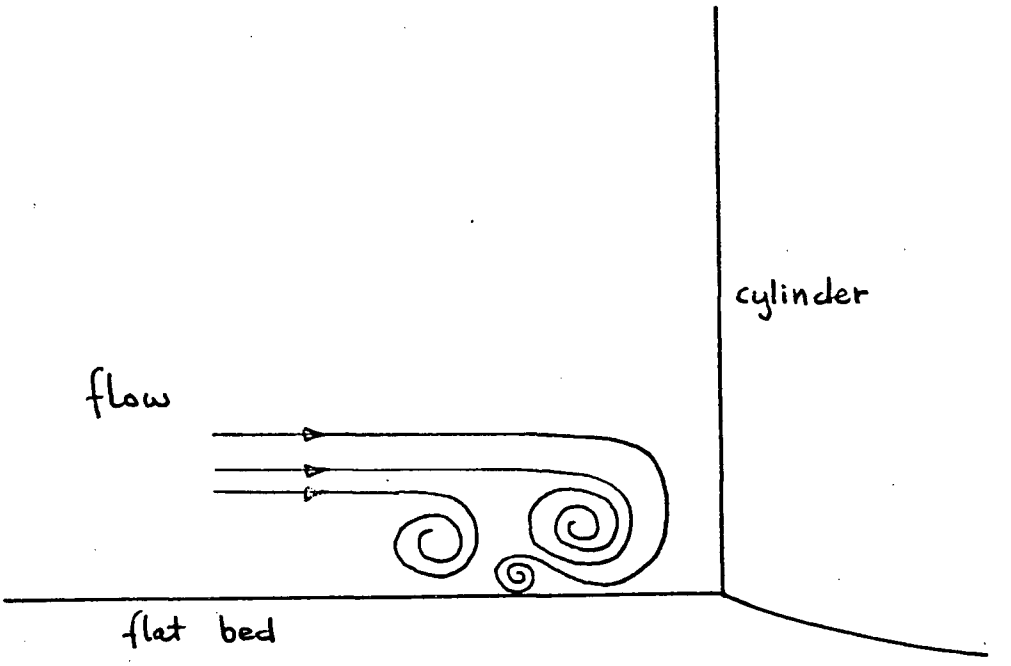

Figure 19. Sketch of the vortex structure on the plane of symmetry in front of a circular cylinder in a laminar boundary layer, from a photograph of an experiment of Gregory and Walker, published in Thwaites[125].

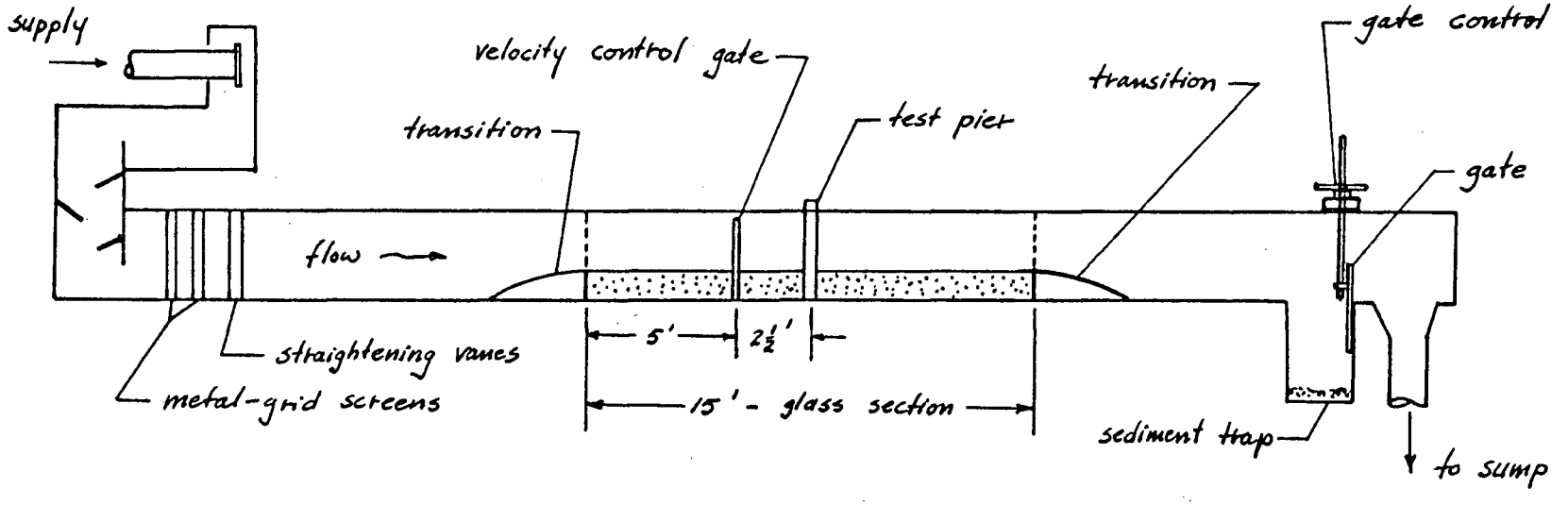

Figure 20. Sketch of laboratory flume cross-section showing general arrangement.

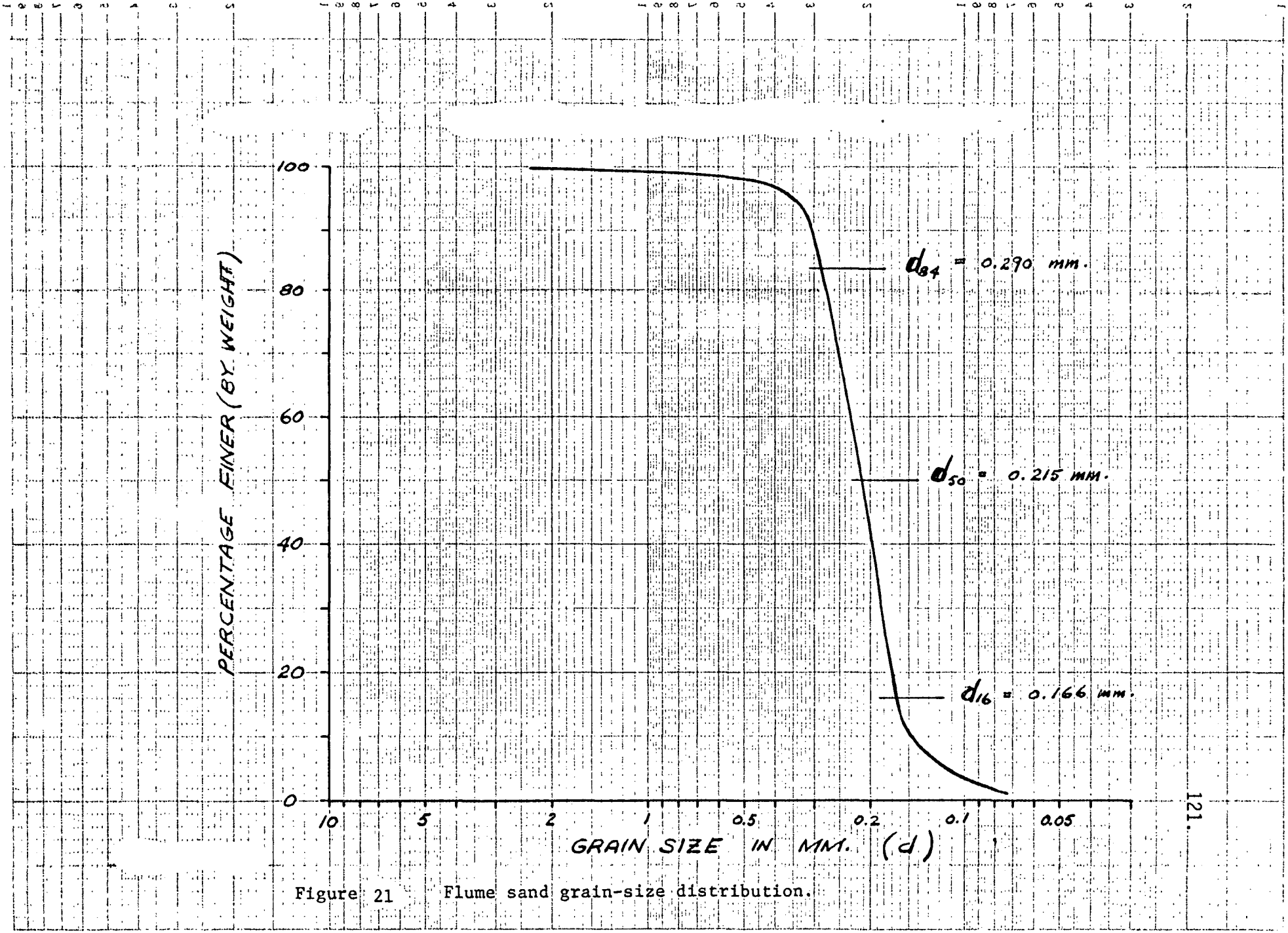

Figure 21 Flume sand grain-size distribution.

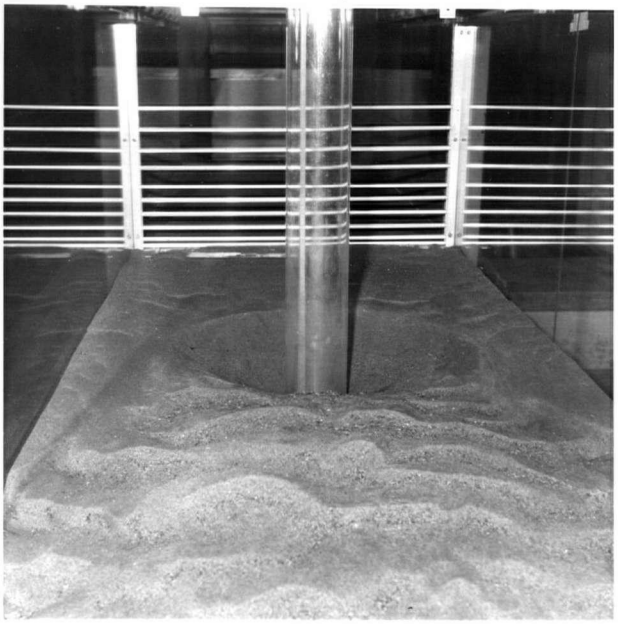

Figure 22. View of velocity-control gate from a position downstream of the pier (gate is reflected in glass walls on either side).

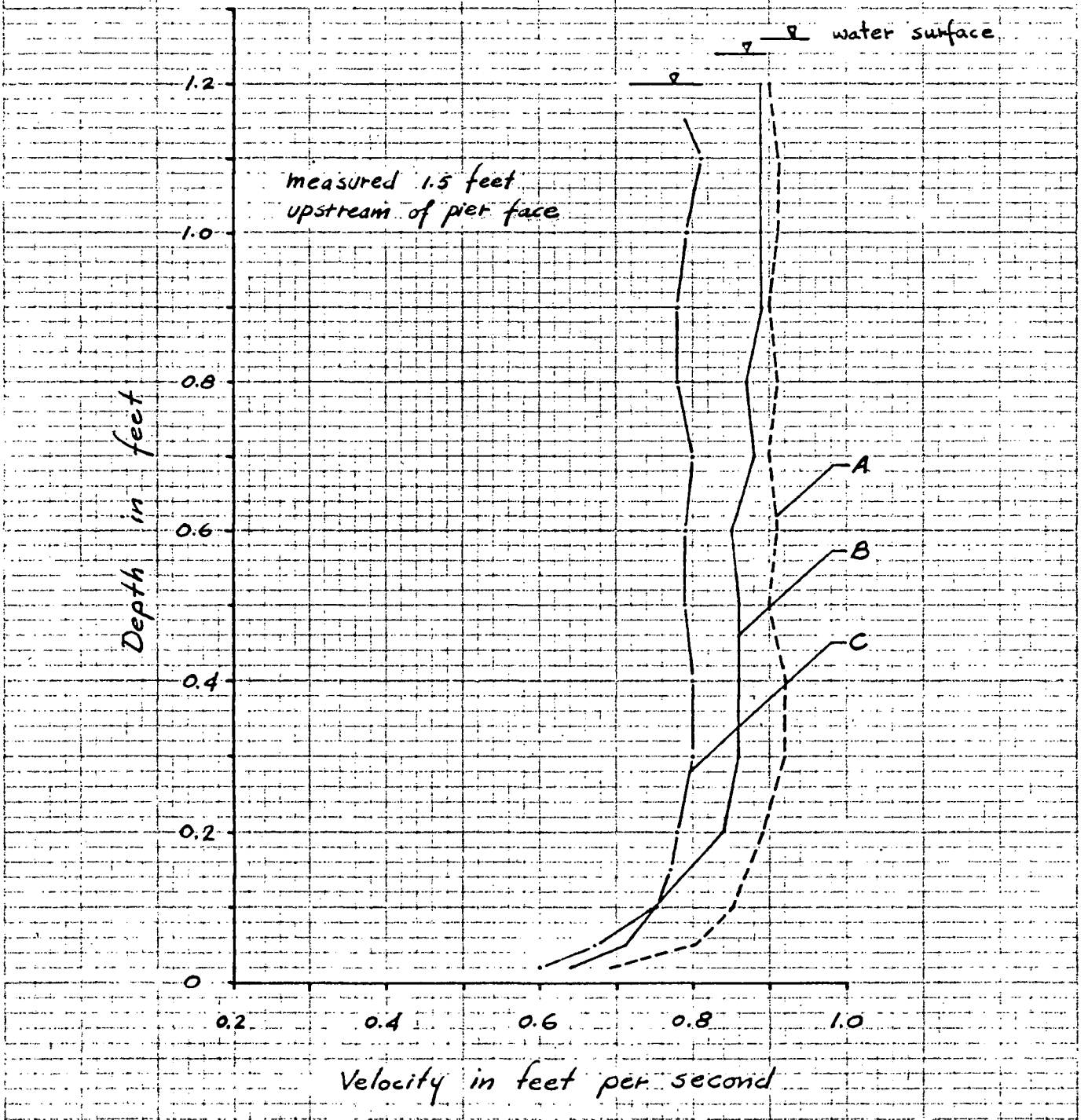

Figure 23. Velocity profiles, series 1.

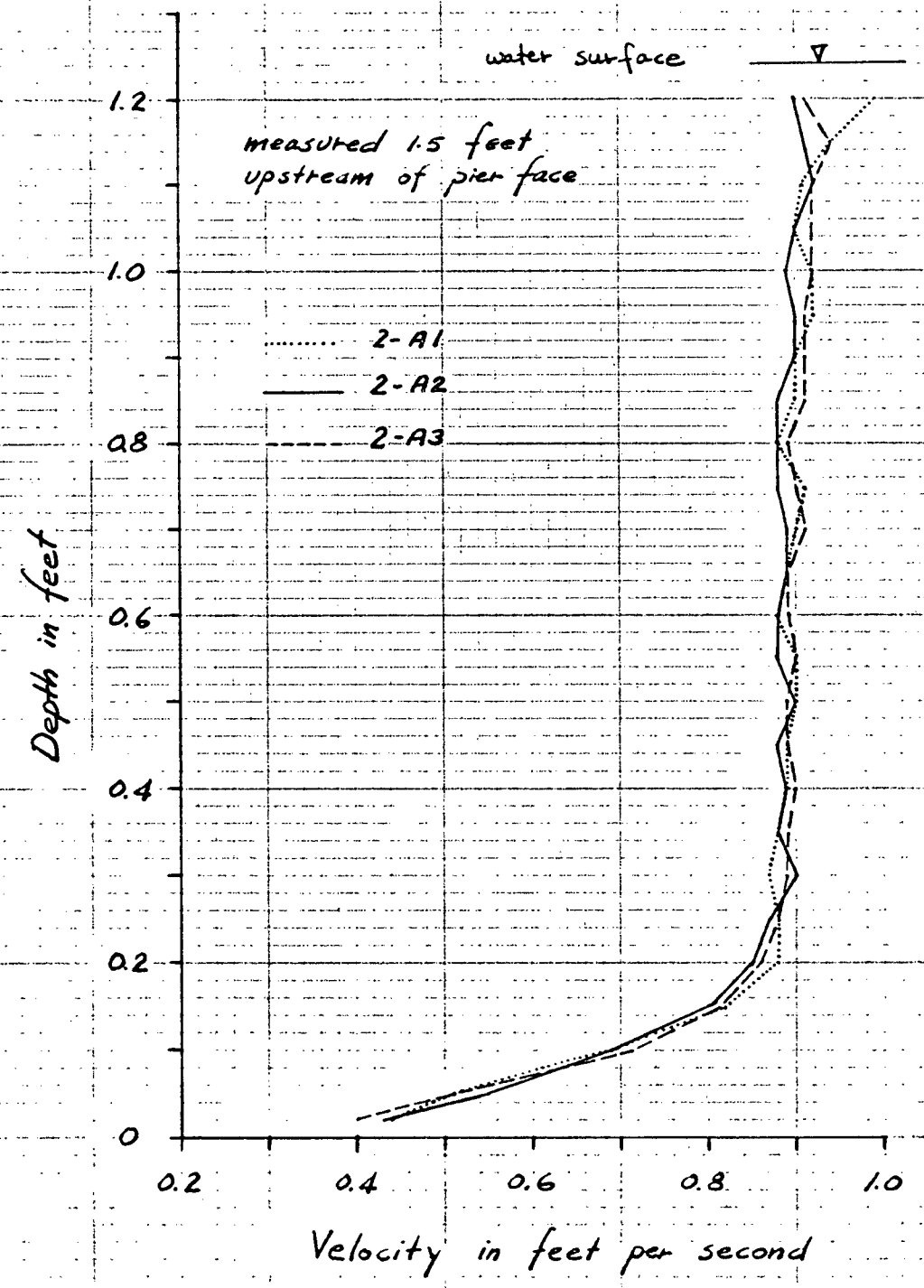

Figure 24. Velocity profiles, series 2-A.

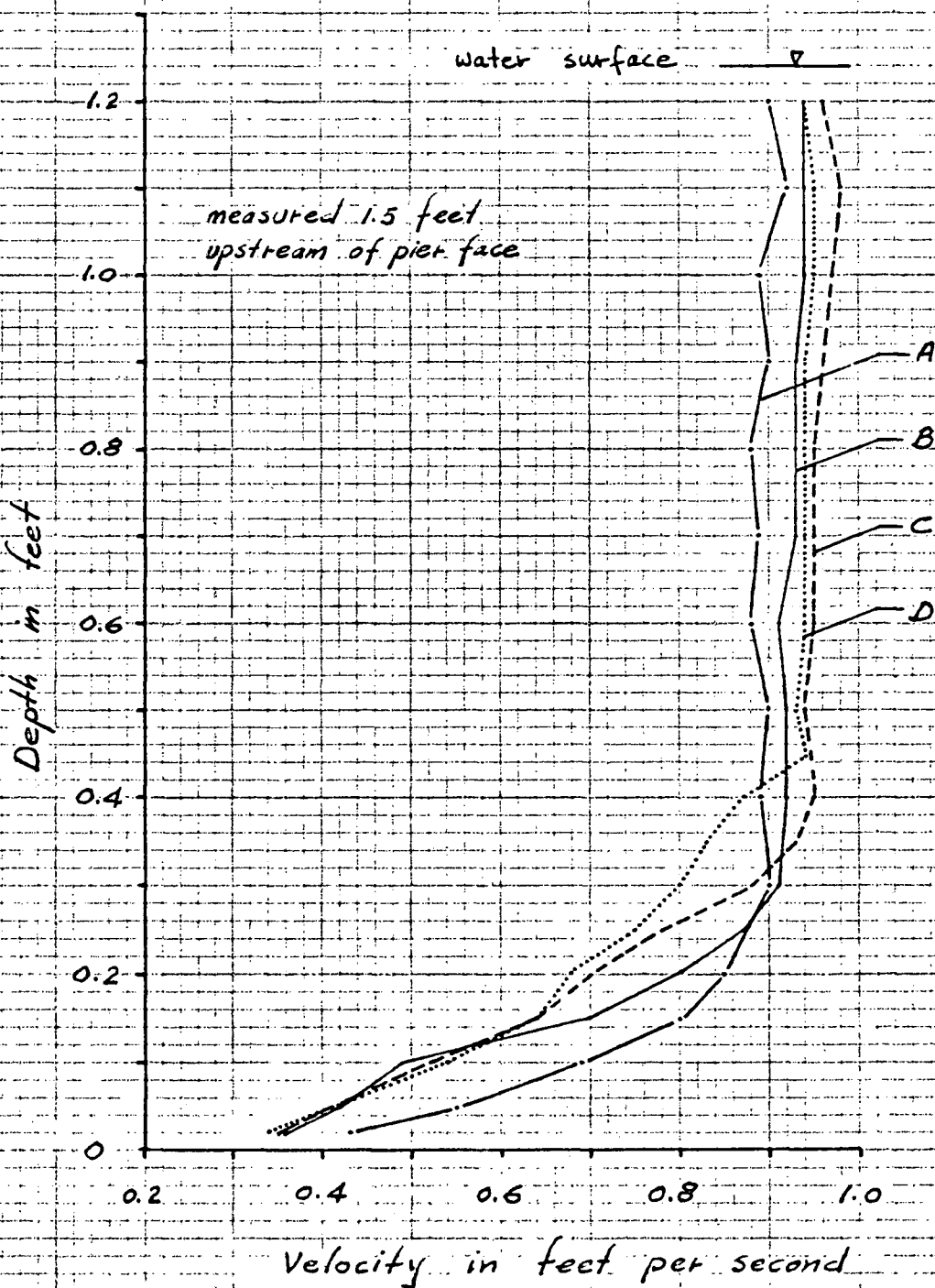

Figure 25. Velocity profiles, series 2.

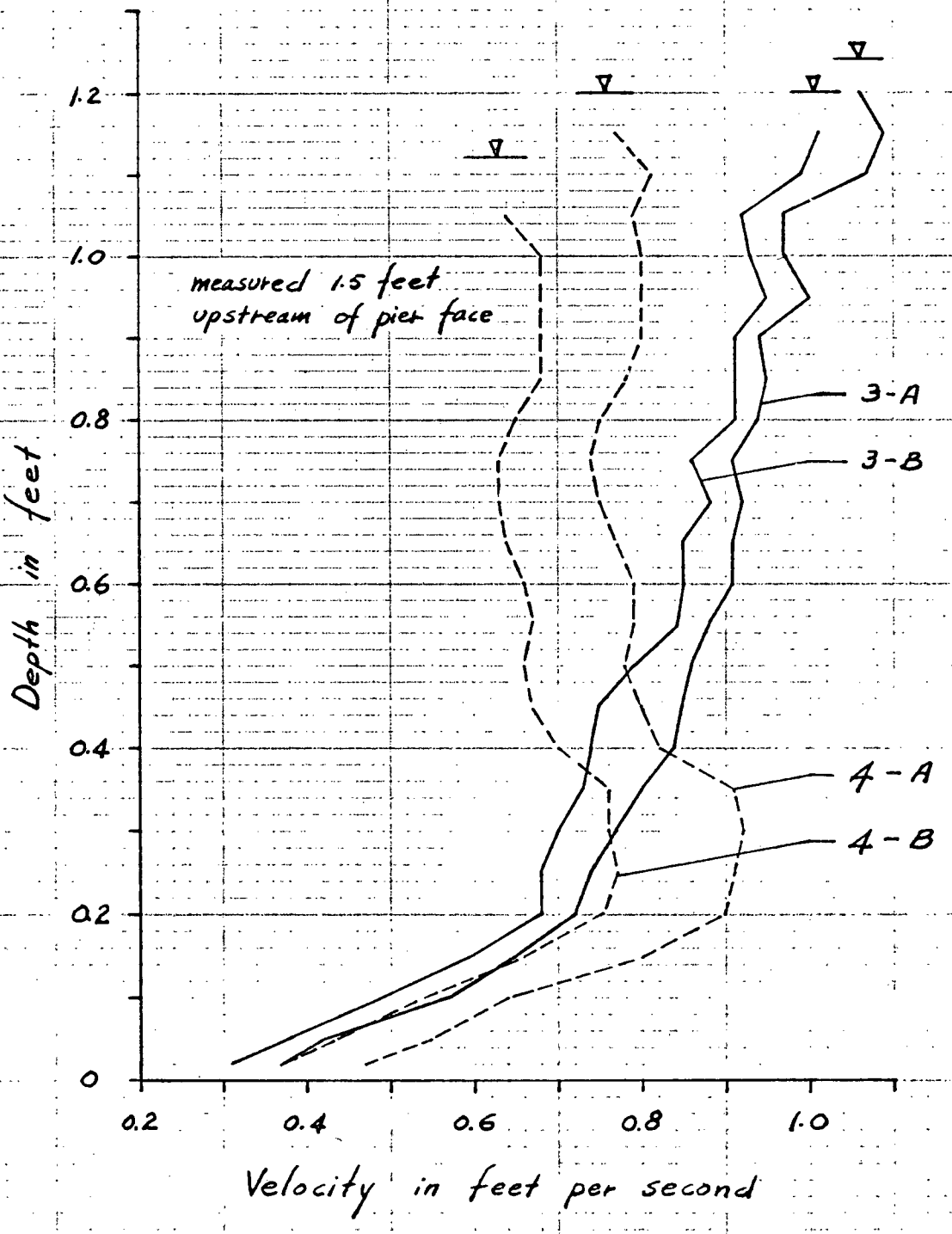

Figure 26. Velocity profiles, series 3 and 4.

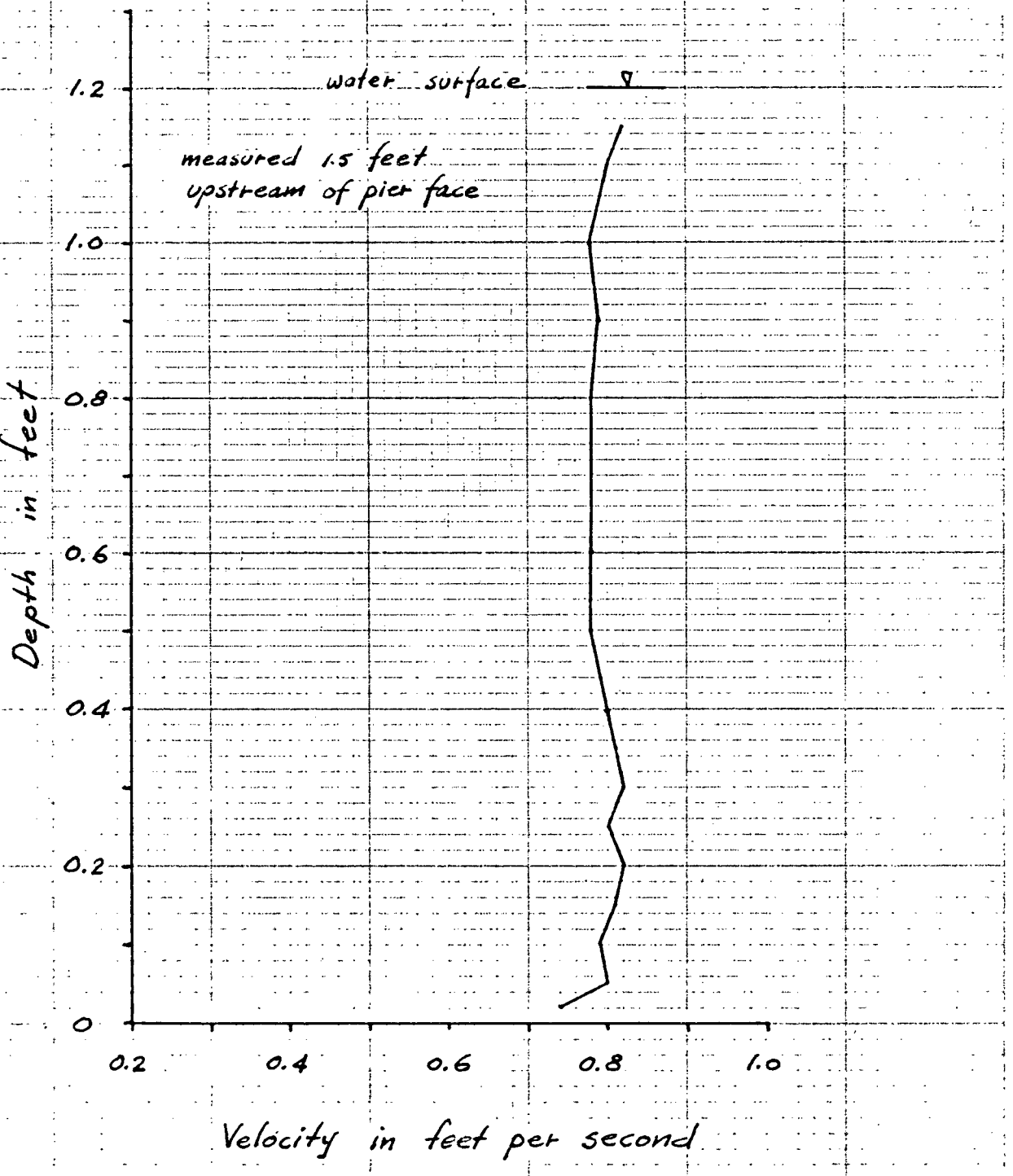

Figure 27. Velocity profile, series 5.

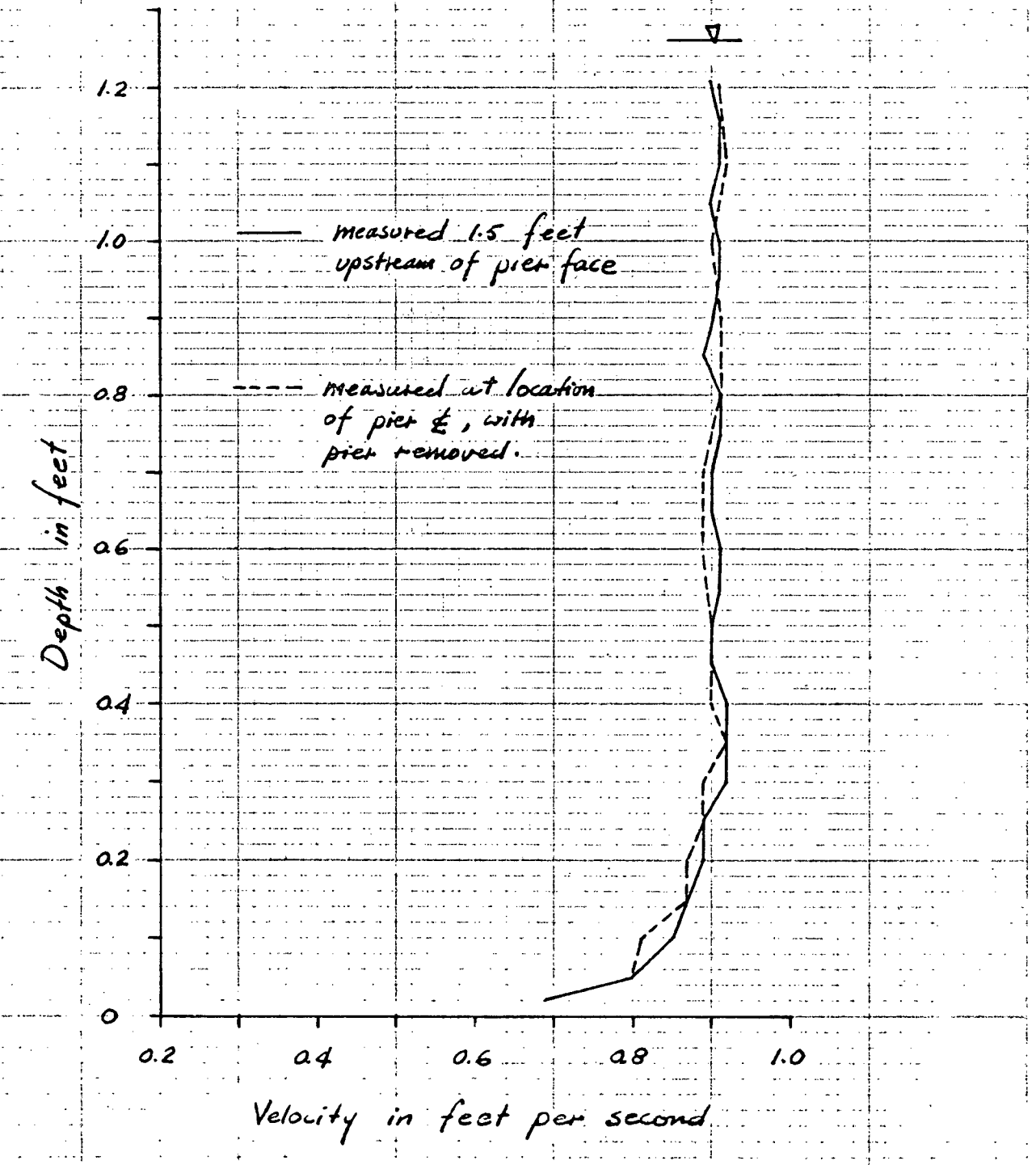

Figure 28. Stability of velocity profiles, series 1-A.

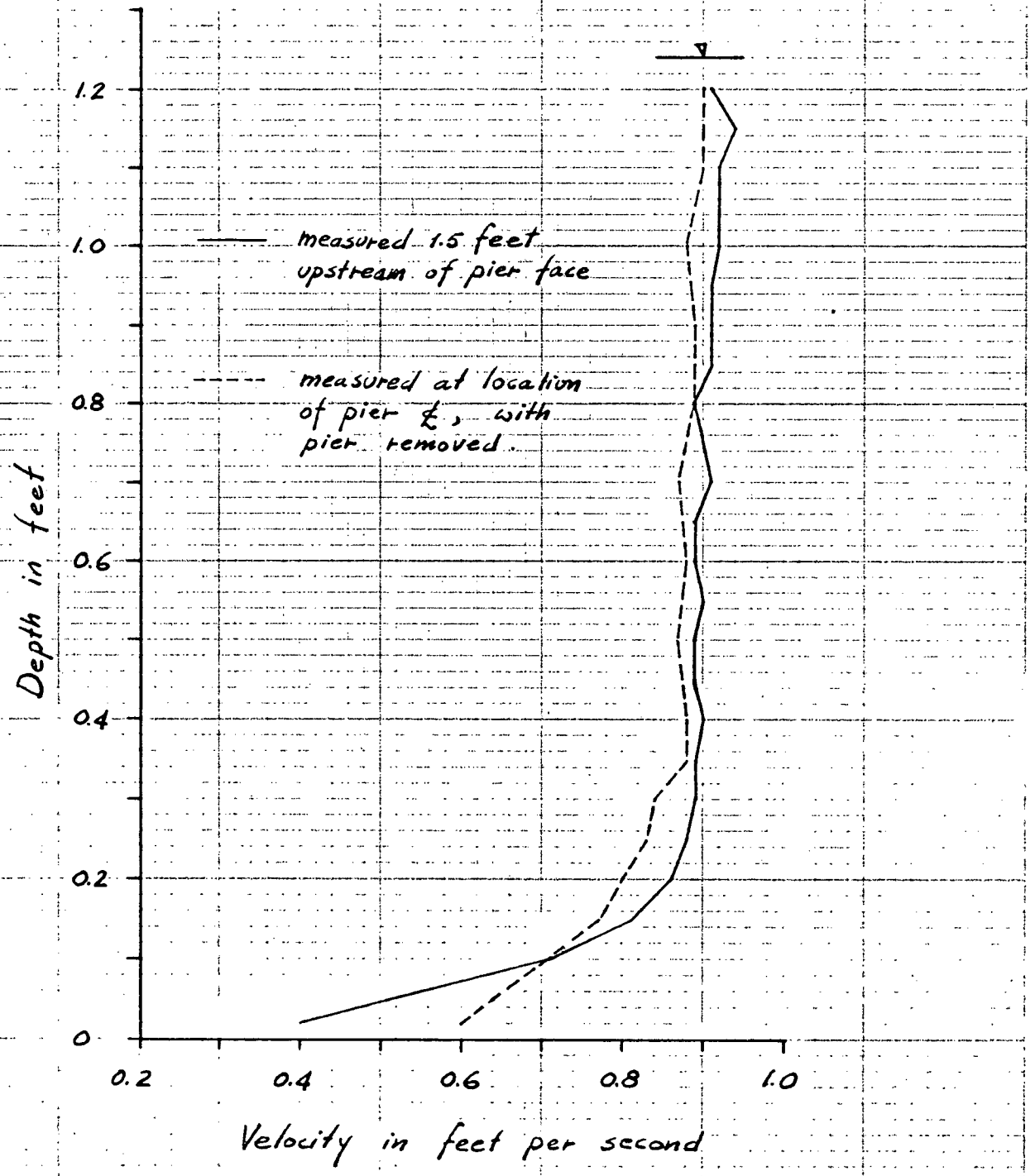

Figure 29. Stability of velocity profile, series 2-A3.

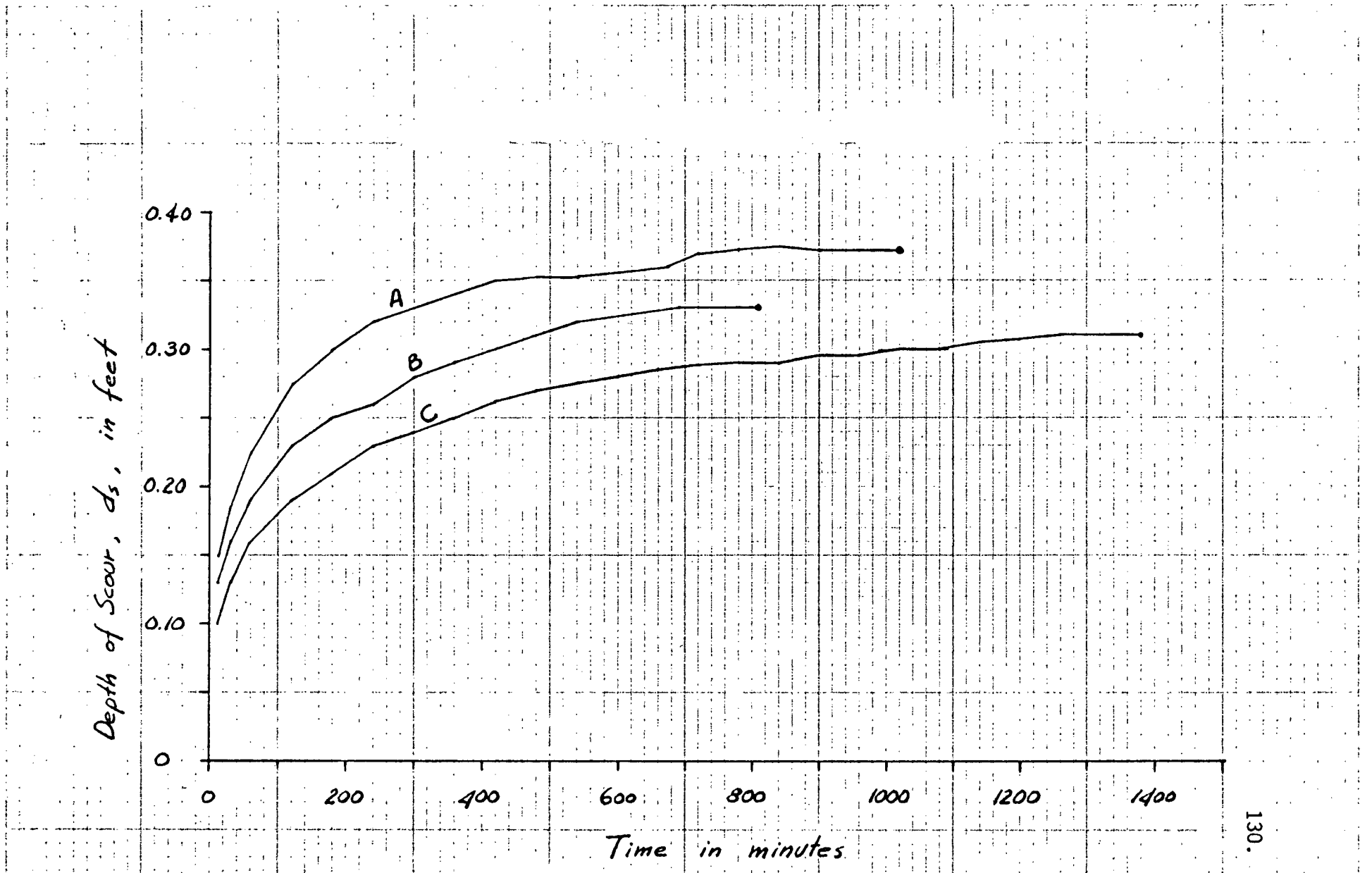

Figure 30. Scour hole development with time, series 1.

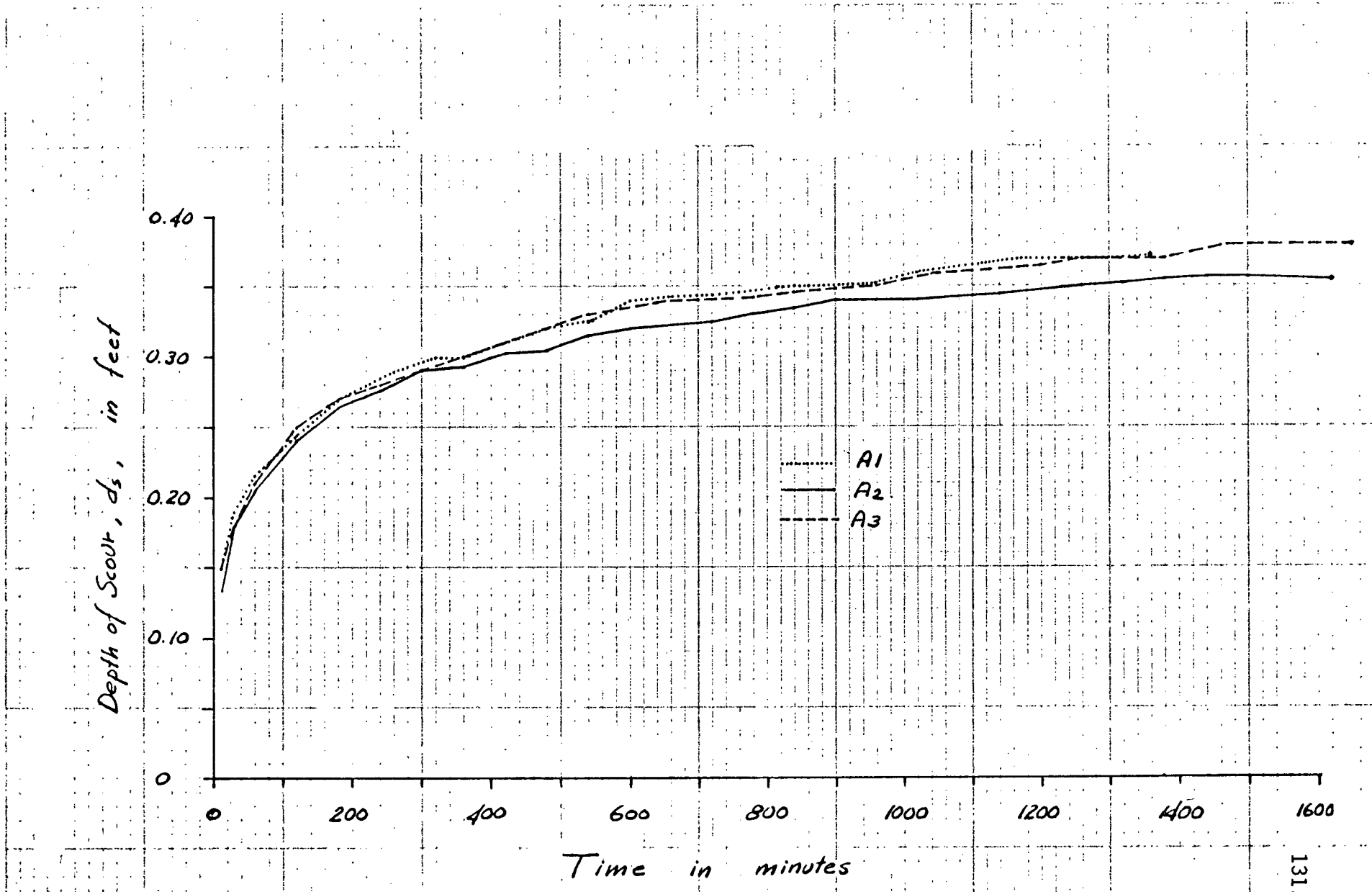

Figure 31 Scour hole development with time, series 2-A.

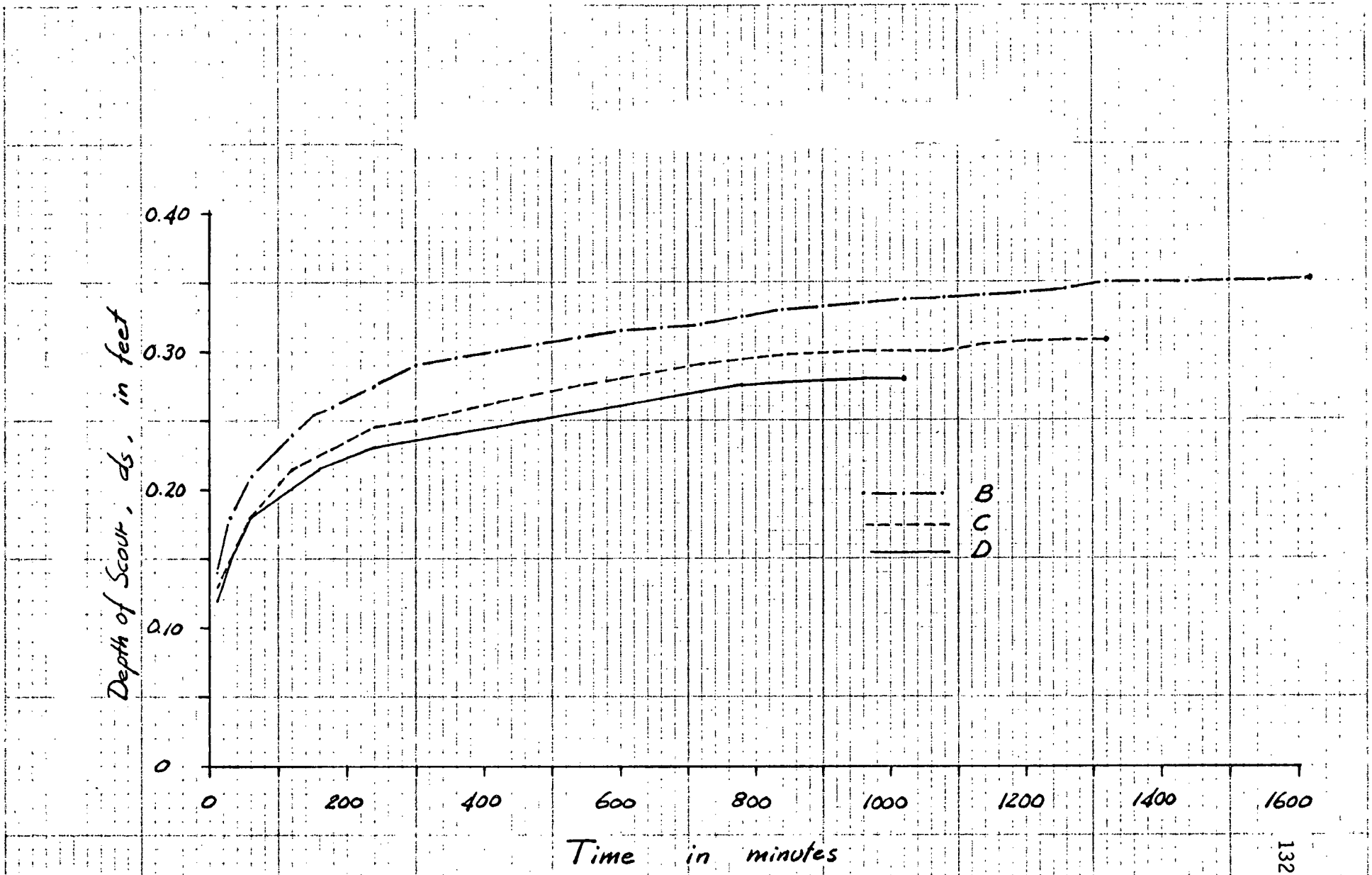

Figure 32. Scour hole development with time, series 2.

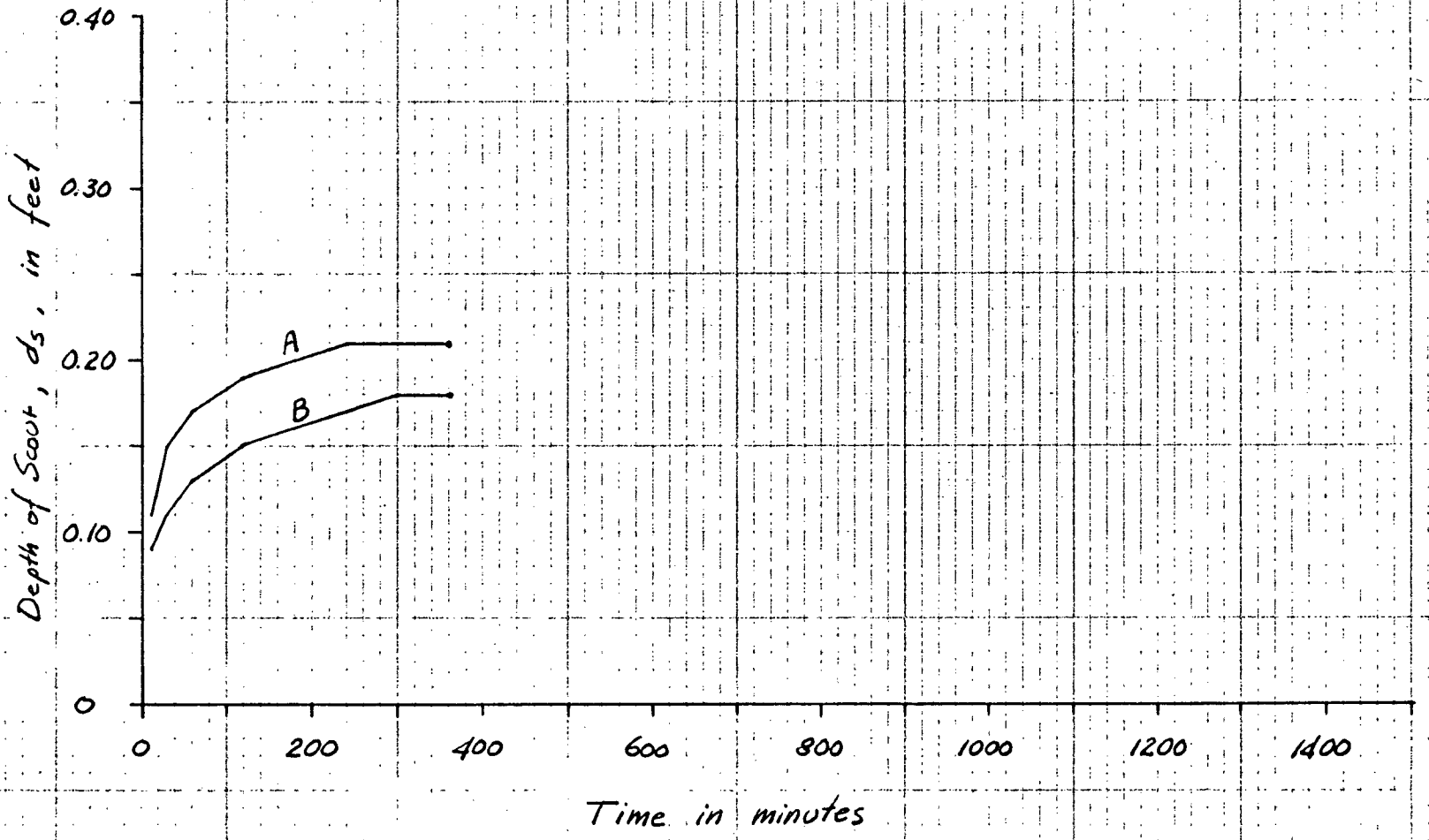

Figure 33. Scour hole development with time, series 3.

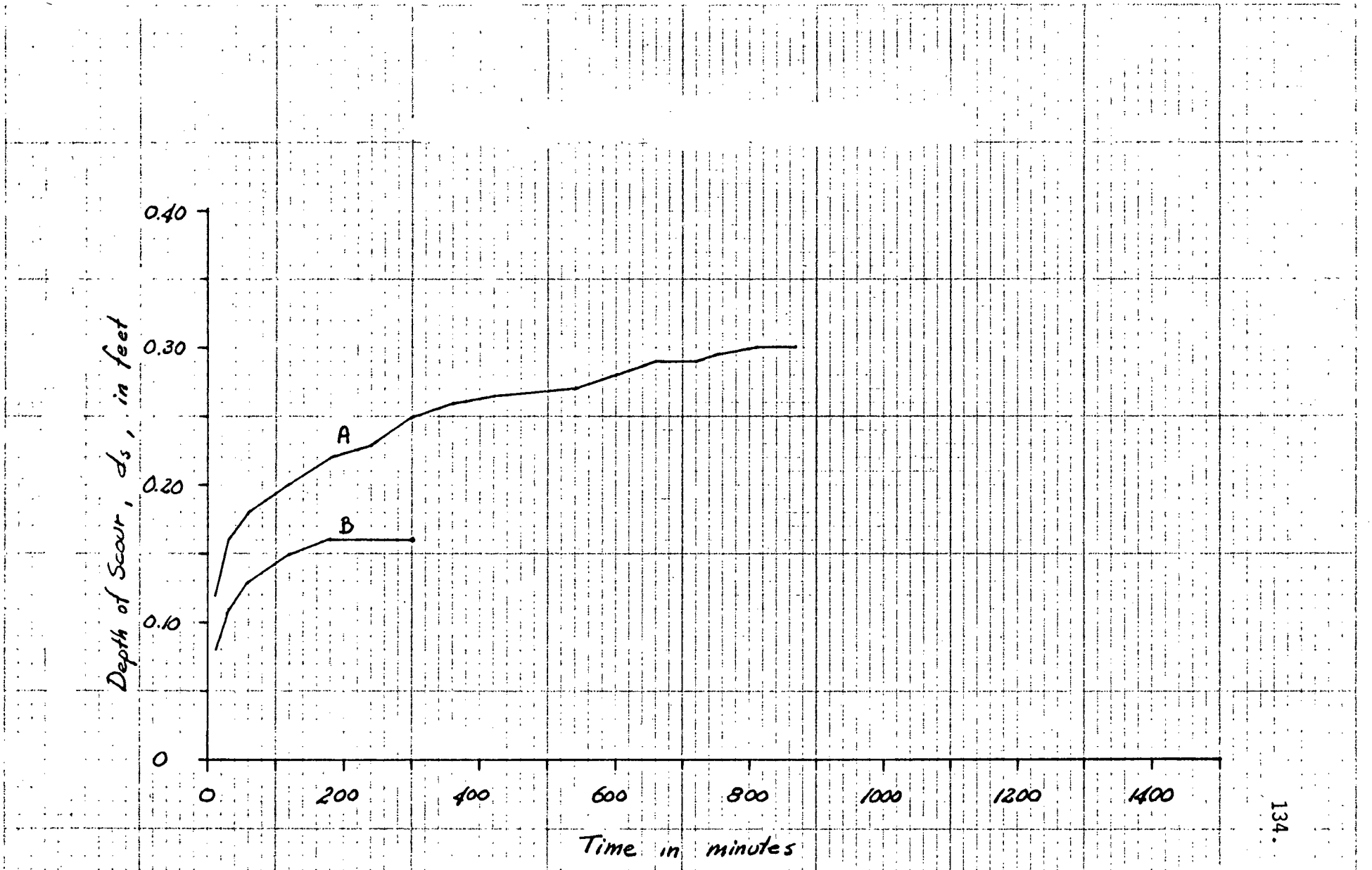

Figure 34. Scour hole development with time, series 4.

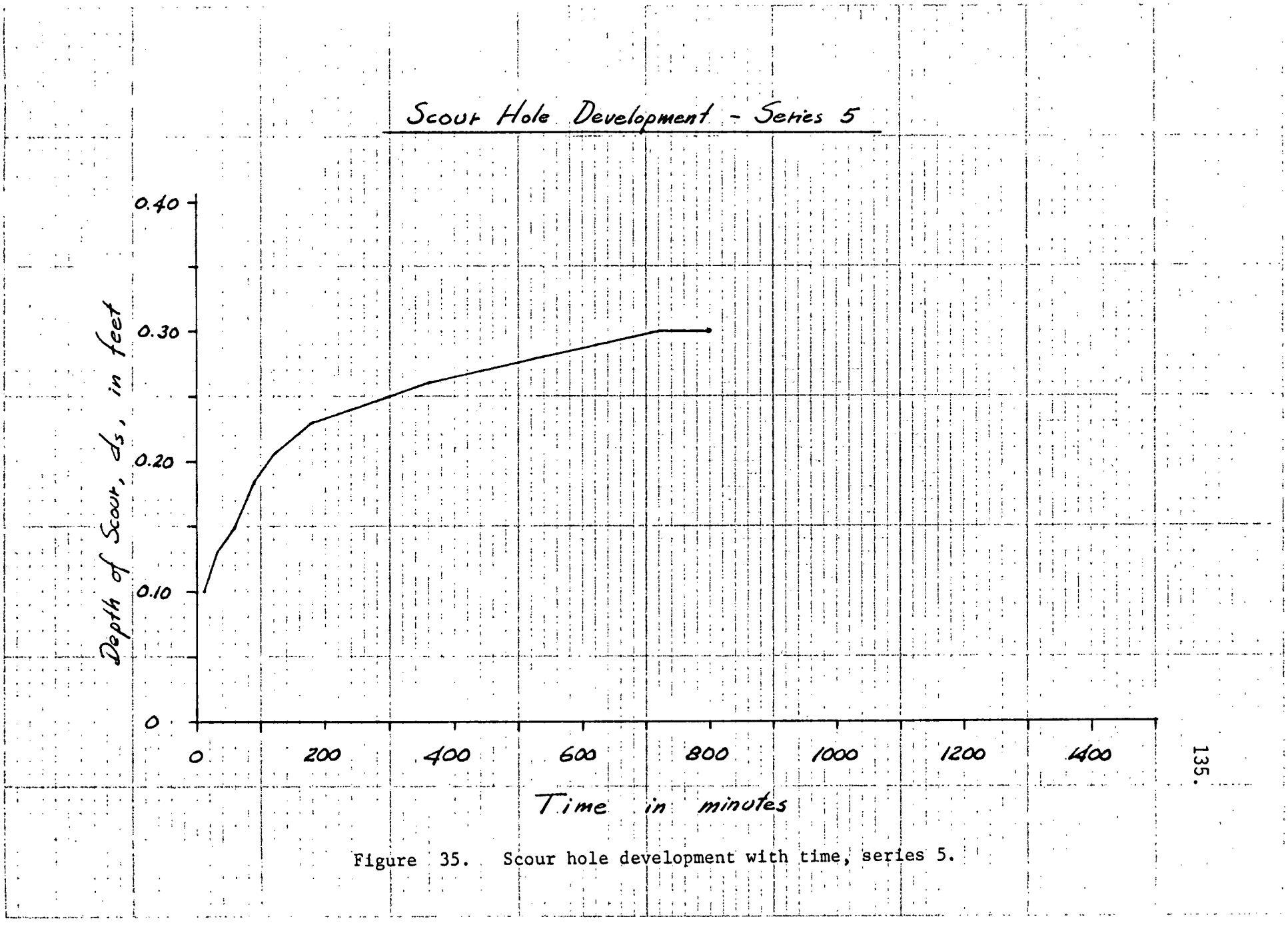

Figure 35. Scour hole development with time, series 5.

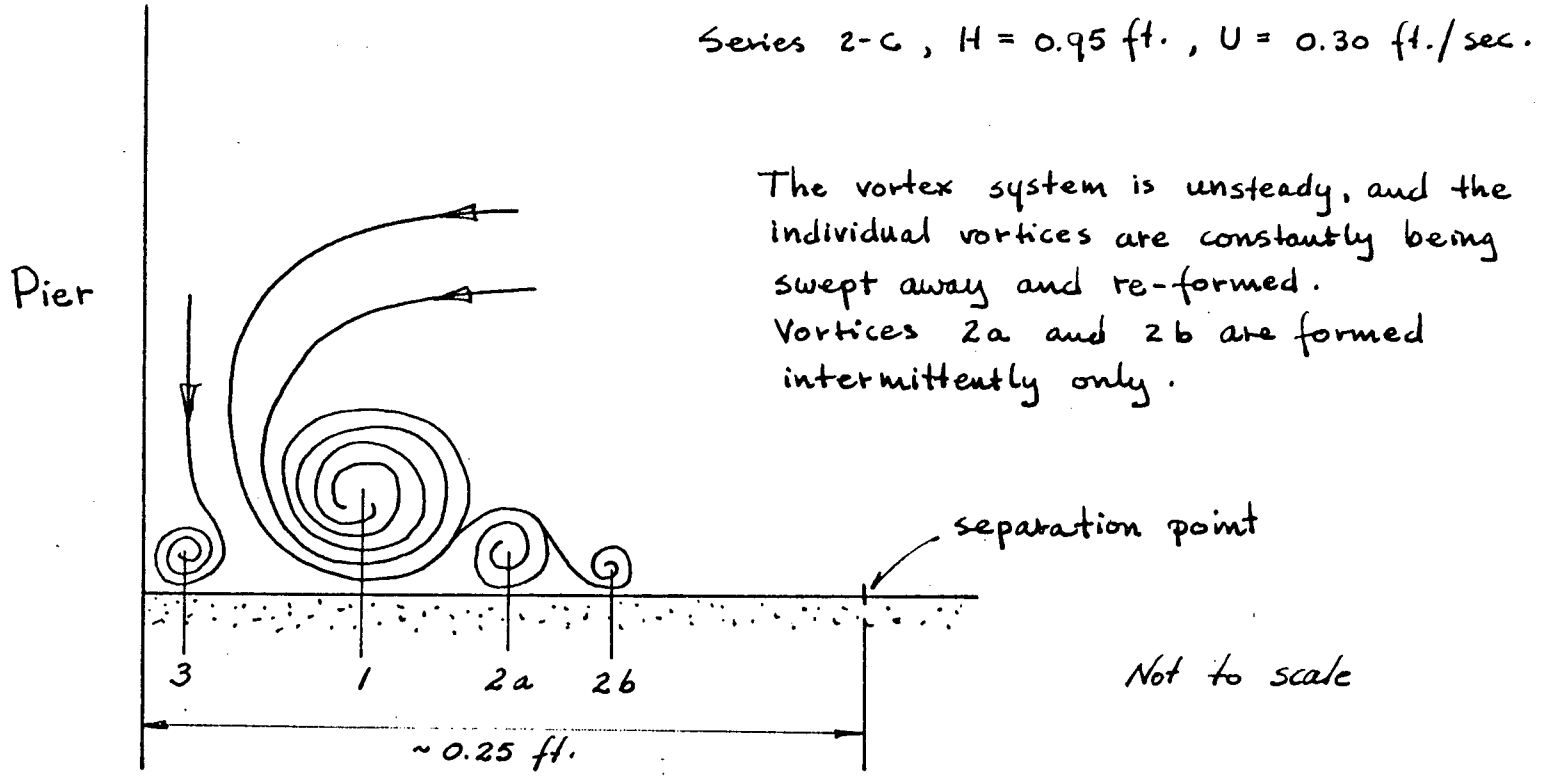

Figure 36. Vortex pattern, flat bed with low flow velocity.

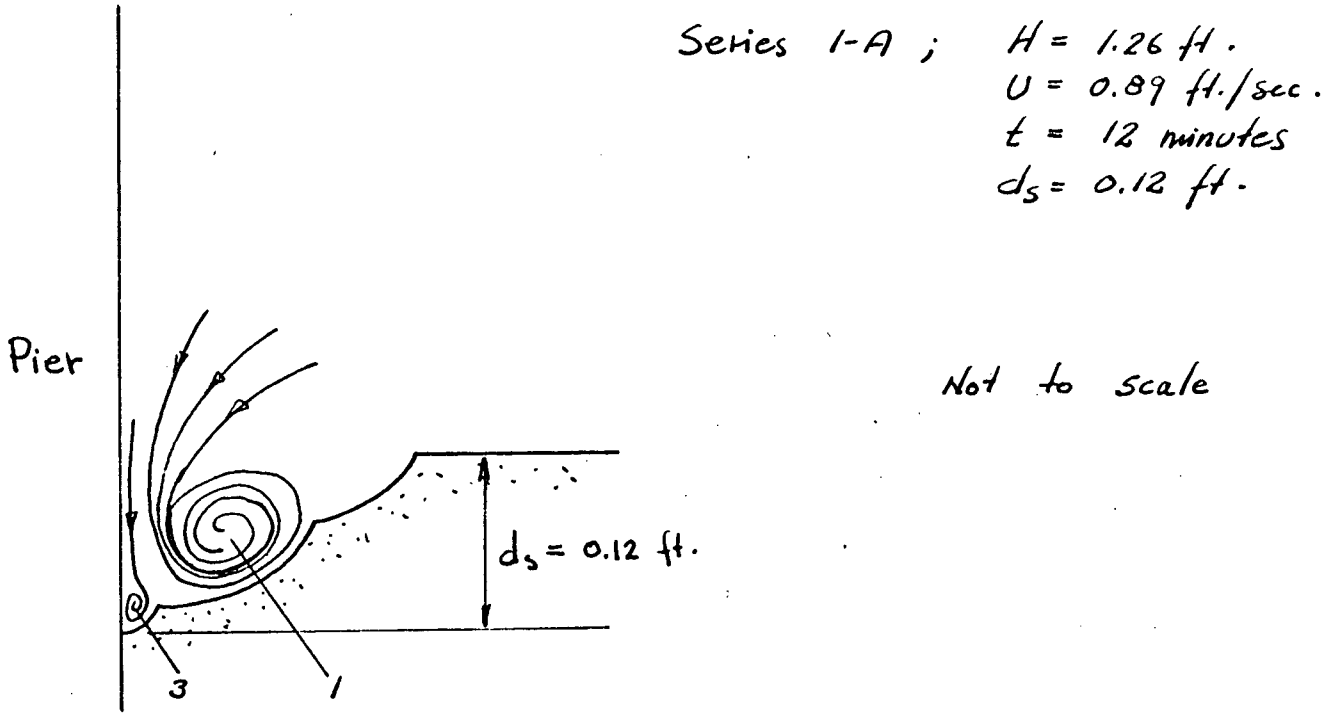

Figure 37. Vortex pattern, beginning of scour (cross-sectional view).

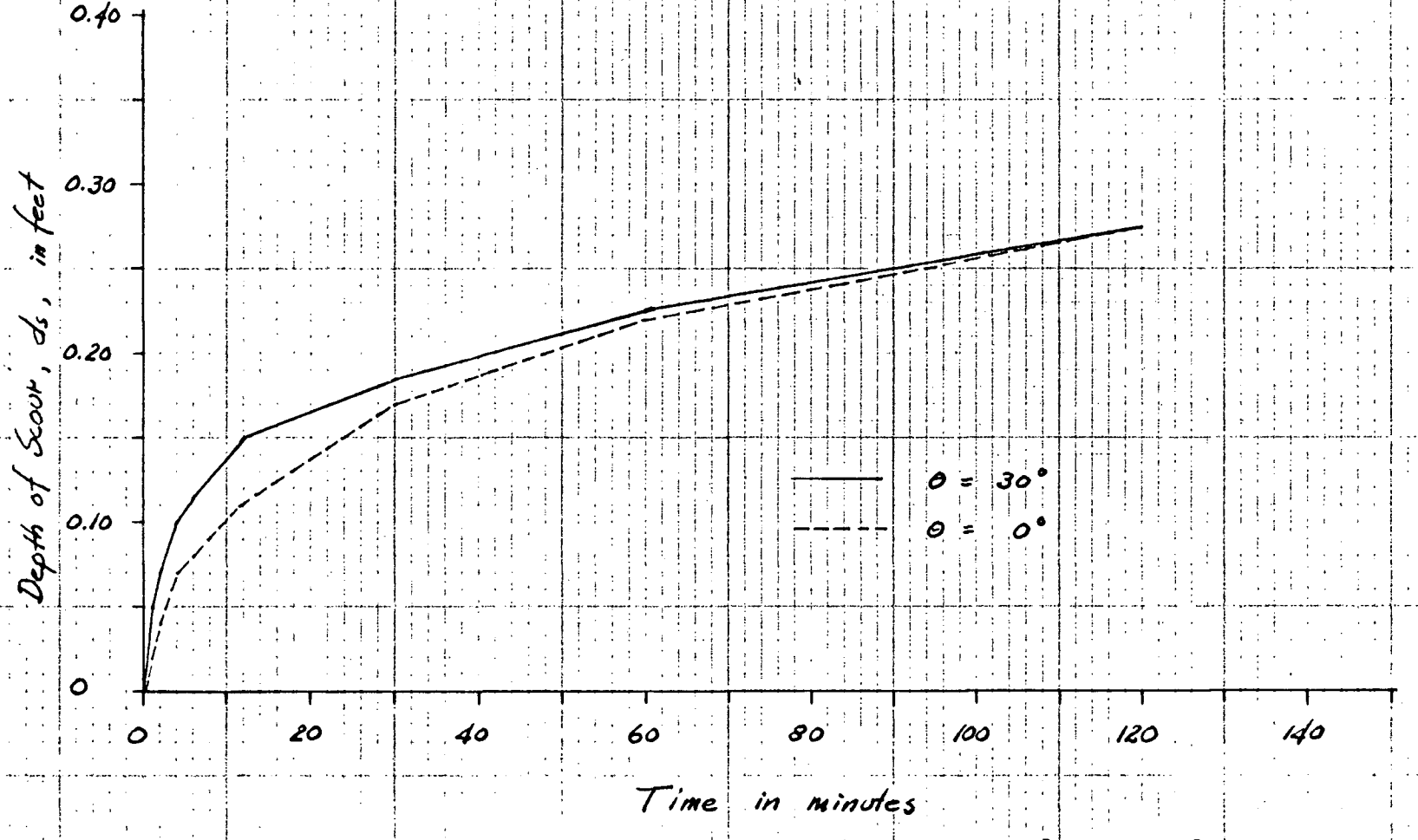

Figure 38. Scour hole development with time, at $\theta = 30^{\circ}$ and $\theta = 0^{\circ}$, series 1-A.

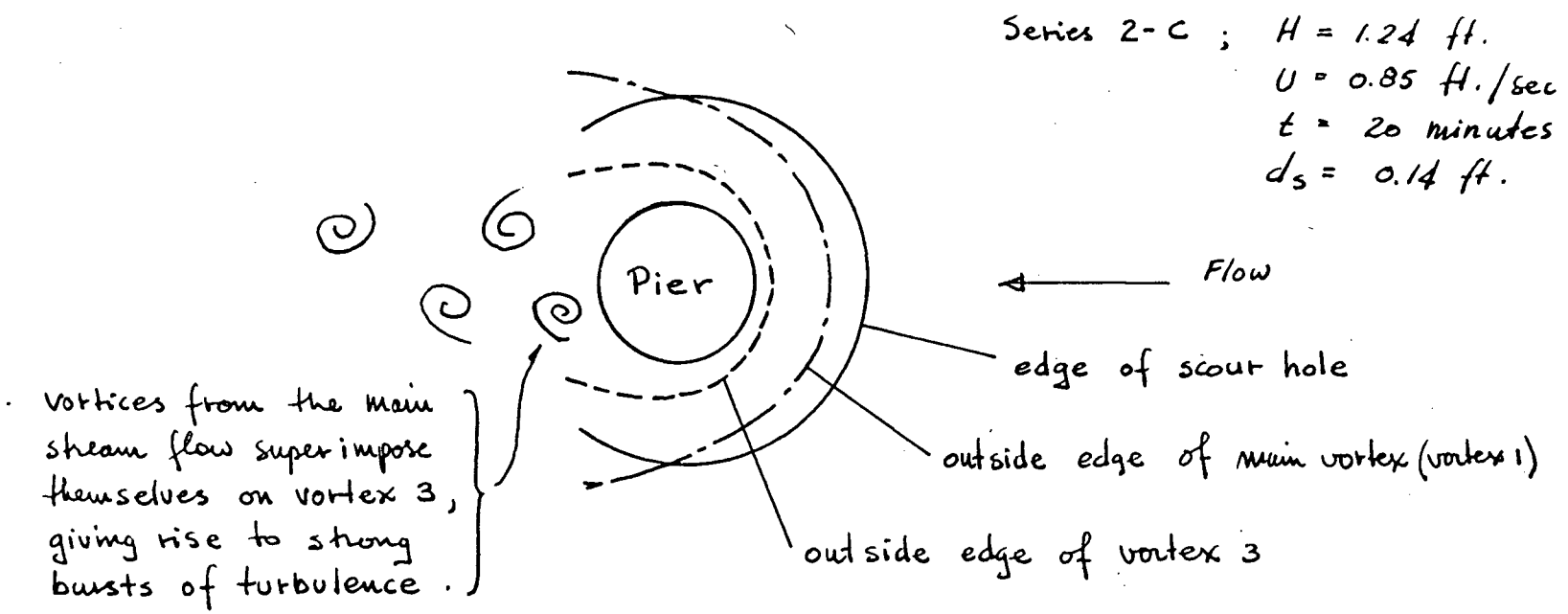

Figure 39. Vortex pattern, beginning of scour (plan view).

The partially developed scour hole was formed by a flow of U = 0.85 ft./sec. and H = 1.24 ft. to a depth d_s = 0.20 ft. The flow was then slowed to U = 0.45 ft./sec. to observe vortex patterns.

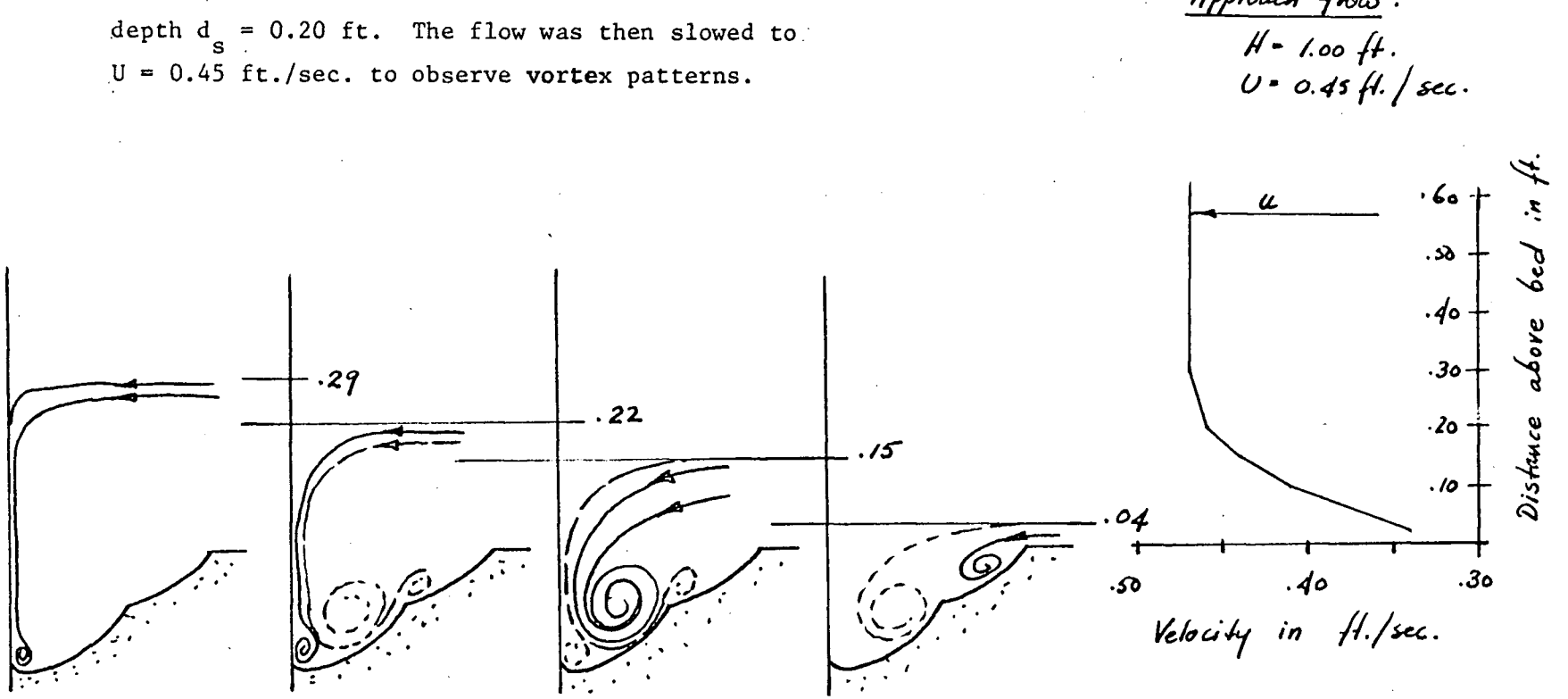

Figure 40. Vortex patterns; partly developed scour hole; showing dependence of the individual vortices on the vertical velocity profile of the approach flow.

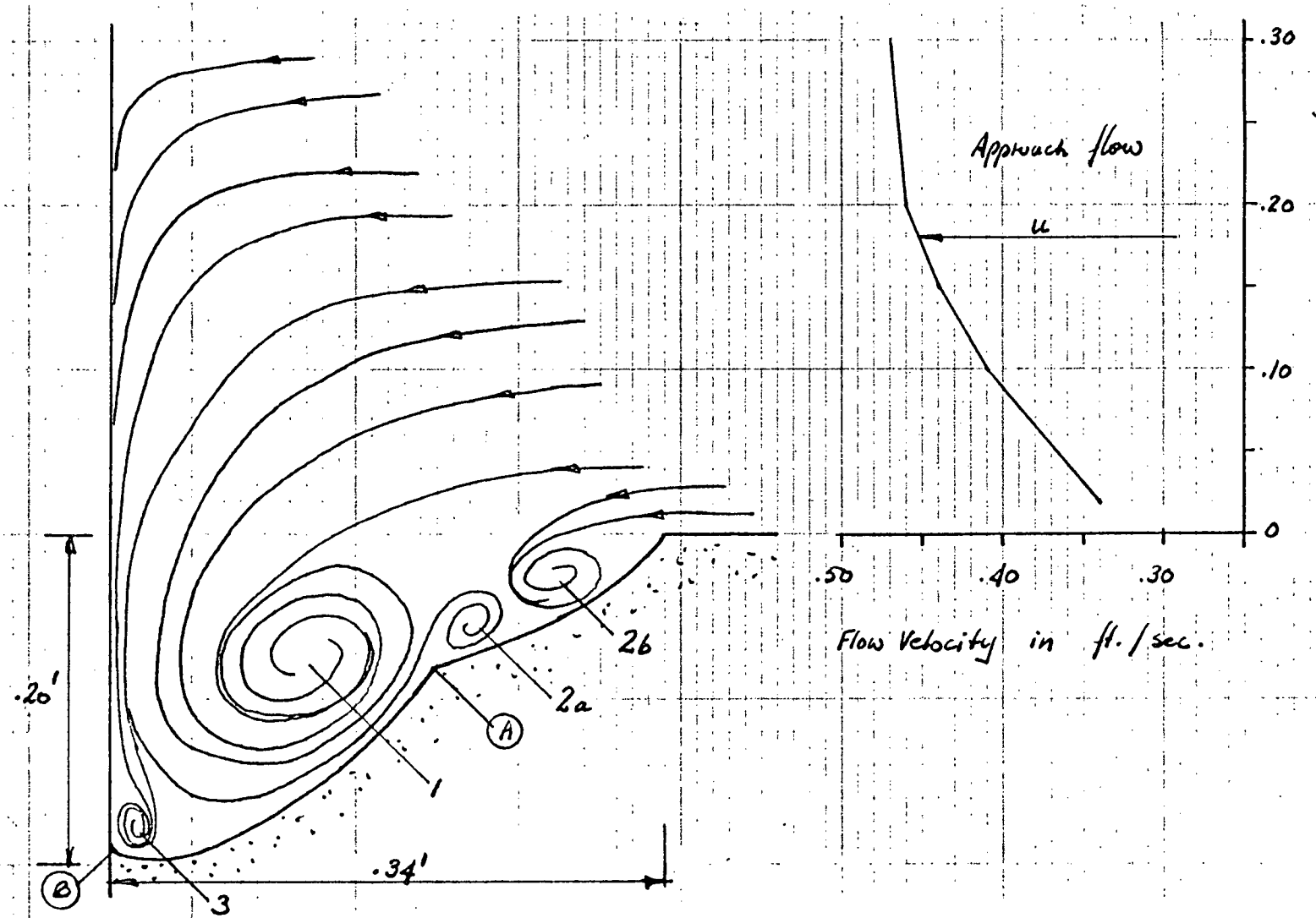

Figure 41. Vortex patterns; partly developed scour hole; showing effect of vertical velocity profile of the approach flow.

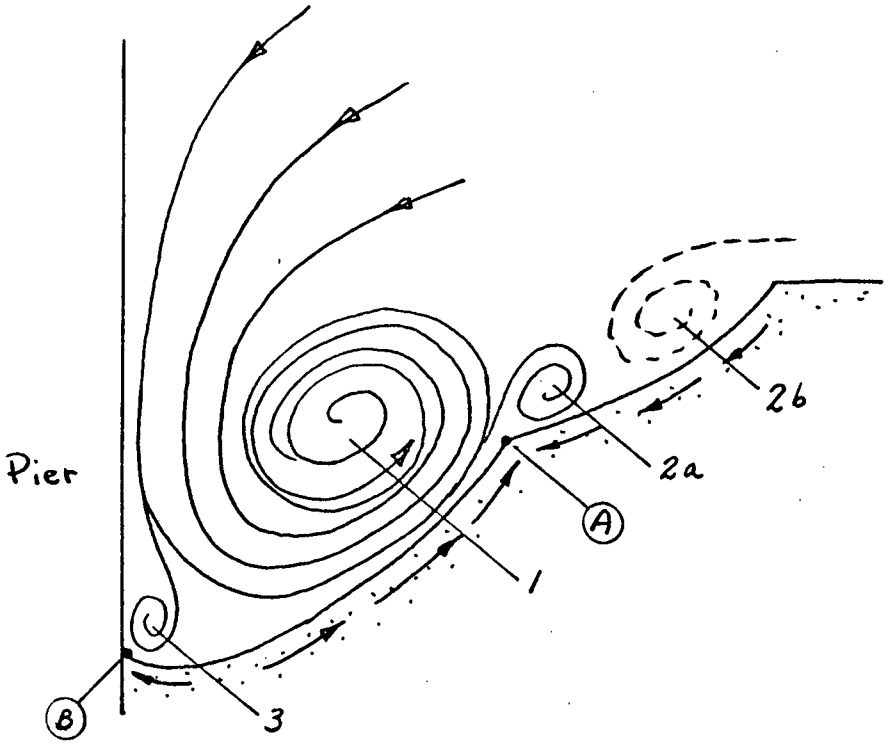

Figure 42. Scour hole development, showing motion of sand grains.

(a) looking downstream

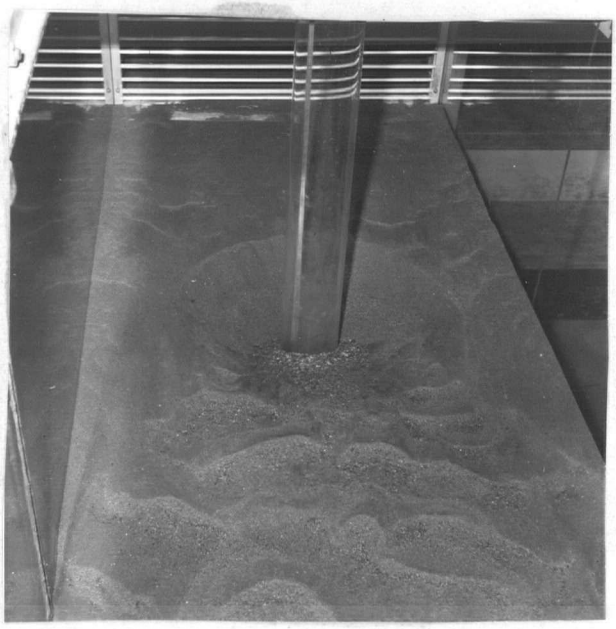

(b) looking upstream

Figure 43. Views of fully-developed scour hole: (a) looking downstream; (b) looking upstream.

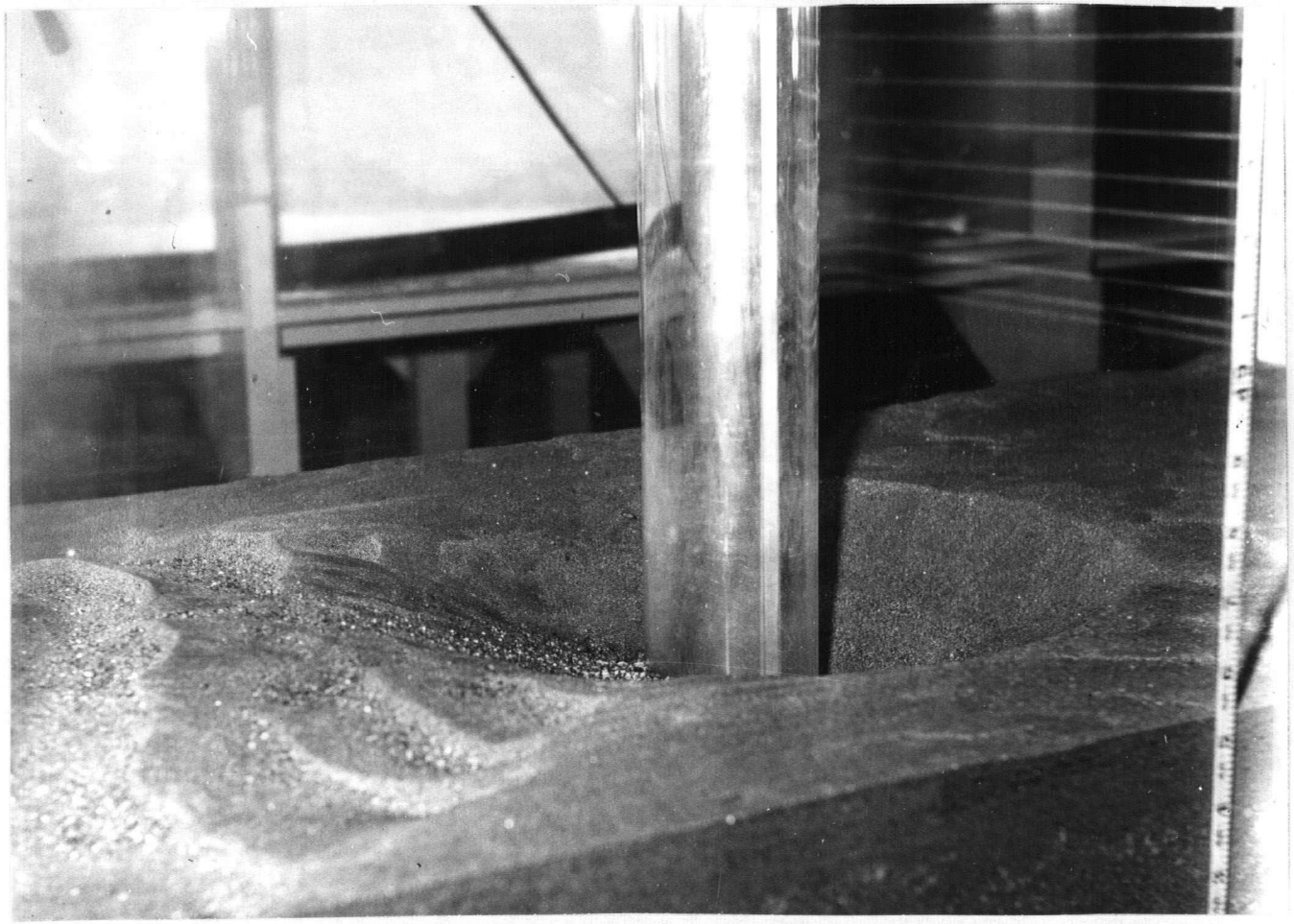

Figure 44. View of fully-developed scour hole, looking diagonally upstream.